

**UNIVERSIDADE FEDERAL DO RIO GRANDE DO SUL
INSTITUTO DE GEOCIÊNCIAS
PROGRAMA DE PÓS-GRADUAÇÃO EM GEOCIÊNCIAS**

**ESTROMATÓLITOS EM SISTEMAS PLATAFORMAIS
DOMINADOS POR ONDAS DO MESOPROTEROZÓICO DA
CHAPADA DIAMANTINA**

JOÃO PEDRO FORMOLO FERRONATTO

ORIENTADOR – Prof. Dr. Clayton Marlon dos Santos Scherer

Porto Alegre, 2021

**UNIVERSIDADE FEDERAL DO RIO GRANDE DO SUL
INSTITUTO DE GEOCIÊNCIAS
PROGRAMA DE PÓS-GRADUAÇÃO EM GEOCIÊNCIAS**

**ESTROMATÓLITOS EM SISTEMAS PLATAFORMAIS
DOMINADOS POR ONDAS DO MESOPROTEROZÓICO DA
CHAPADA DIAMANTINA**

JOÃO PEDRO FORMOLO FERRONATTO

ORIENTADOR – Prof. Dr. Claiton Marlon dos Santos Scherer

BANCA EXAMINADORA

Prof. Dr. Ernesto Luiz Correa Lavina – Universidade do Vale do Rio dos Sinos

Prof. Dr. Juliano Kuchle – Universidade Federal do Rio Grande do Sul

Prof. Dr. Roberto Iannuzzi – Universidade Federal do Rio Grande do Sul

Tese de Doutorado apresentada como
requisito parcial para a obtenção do Título de
Doutor em Ciências.

Porto Alegre, 2021

CIP - Catalogação na Publicação

Ferronatto, João Pedro Formolo
ESTROMATÓLITOS EM SISTEMAS PLATAFORMAIS DOMINADOS
POR ONDAS DO MESOPROTEROZOÍCO DA CHAPADA DIAMANTINA /
João Pedro Formolo Ferronatto. -- 2021.
146 f.
Orientador: Claiton Marlon dos Santos Scherer.

Tese (Doutorado) -- Universidade Federal do Rio
Grande do Sul, Instituto de Geociências, Programa de
Pós-Graduação em Geociências, Porto Alegre, BR-RS,
2021.

1. Estromatólitos do Pré-Cambriano. 2. Mistura de
Sedimentos. 3. Proterozoico. 4. Supergroupa Espinhaço.
5. Formação Caboclo. I. Scherer, Claiton Marlon dos
Santos, orient. II. Titulo.

RESUMO

Estromatólitos são o único registro de vida durante 85% da história geológica da Terra. Estão presentes desde o Arqueano, tendo seu período de acme no Proterozóico e seu declínio no Cambriano. São atualmente definidos como colônias de microorganismos bentônicos que constroem estruturas organo-sedimentares laminadas. As lâminas podem ser formadas por três processos distintos: aglutinação de grãos, precipitação microbial e precipitação inorgânica. Sendo que cada tipo de processo, ou a combinação deles, ocorre preferencialmente em um intervalo de tempo geológico específico. Essa tese tem o objetivo de detalhar dois intervalos específicos da Formação Caboclo, Mesoproterozóico da Chapada Diamantina, em que são encontrados estromatólitos. A partir disso, discutir processos que influenciaram no desenvolvimento e preservação dessas estruturas, e assim construir modelos deposicional para cada intervalo estratigráfico. Os dados utilizados foram obtidos de aproximadamente 367 m de perfis colunares de afloramentos. O artigo 1 foi elaborado com base nos 47 m da seção da Gruta do Cristal, intervalo basal da Fm. Caboclo. Para o detalhamento dos estromatólitos do topo da Fm. Caboclo (artigo 2) foi utilizada a análise sedimentológica de duas seções compostas, Rio Preto (150 m) e Rio Ventura (170 m). Na base da Fm. Caboclo, o ambiente deposicional é caracterizado por uma rampa dominada por tempestades, composta inteiramente por sedimentação híbrida siliciclástica-carbonática e com ampla distribuição de estromatólitos. Por sua vez, o topo da Fm. Caboclo é formada por uma rampa com sedimentação siliciclástica, dominada por ondas de tempestade, com concentrações de estromatólitos siliciclásticos localizados em intervalos específicos e pouco espessos.

PALAVRAS-CHAVE: Estromatólitos do Pré-Cambriano; Mistura de Sedimentos; Proterozóico; Supergrupo Espinhaço; Formação Caboclo

ABSTRACT

Stromatolites are the only record of life during 85% of the Earth's geological history. They are found from the Archean to the present, having their acme in the Proterozoic and their decline in the Cambrian. They are currently defined as colonies of benthic microorganisms that build laminated organosedimentary structures. The laminae can be formed by three distinct processes: grain agglutination, microbial precipitation and inorganic precipitation. And each of these processes, or the combination of them, occurs preferentially in a particular geological time interval. This thesis aims to detail two specific intervals of the Caboclo Formation, Mesoproterozoic of Chapada Diamantina, in which stromatolites are present. From there, discuss processes that influenced the development and preservation of these structures, and thus build depositional models for each stratigraphic interval. The data were obtained from approximately 367 m of outcrop log sections. Article 1 is based on the 47 m of the Cristal Cave section, basal portion of Caboclo Formation. To detail the stromatolites of Article 2 (top of Fm. Caboclo), sedimentological analysis of two composite log sections was used, Preto River (150 m) and Ventura River (170 m). At the base of the Caboclo Formation, the depositional environment is characterized by a storm-dominated ramp, composed entirely of siliciclastic-carbonate hybrid sedimentation and with a wide distribution of stromatolites. At the top, the Caboclo Formation is formed by a storm-dominated ramp with siliciclastic sedimentation, with the occurrence of siliciclastic stromatolites located at specific and thin intervals.

KEYWORDS: Precambrian stromatolites; Sediment mixing; Proterozoic; Espinhaço Supergroup; Caboclo Fm.

LISTA DE FIGURAS

- Figura 1.** As diferentes classificações dos depósitos microbiais com base na sua macrofábrica, retirado de Riding (2011) 11
- Figura 2.** (A) Critérios utilizados por diferentes autores para a definição de estromatólitos (Riding, 1999). (B) Diagrama sumarizando o contraste na definição de estromatólitos pelos mais importantes autores, usando os mesmos critérios mencionados da figura A (Riding, 2011) 12
- Figura 3.** Classificação de estromatólitos e trombólitos baseada na micro e macrofábrica quanto aos processos (aprisionamento de grãos, precipitação microbial e precipitação inorgânica). Modificado de Riding (2011) 14
- Figura 4.** Diagrama ilustrando as estruturas e indicando os termos usados na descrição de características diagnósticas em estromatólitos (Preiss, 1976; no livro de Walter, 1976) 17
- Figura 5.** Níveis de observação e organização de estromatólitos (Awramik, 1991) 18
- Figura 6.** (A) Modelo de estruturas estromatolíticas semi-esféricas lateralmente ligadas (SLL). Exemplos de estruturas semi-esféricas lateralmente ligadas: (B) Feições encontradas no Lago Dalaroo, oeste da Austrália. (C) Estruturas do tipo 'C' encontradas em Coomberdale (Proterozóico) do oeste da Austrália. (D) Estromatólitos do Grupo Missoula, Parque Nacional Glacier, Montana. (E) Estruturas do Grupo Piegan, Parque Nacional Glacier, Montana. Modificado de Logan (1964) 19
- Figura 7.** (A) Modelo de estruturas semi-esféricas verticalmente empilhadas (SVE). Essas estruturas podem ser do tipo 'C' ou do tipo 'V'. (B) Exemplo de um estromatólito SVE do tipo C do Grupo Missoula, Parque Nacional Glacier, Montana. (C) Estrutura SVE do tipo V na zona de intermaré em *Shark Bay*, oeste da Austrália. Modificado de Logan (1964) 20
- Figura 8.** (A) Tipos de estruturas esferoidais 'EE'. (B) Estrutura EE-C, Grupo Missoula, Parque Nacional Glacier, Montana. (C) Estrutura EE-I do recente, coletada de zona de intermaré em Rickenbacker Causeway, Miami, Florida. Modificado de Logan (1964) 21
- Figura 9.** Características físicas e biológicas que controlam a morfologia dos estromatólitos. O quadro indica as características que controlam cada tipo morfológica em Highborne Cay, Bahamas. (A) Conjunto de estromatólitos colunares com mais de 40 cm. (B) Estrutura interna de um estromatólito colunar, com

- laminações contínuas na base que são rompidas em direção ao topo. (C) Estromatólitos em cordões posicionadas em porções rasas atrás do recife. (D) Em estromatólitos com morfologia de cordão a laminação interna é tipicamente mais regular que em estruturas colunares. Modificado de Andres e Reid (2006).....22
- Figura 10.** Modelo conceitual comparando as influências ambientais e microbiais na formação de estromatólitos na escala micro (comunidade microbial), meso (laminação) e macro (morfologia). Retirado de Andres e Reid (2006), baseado em Trompette (1982) e Ginsburg (1991).....23
- Figura 11.** (A) Seção de uma barra de oólitos em um *playa lake*. A aparição e crescimento dos estromatólitos começam com a progressiva estabilização do substrato. (B) Estromatólito de grande porte (escala = 1m). (C) Crescimento de estromatólito entre depósito de oólitos. Raramente os oólitos são incorporados ao estromatólito. Modificado de Paul e Peryt (2000).....24
- Figura 12.** (A) Reconstrução geográfica do período de deposição do Subgrupo Campbellrand. (B) Evolução da sequência carbonática Campbellrand-Malmani. Modificado de Beukes (1987).....26
- Figura 13.** (A) Seção de referência da Formação Wonoka separada em unidades e com a interpretação de ambiente deposicional e profundidade em relação ao nível de ação de ondas normais e de tempestade. (B) Seção e diagrama de roseta representando as paleocorrentes e o eixo dos gutter casts da Unidade 7. No topo da unidade são encontrados os estromatólitos. Em detalhe estão representados dois ciclos. Modificado de Haines (1988).....28
- Figura 14.** (A) Seção estratigráfica geral da unidade estromatolítica e detalhe de parte do afloramento mostrando a relação entre as litofácies. (B) Reconstrução do ambiente deposicional da porção basal 'A' e superior 'B' da unidade. Modificado de Beukes e Lowe (1989)
- Figura 15.** (A) Relação de fácies do Grupo Pethei. (B) Modelos de transição plataforma – bacia. Modificado de Hoffman (1974).....32
- Figura 16.** Fácies estromatolíticas de Strelley Pool Chert, com a reconstrução 3-D e fotografias de afloramento. Escalas: b, h – 18 cm; c, e, k, l, n, s – 1 cm cada incremento; blocos diagramas – 5 cm. Retirado de Allwood *et al.* (2006).....34
- Figura 17.** (A) Diagrama ilustrativo idealizado mostrando a distribuição de associações de fácies com relação ao perfil batimétrico. (B) Modelo de fácies para o sistema misto carbonático-siliciclástico mostrando os principais contextos deposicionais da Formação Abrigo. Modificado de Labaj e Pratt (2016)

Figura 18. Tendências e possíveis controles sobre o desenvolvimento dos microbiais carbonáticos ao longo do tempo geológico. Esse gráfico mostra um longo período de queda (~1.000 Ma) na abundância de estromatólitos (Grotzinger, 1990) e o auge na diversidade morfológica durante o Mesoproterozóico (Awramik e Sprinkle, 1999). A redução de crosta cristalina (*sparry crust*) e estromatólitos híbridos (*hybrid stromatolites*) pode estar vinculada ao declínio da saturação de carbonato nos oceanos (Grotzinger, 1990). As esporádicas ocorrências de crosta cristalina durante o Fanerozóico estão associadas à bacias evaporíticas (Pope et. al, 2000). CCMs – Mecanismos de Concentração de CO₂. PAL – Nível Atmosférico Atual (Present Atmospheric Level). Níveis de CO₂ do Proterozóico inferidos com base em Sheldon (2006), Kah and Riding (2007), Hyde et al., (2000) e Ridgwell et al., (2003). Níveis de CO₂ do Fanerozóico inferidos com base em Berner e Kothavala (2001, Figura 13). Estromatólitos aglutinadores de grãos grossos e trombolitos no Neógeno podem em parte refletir a incorporação de diatomáceas a esteira microbial e pelos baixos valores de saturação de carbonato nos oceanos. Figura retirada de Riding (2011). 38

Figura 19. Mapa geológico do Cráton do São Francisco e seus domínios morfotectônicos: Bacia do São Francisco e Aulacógeno do Paramirim (Modificado de Alkmim et al., 1993).....41

Figura 20. Correlação regional do Supergrupo Espinhaço (Espinhaço Sul, Espinhaço Norte e Chapada Diamantina), indicando características gerais como os eventos e ambientes tectônicos relacionados, sequências deposicionais e datações realizadas por diversos pesquisadores ao longo do supergrupo. Retirado de Guadagnin et al., (2015).....42

Figura 21. Coluna estratigráfica composta da Formação Caboclo. Modificado de Guimarães e Pedreira (1990), retirada de Pedreira (1994).44

SUMÁRIO

ESTRUTURA DA TESE	7
1 INTRODUÇÃO.....	8
2 OBJETIVOS.....	10
3 ESTADO DA ARTE.....	11
3.1 Estromatólitos - Introdução	11
3.2 Tipos de Estromatólitos.....	13
3.3 Estruturas Estromatolíticas	16
3.4 Morfologia e Ambiente Deposicional.....	18
3.5 Estromatólitos no Proterozóico	37
4 DADOS E MÉTODOS.....	39
5 CONTEXTO GEOLÓGICO	40
5.1 Cráton do São Francisco.....	40
5.2 Supergrupo Espinhaço.....	41
5.3 Formação Caboclo.....	43
6 RESUMO DOS RESULTADOS E DISCUSSÕES	45
7 CONCLUSÕES.....	47
8 REFERÊNCIAS BIBLIOGRÁFICAS	49
9 ARTIGOS.....	56
9.1 ARTIGO 1 - Mixed carbonate-siliciclastic sedimentation in a Mesoproterozoic storm-dominated ramp: depositional processes and stromatolite development....	56
9.2 ARTIGO 2 – Mesoproterozoic siliciclastic stromatolites of Chapada Diamantina (Brazil): morphological types, genesis and environmental context....	103

ESTRUTURA DA TESE

Essa tese de doutorado está estruturada em um texto integrador e dois artigos científicos. O artigo 1, “*Mixed carbonate-siliciclastic sedimentation in a Mesoproterozoic storm-dominated ramp: depositional processes and stromatolite development*”, foi publicado no periódico Precambrian Research (Qualis-CAPES A1). O artigo 2, intitulado “*Mesoproterozoic siliciclastic stromatolites of Chapada Diamantina (Brazil): morphological types, genesis and environmental context*”, foi submetido para o periódico Precambrian Research (Qualis-CAPES A1). O texto integrador compreende os seguintes capítulos: (1) introdução; (2) estado da arte; (3) contexto geológico; (4) dados e métodos; (5) resultados e discussões; (6) conclusões; (7) referências bibliográficas.

1 INTRODUÇÃO

Estromatólitos são o único registro de vida durante 85% da história geológica da Terra, sendo encontrados desde o Arqueano até os dias atuais (Logan, 1961; Hofmann, 1973; Walter, 1977; Pratt, 1982; Knoll e Semikhatov, 1998; Grotzinger e Knoll, 1999; Reid et al., 2000; Allwood et al., 2006). São depósitos microbiais bentônicos que formam estruturas organo-sedimentares laminadas que podem ser compostas por três processos distintos: (i) trapeamento de grãos; (ii) precipitação microbial; (iii) precipitação inorgânica. Cada um desses processos dominam em determinado período geológico (Awramik e Riding, 1988; Grotzinger, 1990; Riding, 2011; Frantz et al., 2015). De acordo com Riding (2000), construções microbiais são biologicamente estimuladas, no entanto, as condições hidrodinâmicas e de saturação do ambiente necessitam ser favoráveis para que esses depósitos se desenvolvam. A ocorrência de estromatólitos é dependente da relação entre fatores bióticos e abióticos. Essa relação vai controlar a composição da fábrica, o crescimento e a geometria desses depósitos organo-sedimentares.

A Formação Caboclo (Branner, 1910; Srivastava, 1988; Rocha et al., 1992; Babinski et al., 1993; Pedreira, 1994) é interpretada como uma rampa mista carbonática-siliciclástica dominada por tempestades. A sedimentação é dominada por depósitos siliciclásticos (pelíticos e areníticos) com depósitos mistos siliciclásticos-carbonáticos subordinados. Foram detalhados dois intervalos estratigráficos da Formação Caboclo em que ocorrem estromatólitos. O primeiro, próximo à base da formação, está inserido em um contexto de sedimentação híbrida, enquanto o segundo, no topo da formação, está inserido em um contexto puramente siliciclástico.

Este trabalho apura a hipótese de que esses intervalos apresentam estromatólitos com características peculiares quando comparados com outros descritos no registro geológico, tanto em idade quanto em modelo deposicional, que seriam resultado de condições ambientais bastante específicas. No caso do intervalo basal (artigo 1), a particularidade estaria na ampla distribuição de depósitos estromatolíticos e a homogeneidade composicional dos sedimentos (carbonática/siliciclástica). Por sua vez, no intervalo do topo da Formação Caboclo (artigo 2) é investigada a hipótese de que esses estromatólitos se formaram em condições favoráveis para a aglutinação de material detritico siliciclástico. Esse

último processo não é comum no Mesoproterozóico e pode estar vinculado a queda abrupta da saturação de CaCO₃ dos oceanos nesse intervalo de tempo.

2 OBJETIVOS

Essa tese tem como foco de estudo dois intervalos que apresentam como características distintivas do resto da sucessão estratigráfica a presença de construções microbiais na forma de estromatólitos. O principal objetivo deste trabalho é entender os processos formadores e as variáveis controladoras da distribuição de estromatólitos em uma rampa dominada por ondas de idade mesoproterozóica, tendo como estudo de caso a Formação Caboclo, Chapada Diamantina, Brasil.

Os objetivos específicos são:

- (i) Estabelecer a relação entre a morfologia dos estromatólitos e os processos sedimentares operantes em uma plataforma mista carbonática-siliciclástica dominada por ondas;
- (ii) Descrever e interpretar um dos exemplos mais antigos de estromatólitos formados por trapeamento de grãos siliciclásticos, além de discutir os mecanismos que controlaram a acumulação e preservação dessas estruturas organo-sedimentares.

3 ESTADO DA ARTE

3.1 Estromatólitos - Introdução

Depósitos estromatolíticos dominam o registro fóssil de 85% da história da Terra. Essas estruturas tiveram seu pico de abundância durante o Proterozóico, porém são encontradas desde o Arqueano até os tempos de hoje (Logan, 1961; Hofmann, 1973; Walter, 1977; Pratt, 1982; Knoll and Semikhatov, 1998; Reid et al., 2000; Allwood et al., 2006). Estromatólitos estão inseridos em um grupo maior denominado de microbialitos (Figura 1), sendo a sua macrofábrica laminada a característica que o diferencia de trombólitos (grumosos), dendrólitos (dendríticos) e leiólitos (afanítico).

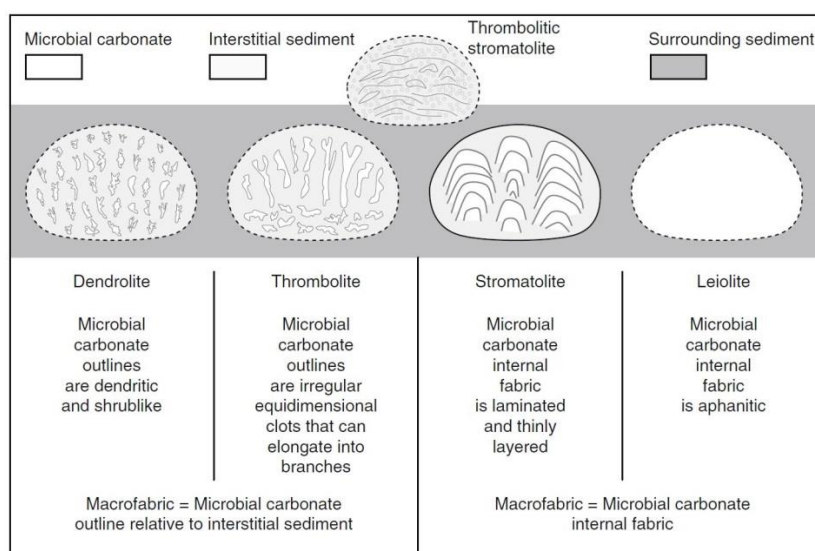


Figura 1. As diferentes classificações dos depósitos microbiais com base na sua macrofábrica, retirado de Riding (2011).

Porém, antes de se chegar a essa definição de microbialitos houveram muitas discussões quanto à definição de estromatólitos (Figura 2). Segundo Kalkowsky (1908), os estromatólitos são depósitos laminados gerados por organismos microbiais bentônicos. Awramik e Margulis (1974) definiram estromatólitos como estruturas organo-sedimentares que se acumulam devido ao trapeamento e aprisionamento de material detritíco e/ou por precipitação mineral gerado pelo crescimento e atividade metabólica de microrganismos, sem apresentar uma macrofábrica específica. Essa descrição de estromatólitos é a mesma que Burne e Moore (1987) utilizaram para definir os microbialitos. Entretanto, os microbialitos foram individualizados conforme a sua macrofábrica (Figura 1). Semikhatov et al.

(1979) define estromatólitos como estruturas de crescimento sedimentar, laminadas e litificadas que são acrescionadas a partir de um ponto ou superfície, não sendo necessária a atividade microbial. Essa definição incluiria como estromatólitos estruturas abiogênicas do tipo calcretes, estalagmites, ooides, sendo uma definição muito ampla e puramente descritiva. Grotzinger e Rothman (1996) defendem a hipótese de que embora a definição de estromatólito exija uma atividade microbial, existe um componente de precipitação abiótico na construção de estromatólitos, além de aprisionamento e precipitação estimulada por organismos. Os principais organismos envolvidos nos processos formadores de estruturas microbiais são bactérias, especialmente cianobactérias, pequenas algas e fungos.

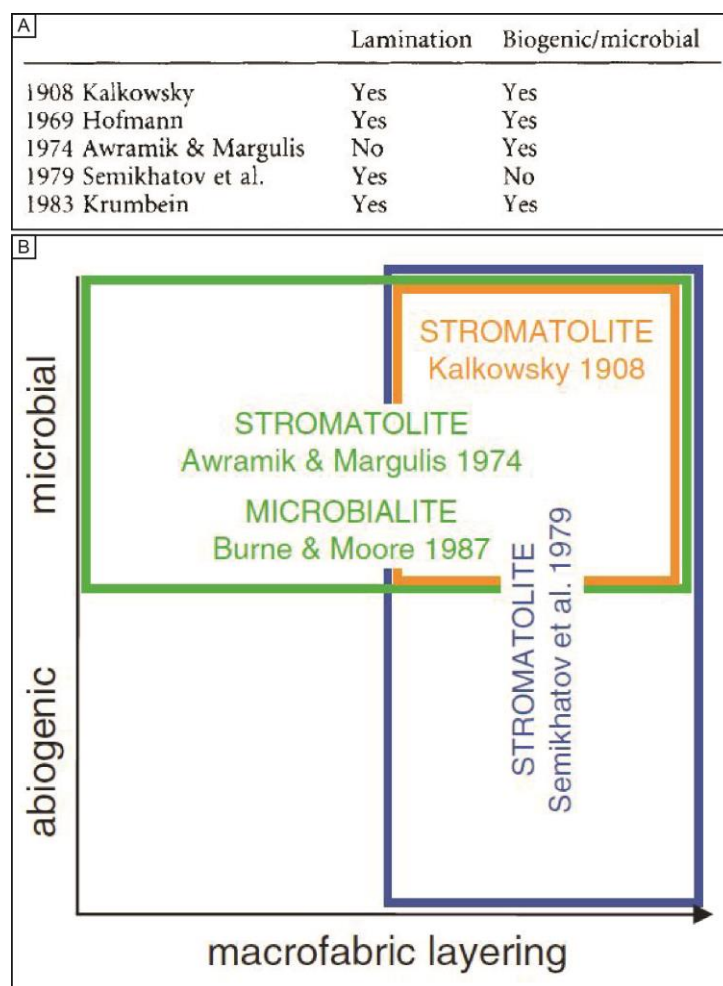


Figura 2. (A) Critérios utilizados por diferentes autores para a definição de estromatólitos (Riding, 1999). (B) Diagrama sumarizando o contraste na definição de estromatólitos pelos mais importantes autores, usando os mesmos critérios mencionados da figura A (Riding, 2011).

Estromatólitos se formam em uma ampla variedade de ambientes. São de grande importância no registro geológico, fornecendo informações paleoambientais, de biodiversidade e mudanças globais. Segundo Riding (2000), depósitos microbiais são biologicamente estimulados, porém também necessitam de fatores de saturação favoráveis do ambiente aquoso. Assim, a ocorrência dessas estruturas é dependente de uma relação entre fatores bióticos e abióticos, que em conjunto controlam o crescimento e geometria desses depósitos organosedimentares.

3.2 Tipos de Estromatólitos

Existem atualmente diferentes classificações de estromatólitos, baseados na microfábrica, na textura e na taxonomia dos organismos. A seguir faremos uma discussão dos tipos de estromatólitos baseada nos processos envolvidos na construção da fábrica estromatolítica, que resultam em microfábricas e texturas distintas, propostas nos trabalhos de Riding (2008 e 2011).

Nessa classificação, mesmo acreditando na origem microbial dos estromatólitos, o autor incorpora a precipitação inorgânica de carbonato aos processos formadores dessas construções (Figura 3). Isso, por existir muitas vezes uma relação conjunta entre processos inorgânicos e o biológicos. Sendo assim, a formação dessas estruturas organosedimentares envolve três processos: (i) trapeamento de grãos (*grain trapping*); (ii) precipitação microbial (*microbial precipitation*); (iii) precipitação inorgânica (*inorganic precipitation*).

Com base nos processos formadores da microfábrica estromatolítica, o autor define três grupos de estromatólitos (Figura 7):

- (i) Esteiras estromatolíticas litificadas (*lithified microbial mat stromatolites*);
- (ii) Crosta cristalina (*sparry crust*);
- (iii) Estromatólitos de crosta híbrida (*hybrid crust stromatolites*).

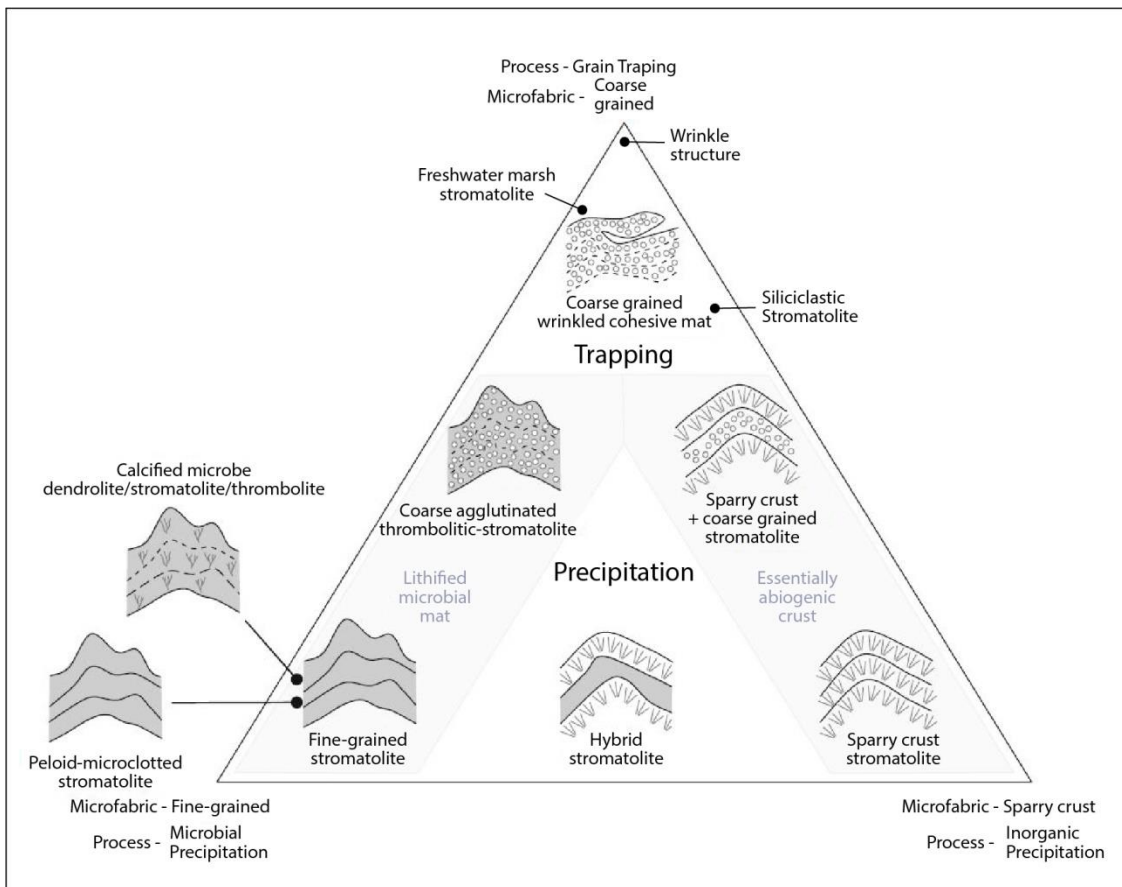


Figura 3. Classificação de estromatólitos e trombólitos baseada na micro e macrofábrica quanto aos processos (aprisionamento de grãos, precipitação microbial e precipitação inorgânica). Modificado de Riding (2011).

Esteiras estromatolíticas litificadas (lithified microbial mat stromatolites)

Os dois principais tipos são: (1) estromatólitos de grãos finos e (2) estromatólitos aglutinadores de grãos grossos. Morfológicamente formam depósitos estratiformes, dômicos e colunares, e tendem a formar camadas irregulares a descontínuas, podendo ter abundante porosidade fenestral e incorporar grãos alóctones.

Os estromatólitos de grãos finos (fine-grained stromatolites) são resultado de precipitação microbial sin-sedimentar e sua fábrica é composta por micrita, microespatito e feições filamentosas. A microfábrica de gãos finos tem características tipicamente grumosa e peloidal, possivelmente formada por processos metabólicos de microorganismos que resultam na precipitação de minerais, tendo como resultado a calcificação do EPS (Extracellular Polymeric Substances) e de outros produtos celulares. Esses estromatólitos também podem incorporar, em pequenas quantidades, grãos alóctones.

Os estromatólitos aglutinadores de grãos grossos (agglutinated stromatolites) são reconhecidos pela fábrica composta pelo trapeamento e aprisionamento de grãos maiores que silte pelo EPS não calcificado e/ou por filamentos eretos de microrganismos. Geralmente apresentam fábrica grosseira, com laminação pouco desenvolvida quase trombolítica. Exemplos de estromatólitos aglutinadores de grãos grossos são raros no registro geológico.

Crosta cristalina (sparry crust)

Formam precipitados abiogênicos “tipo estromatólitos”, frequentemente isópicos, homogêneos e com boa persistência lateral. Sua microfábrica é formada geralmente por cristais radiais/fibrosos. Exemplos incluem tamanhos variáveis de botrióides radiais e pseudomorfos de cristais, micro interdigitação com estromatólitos do tipo tufa, dendritos, laminitos isópicos e calcita herringbone. Podem formar domos, crescimentos de cristais verticais e apresentar uma grande extensão lateral. Esses estromatólitos também podem incorporar ou se intercalar com grãos alóctones.

Crosta cristalinas são comuns desde o fim do Arqueano até o Mesoproterozóico. Depósitos interdigitados milimétricamente ocorrem em ambientes de supra e intermaré enquanto que laminitos isópicos precipitam em águas relativamente profundas.

Estromatólitos de crosta híbrida (hybrid crust stromatolites)

Tipicamente consistem em alternações milimétricas de crosta cristalinas e de crostas de grãos finos, interdigitando lâminas de coloração clara (crosta cristalina) e escura (esteiras estromatolíticas). Essa alternância de processos constrói estromatólitos com camadas bem regulares e bastante persistentes. Sendo assim, esse acamamento coloca esses depósitos em um intermediário entre estromatólitos de crosta cristalina e estromatólitos de crosta de grãos finos. Esses estromatólitos são um importante componente dos estromatólitos do Paleoproterozóico e do Mesoproterozóico, formando grandes corpos com morfologia dômica e cônicas.

3.3 Estruturas Estromatolíticas

A caracterização de estromatólitos em campo nem sempre é fácil, depende muito do grau de exposição e preservação do depósito. As principais características que devem ser detalhadas são a geometria, o arranjo e forma das colunas, as laminações e a relação entre os estromatólitos. Com essas informações é possível sugerir um possível ambiente de deposição (lâmina d'água, energia, sentido de correntes, exposição) e como ele se comportou ao longo do tempo de deposição dessas bioconstruções.

Preiss (1976) indica uma lista de características que devem ser observadas para a descrição desses depósitos, em grande e média escalas. O autor também criou um esquema ilustrativo das estruturas que podem ser descritas (Figura 4).

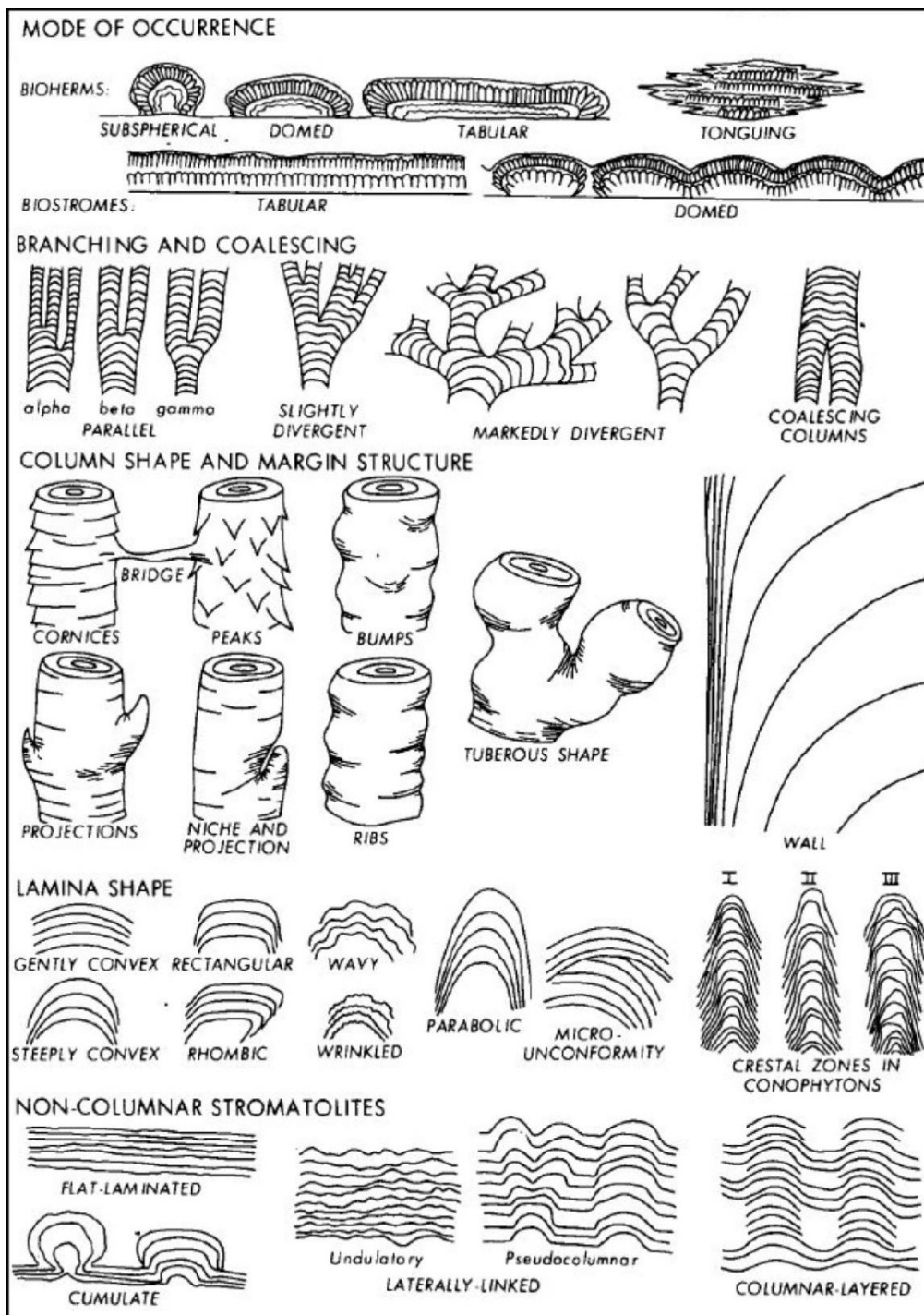


Figura 4. Diagrama ilustrando as estruturas e indicando os termos usados na descrição de características diagnósticas em estromatólitos (Preiss, 1976; no livro de Walter, 1976).

Segundo Awramik (1991), a maneira ideal de estudar estromatólitos é considerar todas as escalas de observação, desde grandes estruturas (biostromas e biohermas) até a escala de microscópio (microestruturas e microfósseis). A figura 5 ilustra as escalas de observação citadas anteriormente. A descrição realizada nessas diversas escalas permite uma interpretação precisa sobre o desenvolvimento de um estromatólito em diferentes escalas de tempo, desde um simples evento de

trapeamento de grãos ou de precipitação mineral, até variações na morfologia em macro escala que podem ser relacionadas a mudanças hidrodinâmicas associada aos ambientes deposicionais.

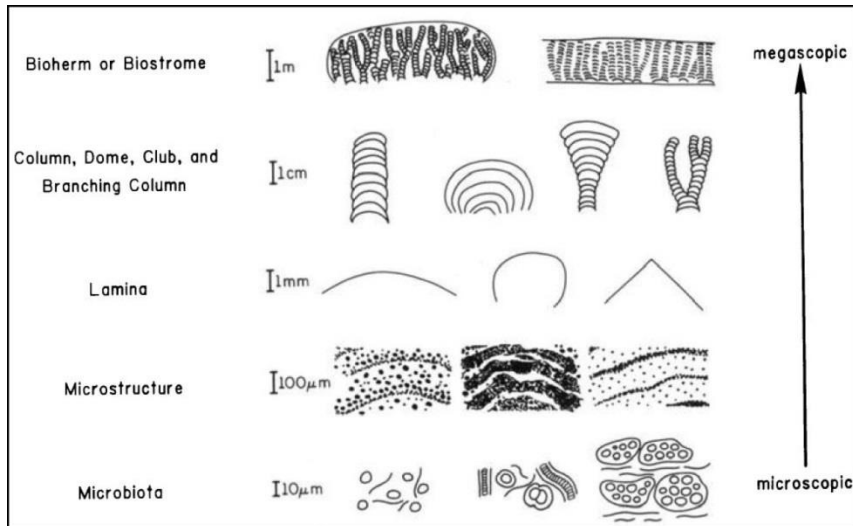


Figura 5. Níveis de observação e organização de estromatólitos (Awramik, 1991).

3.4 Morfologia e Ambiente Deposicional

Segundo Hofmann (1973), a maioria dos estromatólitos carbonáticos se forma em águas rasas de bacias marinhas, lagos salinos e nascentes termais. A ocorrência de depósitos de água doce e de águas profundas ocorre em menores quantidades.

Estromatólitos são moldados por uma interação de fatores. Segundo Walter (1977), duas variáveis controlam a morfogênese dos estromatólitos: (a) correntes aquosas e (b) reação a luz.

Logan et al. (1964) propõe uma classificação descritiva para estromatólitos baseada na geometria de depósitos recentes. A organização geométrica ocorre em função da reação da esteira algal às condições ambientais. Através dessa identificação morfológica os autores sugerem possíveis ambientes de crescimento. Sendo assim, foi determinado três principais arranjos geométricos: semi-esféricos lateralmente ligados (*SLL*), semi-esféricos verticalmente empilhados (*SVE*) e estruturas esféricas (*EE*), conhecidas como oncólitos. A maioria das estruturas

estromatolíticas são compostas por SLL e SVE. Essa mudança de empilhamento é resultado de alterações no ambiente deposicional.

Estruturas SLL (Figura 6) ocorrem em ambientes de intermaré, geralmente em ambientes protegidos de baías ou atrás de cordões e ilhas barreiras onde a ação de ondas é baixa. Periódicamente esses depósitos podem se estender para zonas supramaré. Isso ocorre em períodos de marés anômalas ou eventos de tempestades. Normalmente SLL de supramaré apresentam feições de ressecamento e exposição, são blocosos e podem estar associados a conglomerados e brechas.

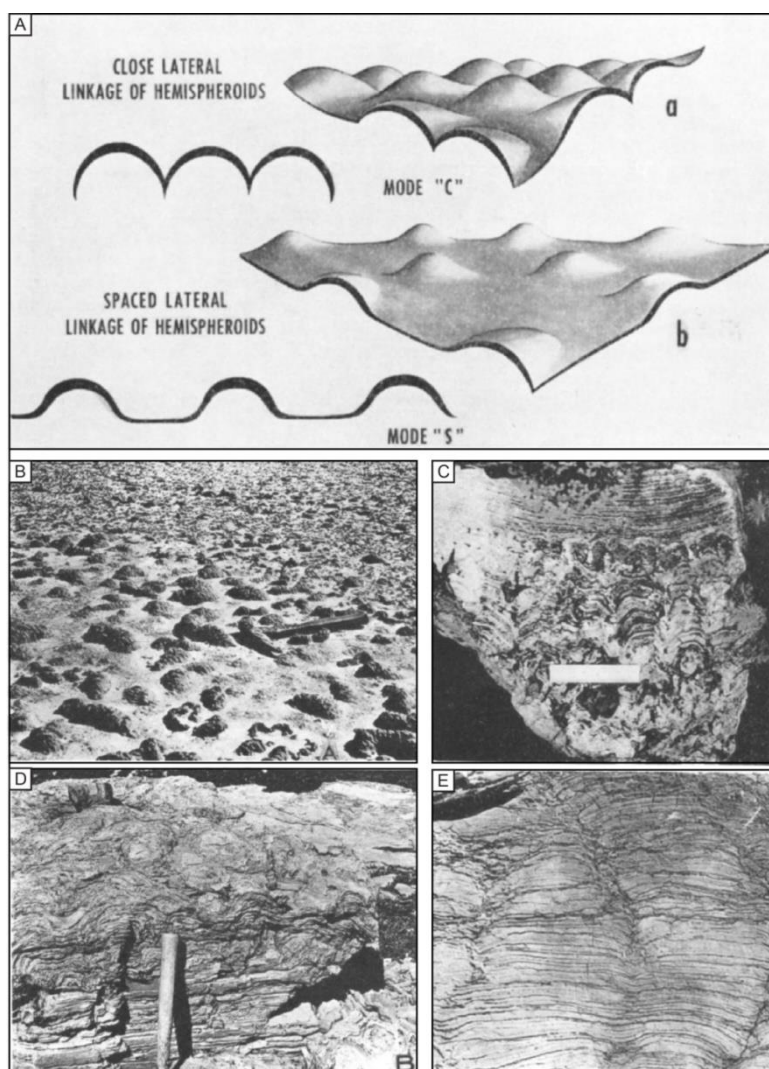


Figura 6. (A) Modelo de estruturas estromatolíticas semi-esféricas lateralmente ligadas (SLL). Exemplos de estruturas semi-esféricas lateralmente ligadas: (B) Feições encontradas no Lago Dalaroo, oeste da Austrália. (C) Estruturas do tipo 'C' encontradas em Coomberdale (Proterozóico) do oeste da Austrália. (D) Estromatólitos do Grupo Missoula, Parque Nacional Glacier, Montana. (E) Estruturas do Grupo Piegan, Parque Nacional Glacier, Montana. Modificado de Logan (1964).

A formação e preservação de estruturas SVE (Figura 7) ocorre devido a inabilidade das esteiras microbiais ou domos em se conectar lateralmente ou ainda pela destruição da esteira nas áreas entre domos. O exemplo clássico desses estromatólitos no recente são os de Shark Bay, oeste da Austrália. Comparando com estruturas SLL, depósitos SVE se estabelecem em ambientes de maior energia de ondas e marés. São comuns em recifes e locais de energia de onda moderada.

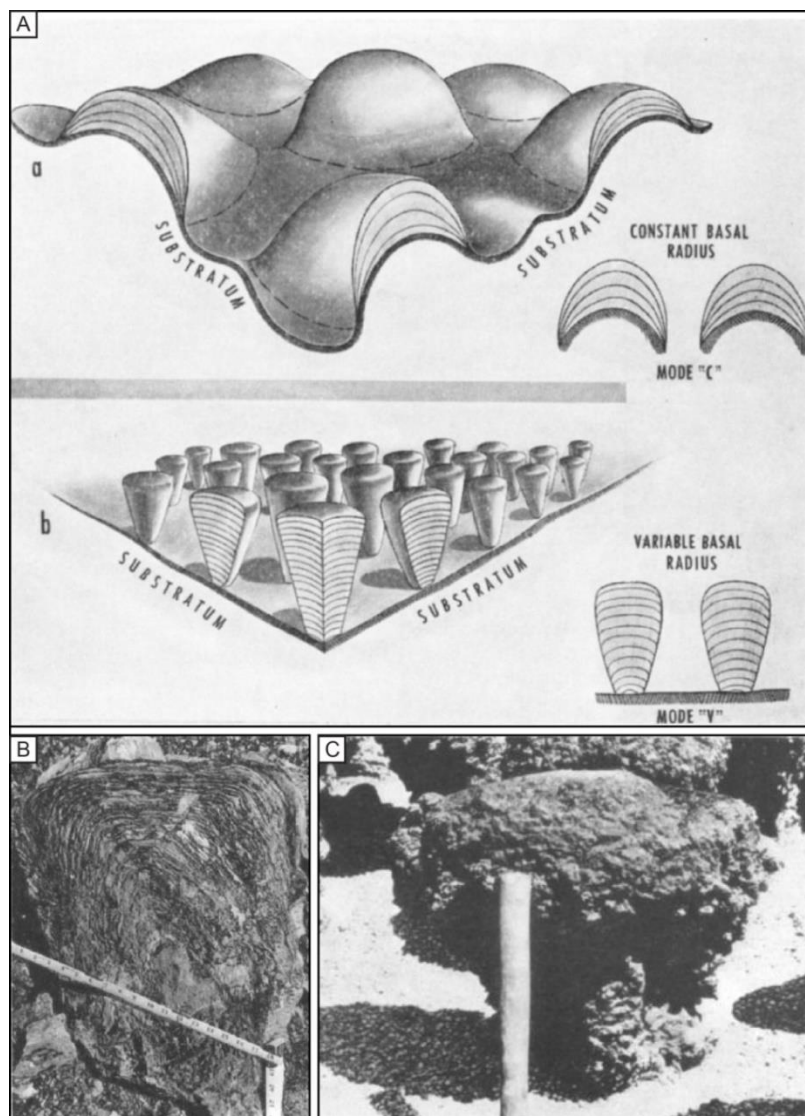


Figura 7. (A) Modelo de estruturas semi-esféricas verticalmente empilhadas (SVE). Essas estruturas podem ser do tipo 'C' ou do tipo 'V'. (B) Exemplo de um estromatólito SVE do tipo C do Grupo Missoula, Parque Nacional Glacier, Montana. (C) Estrutura SVE do tipo V na zona de intermaré em *Shark Bay*, oeste de Austrália. Modificado de Logan (1964).

A ocorrência de estruturas do tipo EE (oncólitos; Figura 8) geralmente indicam ambientes permanentemente submersos, abaixo da zona intermaré. A presença de

estruturas do tipo EE indica a ação de onda e/ ou correntes no substrato. Conforme o grau de agitação do ambiente estruturas distintas se formam.

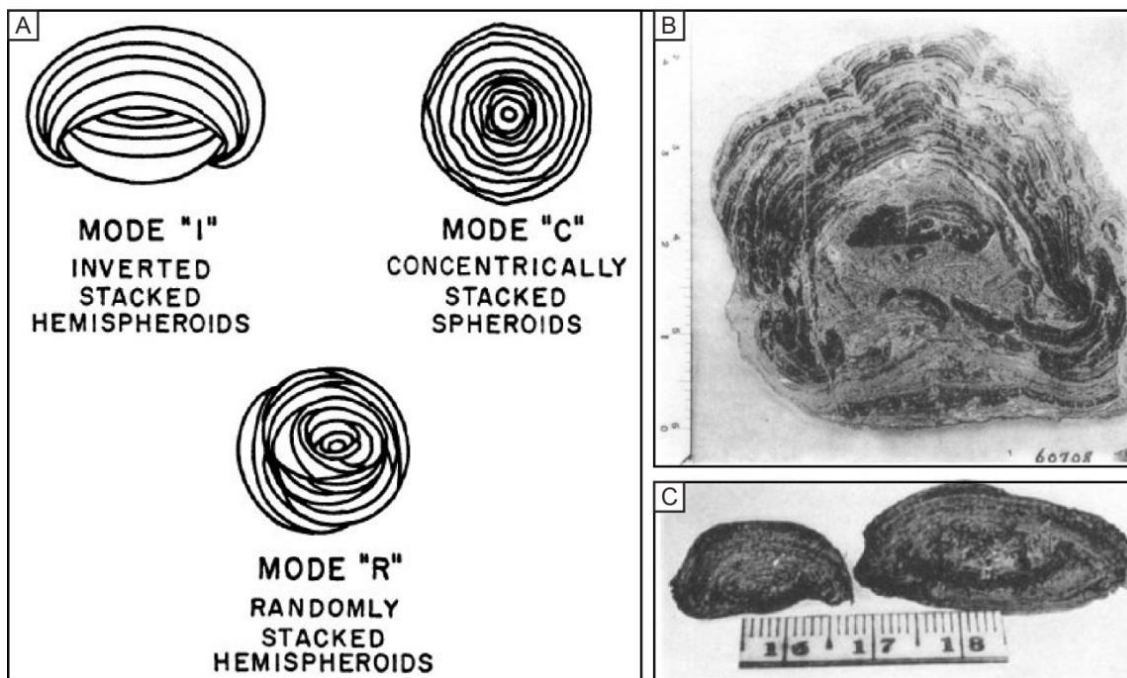


Figura 8. (A) Tipos de estruturas esferoidais ‘EE’. (B) Estrutura EE-C, Grupo Missoula, Parque Nacional Glacier, Montana. (C) Estrutura EE-I do recente, coletada de zona de intermaré em Rickenbacker Causeway, Miami, Florida. Modificado de Logan (1964).

Andres e Reid (2006) em seu trabalho sobre a morfologia dos estromatólitos atuais de Highborne Cay nas Bahamas sugerem que a morfologia em macroescala dos estromatólitos estudados é controlada principalmente pelo espaço de acomodação, a hidrodinâmica do ambiente e pelo padrão de sedimentação (Fig. 9). A dinâmica de sedimentação é uma variável fundamental para a acresção desses depósitos, pois o sedimento em suspensão fornece grãos que podem ser aprisionados e cimentados pelos microrganismos.

Na área de estudo de Andres e Reid (2006) os estromatólitos apresentam duas morfologias distintas: colunas (Figura 9A e B) e cordões (Figura 9C e D). Os colunares tem mais de 40 cm de altura e 50 cm de diâmetro e ocorrem isolados ou como montes coalescentes sem orientação preferencial. São estruturas compostas que variam da base para o topo entre laminações estratiformes e colunas ramificadas. As estruturas em cordões tem entre 5 e 10 cm de altura, variam de 10 a 20 cm de largura e internamente as laminações são subparalelas a superfície. As construções em forma de cordões são melhor desenvolvidas em águas mais rasas, em lagunas atrás dos recifes com uma dinâmica de sedimentação em que o

soterramento e retirada de sedimentos são muito frequentes, na ordem de dias ou semanas. Em contraste, os estromatólitos colunares são encontrados predominantemente em porções mais profundas, com períodos de sotterramentos e remobilização de sedimentos de escala anual.

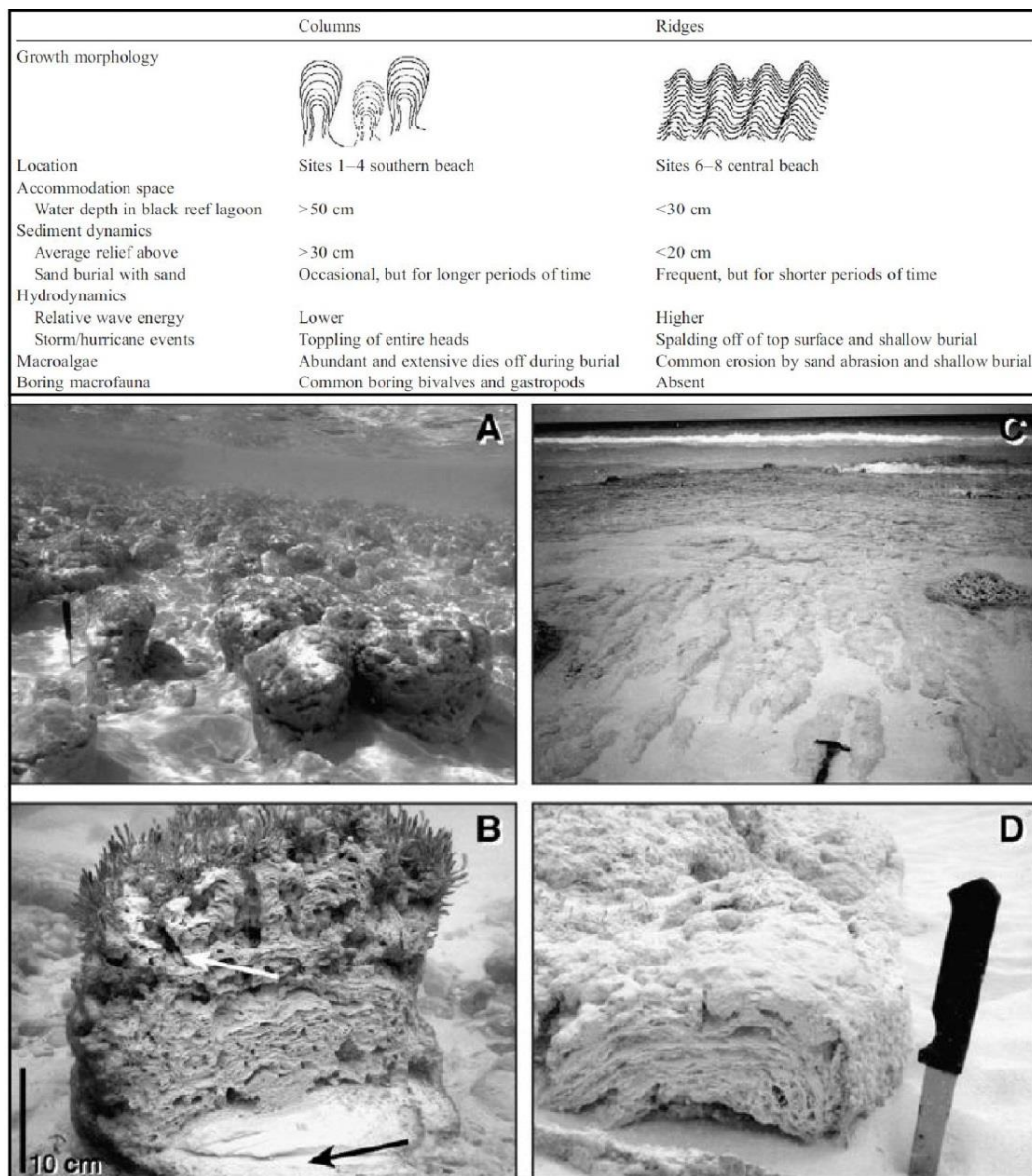


Figura 9. Características físicas e biológicas que controlam a morfologia dos estromatólitos. O quadro indica as características que controlam cada tipo morfológica em Highborne Cay, Bahamas. (A) Conjunto de estromatólitos colunares com mais de 40 cm. (B) Estrutura interna de um estromatólito colunar, com laminações contínuas na base que são rompidas em direção ao topo. (C) Estromatólitos em cordões posicionadas em porções rasas atrás do recife. (D) Em estromatólitos com morfologia de cordão a laminação interna é tipicamente mais regular que em estruturas colunares. Modificado de Andres e Reid (2006).

Nesse trabalho as autoras também sugerem que os microorganismos tem maior influência na microfábrica, enquanto os parâmetros físicos ambientais controlariam a morfologia em macroescala dos estromatólitos (Figura 15). A influência microbial e as influências físicas ambientais seriam inversamente proporcionais.

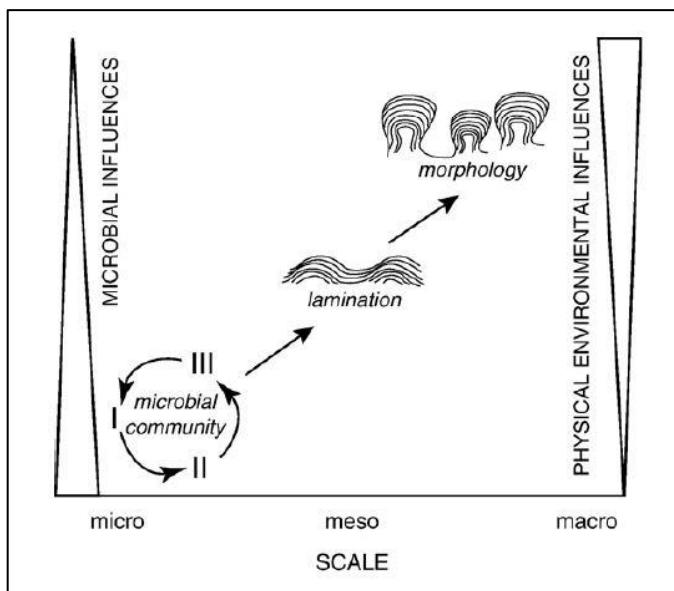


Figura 10. Modelo conceitual comparando as influências ambientais e microbiais na formação de estromatólitos na escala micro (comunidade microbial), meso (laminação) e macro (morfologia). Retirado de Andres e Reid (2006), baseado em Trompette (1982) e Ginsburg (1991).

Paul e Peryt (2000) trabalharam com os carbonatos de Buntsandstein, Montanhas Harz, Alemanha. Foi nessas rochas que Kalkowsky criou o termo “estromatólito” em 1908. São datadas do Triássico inferior, com gênese relacionada a uma bacia lacustrina fechada, em um sistema de *playa lake* com variações de salinidade. No centro da bacia camadas de oólitos se intercalam com depósitos siliciclásticos que compõem ciclos de granodecrescência ascendente vinculados a variações climáticas.

Nesse contexto, os estromatólitos geralmente se desenvolvem em um tempo subsequente ao aparecimento dos oólitos (Figura 11). São formados por laminações milimétricas que compõem estruturas centimétricas colunares ramificadas, geralmente de mais de 4 cm (Figura 11C). Essas formas menores, que comumente se iniciam como crostas milimétricas sobre areias oolíticas, se agrupam em grandes

estruturas dômicas (> 2 m, Figura 11B) e ocasionalmente apresentam estruturas de dissolução sindepositinal no topo.

A passagem de estruturas colunares para grandes domos reflete mudanças nas condições hidrodinâmicas. O influxo de oóides ou sedimento lamoso siliciclástico interrompe a construção microbial. A alta taxa de evaporação faz com que ocorram altas concentrações de Ca, favorecendo a precipitação biologicamente induzida de carbonatos na forma de oóides e estromatólitos. Sendo assim, é possível associar a presença desses depósitos á períodos áridos.

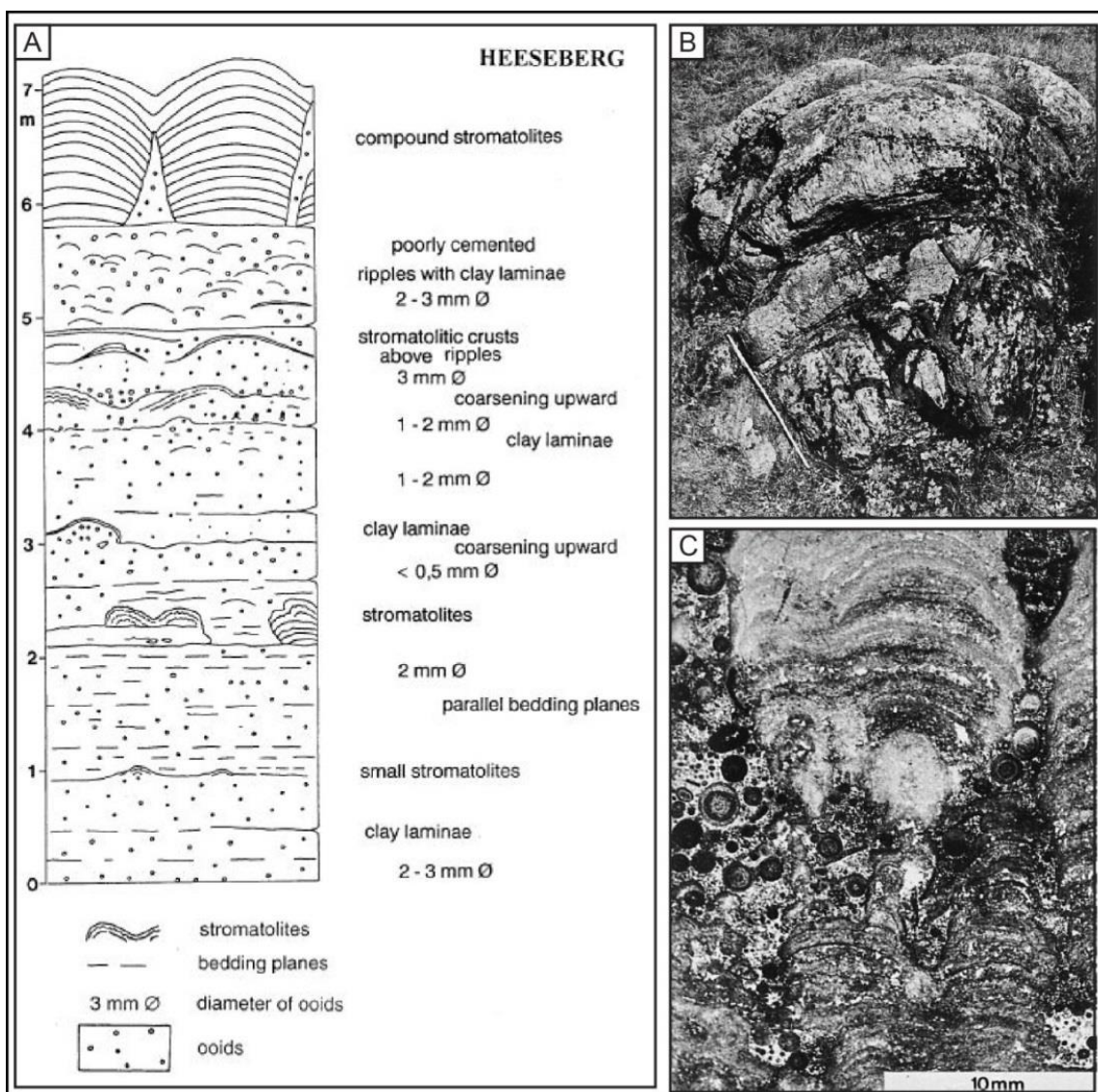


Figura 11. (A) Seção de uma barra de oólitos em um *playa lake*. A aparição e crescimento dos estromatólitos começam com a progressiva estabilização do substrato. (B) Estromatólito de grande porte (escala = 1m). (C) Crescimento de estromatólito entre depósito de oólitos. Raramente os oólitos são incorporados ao estromatólito. Modificado de Paul e Peryt (2000).

Beukes (1987) caracterizou os depósitos estromatolíticos plataformais Proterozóicos (2,3 – 2,6 G.a.) do Subgrupo Campbellrand, Transvaal Supergrupo, sul do continente africano. Uma grande sequência carbonática com aproximadamente 1.500 - 1.700 metros de espessura e litofácies carbonáticas cobrindo a plataforma desde porções distais até proximais.

Os estromatólitos ocorrem como fácies de ambientes rasos plataformais (Figura 12). A borda da plataforma é definida pela presença de estromatólitos colunares, oólitos e arenitos carbonáticos. Em direção ao depocentro da bacia esses depósitos são limitados por recifes de estromatólitos gigantes de submaré formando montes alongados, perpendiculares à margem da plataforma (Figura 12A), que gradam para fácies mais profundas, como carbonatos laminados intercalados com brechas dolomíticas e estromatólitos conófitos. Na laguna são encontrados estromatólitos estratiformes que, em direção ao continente, intercalam-se com estromatólitos dômicos e estratiformes com estruturas de exposição (tepee) e conglomerados, interpretados como ambientes de intermaré e supramaré.

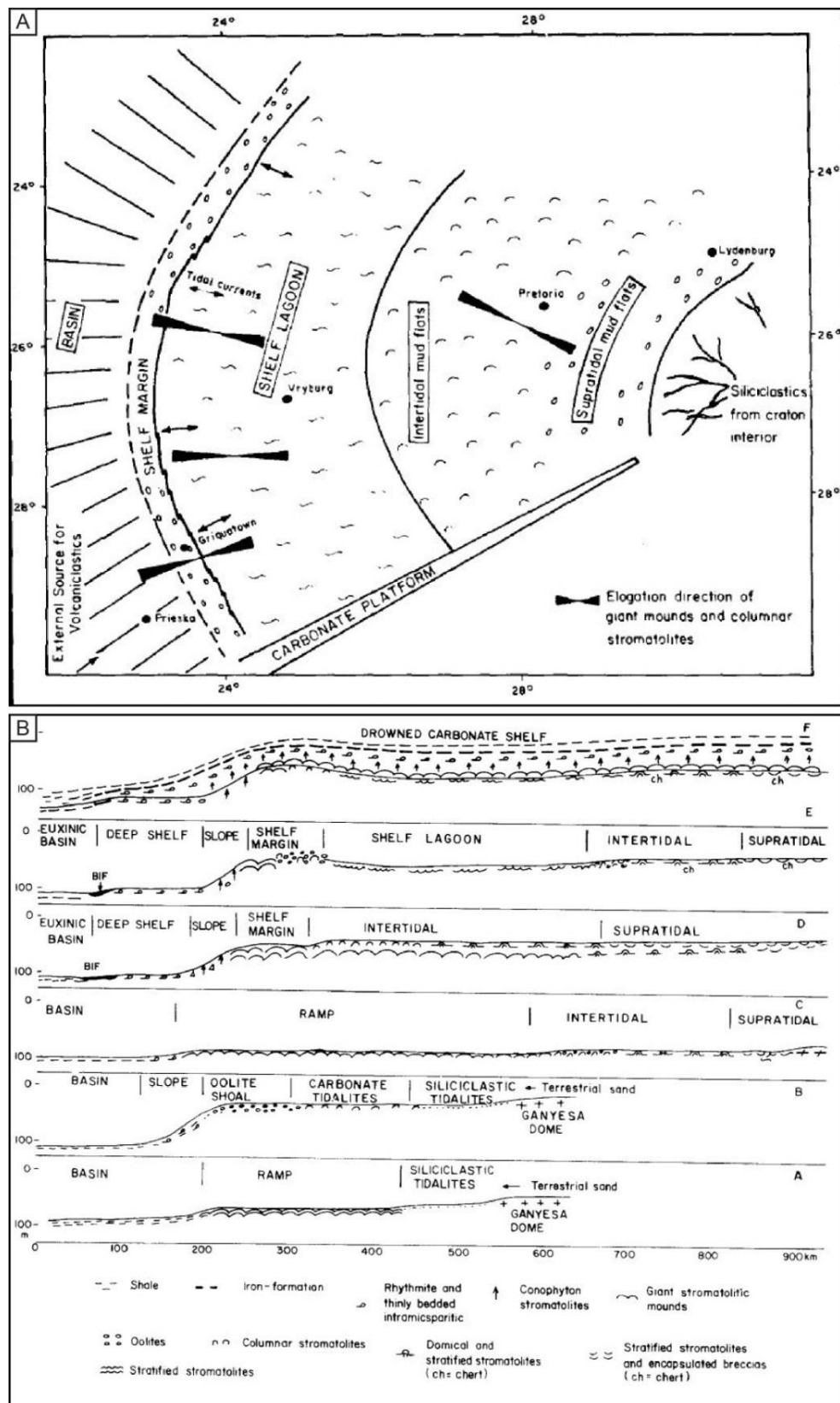


Figura 12. (A) Reconstrução geográfica do período de deposição do Subgrupo Campbellrand. (B) Evolução da sequência carbonática Campbellrand-Malmani. Modificado de Beukes (1987).

Haines (1988) trabalhou com depósitos de plataforma mista carbonática/siliciclástica regressiva dominada por tempestades da Formação Wonoka, Proterozóico superior no Sul da Austrália. Os depósitos apresentam uma grande quantidade de estruturas do tipo hummocky, com tamanhos variados, e outras estruturas sedimentares formadas por ondas.

A Formação Wonoka é dividida em 11 unidades (Figura 13A), sendo a unidade 7 a única em que ocorre deposição estromatolítica (Figura 13B). A unidade 7 apresenta aproximadamente 100 m de espessura e é formada por um padrão de empilhamento dos estratos que caracteriza um grande raseamento para o topo. Domina deposição de lama carbonática e em direção ao topo, arenitos carbonáticos com estruturas geradas por ondas e conglomerados intraclásticos progressivamente vão aparecendo com mais frequência. No topo da seção, na porção mais rasa da unidade (zona fótica), são descritos estromatólitos colunares e dônicos, distribuídos continuamente em um único horizonte, associados a calcarenitos.

Segundo o autor, essa unidade é aparentemente depositada em um ambiente relativamente proximal dominado por tempestade. A boa continuidade lateral e a regularidade nas espessuras das camadas é interpretada como resposta a um ambiente deposicional de baixo gradiente e com subsidência uniforme da bacia.

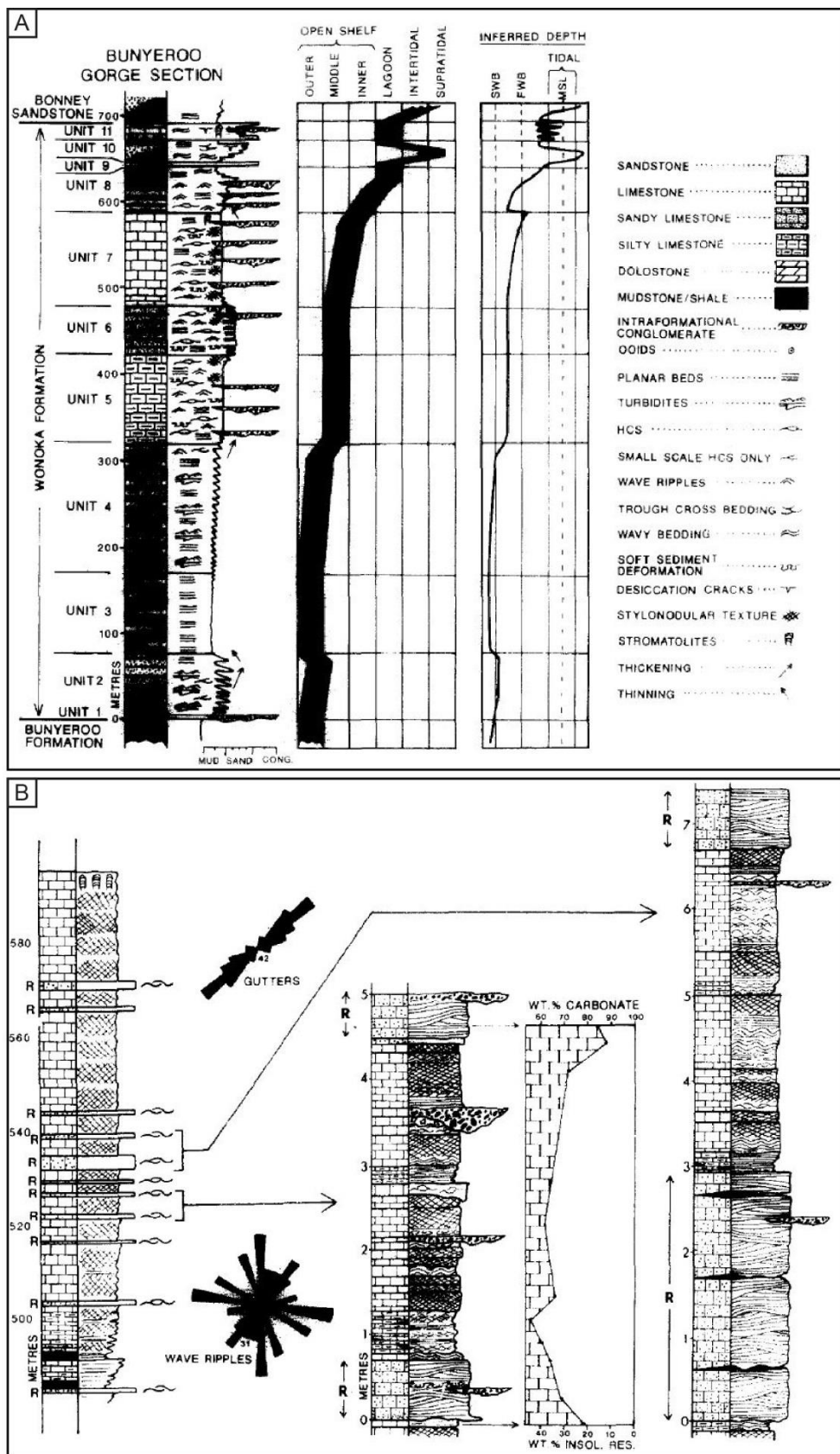


Figura 13. (A) Seção de referência da Formação Wonoka separada em unidades e com a interpretação de ambiente deposicional e profundidade em relação ao nível de ação de ondas normais e de tempestade. (B) Seção e diagrama de roseta representando as

paleocorrentes e o eixo dos gutter casts da Unidade 7. No topo da unidade são encontrados os estromatólitos. Em detalhe estão representados dois ciclos. Modificado de Haines (1988).

Beukes e Lowe (1989) discutem sobre o controle ambiental na morfologia dos estromatólitos do Supergrupo Pongola (3,0 G.a.) na África do Sul. Os dados que foram obtidos indicam uma grande diversidade de estromatólitos relacionados a ambientes rasos em um contexto de canal de maré (Figura 19).

O afloramento estudado apresenta uma boa preservação, sendo possível caracterizar o contexto deposicional e as relações entre estromatólitos de distintas morfologias (Figura 14A). Sendo assim, foram identificadas quatro litofácies: dolarenitos/lamitos com ripples, dolarenitos canalizados, estromatólitos estratiformes e biohermas. A morfologia dos estromatólitos varia de acordo com o ambiente deposicional (Figura 14B). Os estratiformes ocorrem em áreas protegidas intermaré superior, dônicos no intermaré médio, colunar no intermaré inferior e os cônicos em ambientes de alta energia de submaré (canal). Os grandes biohermas (até 1,6 m), compostos por estruturas colunares, se formam nas margens do canal de maré em um ambiente de micromaré.

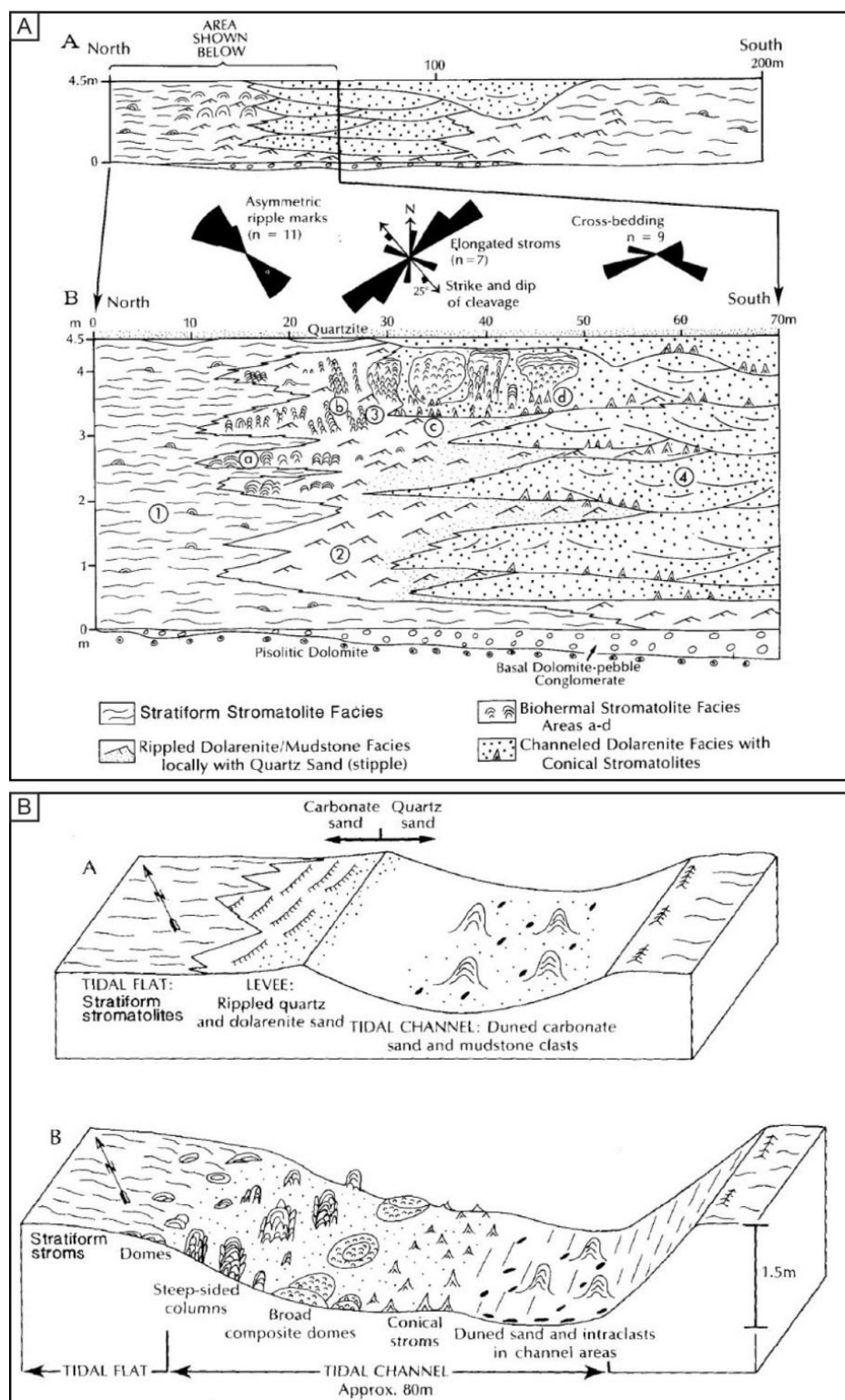


Figura 14. (A) Seção estratigráfica geral da unidade estromatolítica e detalhe de parte do afloramento mostrando a relação entre as litofácies. (B) Reconstrução do ambiente deposicional da porção basal 'A' e superior 'B' da unidade. Modificado de Beukes e Lowe (1989).

Hoffman (1974) caracterizou os estromatólitos plataformais de águas rasas e profundas do Grupo Pathei, Proterozóico inferior (1,795 – 1,872 G.a.), Great Slave Lake, Canadá. O autor separa o grupo em sequência cratônica e bacinal. A cratônica é dividida em fácies rasa e submersa, já a bacinal em fácies de talude e de assoalho. Os estromatólitos apresentam abundância e ampla distribuição ambiental, estendem-se de ambientes proximais de maré até o assoalho da bacia (Figura 15).

Nas porções rasas da plataforma são encontrados estromatólitos heterogêneos colunares e laminados associados com oóides e *grainstones* de intraclastos. Abundância de oóides e intraclastos de *grainstones* associados a estromatólitos assimétricos indica um ambiente de alta energia, no caso a zona de *surf*. A plataforma rasa é limitada por uma quebra de relevo. Nessa borda de plataforma ocorrem cinturões de montes estromatolíticos associados com canais de maré preenchidos com intraclastos de *grainstones* (Figura 15).

Nas partes profundas da plataforma os estromatólitos são colunares, homogêneos e com laminações mal definidas, localmente são encontrados estromatólitos cônicos. A homogeneidade dos depósitos e a relação com as fácies rasa indica um ambiente abaixo do nível de ação de ondas. No talude as fácies são representadas por ritmitos calcáreos e brechas de escorregamento. Enquanto que no assoalho da bacia se depositam lamitos siliciclásticos e estromatólitos calcáreos colunares pobemente laminados intercalados com turbiditos. O contexto de águas profundas para as porções bacinais é confirmado pela interdigitação com brechas de escorregamentos e turbiditos.

Os estromatólitos de profundidade diferem-se dos de águas rasas por sua laminação fracamente marcada e por se desenvolverem em sedimentos siliciclásticos sem oóides e intraclastos de *grainstones* associados. A transição de depósitos rasos para profundos é marcada pelo aparecimento de estromatólitos com laminações cônicas (conófitos).

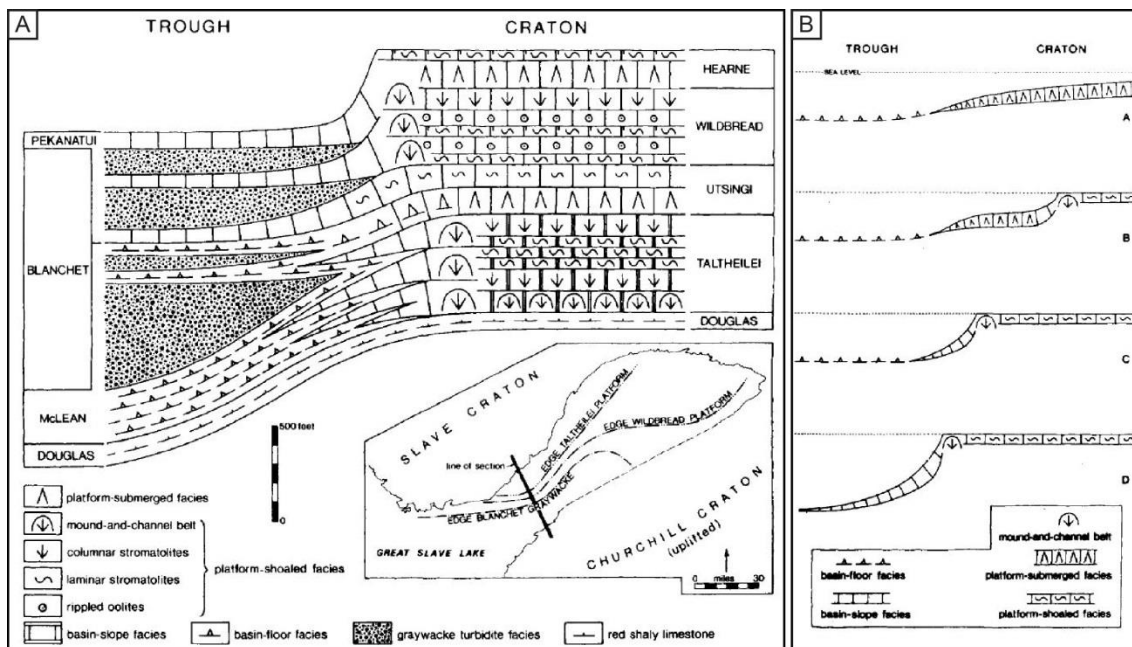


Figura 15. (A) Relação de fácies do Grupo Pethei. (B) Modelos de transição plataforma – bacia. Modificado de Hoffman (1974).

Os recifes de estromatólitos de Strelley Pool Chert, Arqueano da Austrália, são questão de discussões sobre a sua formação biogênica. Porém, Allwood *et al.* (2006) sugerem algumas características que indicariam atividade microbial envolvida na formação desses depósitos: (i) o contexto paleoambiental; (ii) atributos combinados dos estromatólitos; (iii) a distribuição morfológica; (iv) a similaridade com depósitos mais recentes no tempo geológico.

A formação é dividida em quatro membros (M1, M2, M3 e M4), sendo o M2 o mais importante quanto à presença de estromatólitos. Os autores identificaram sete morfotipos de estromatólitos (Figura 16), seis no M2 e um no M3, formados em diferentes estágios e porções de uma plataforma carbonática isolada retrabalhada por maré em um contexto transgressivo. Os estromatólitos estariam restritos espacialmente a porções de águas mais rasas. O início do desenvolvimento das estruturas estromatolíticas está vinculado com o final do influxo de sedimento siliciclástico, enquanto o desaparecimento dos estromatólitos coincide com a retomada da sedimentação siliciclástica, vulcanismo e atividade hidrotermal (M3-M4).

Os ciclos carbonáticos do membro M2 são formados por três raseamentos. Resumidamente, estruturas de maiores amplitudes na base e menores amplitudes no topo, apresentando feições de exposição (brechas, gretas). O primeiro ciclo é formado por laminitos dômicos/incrustações (Fig 16a) que verticalmente dão lugar para pequenas cristas cônicas (Fig 16d). O segundo raseamento reflete uma construção carbonática contínua formada por quatro tipos de estromatólitos. Na base e lateralmente associados, ocorrem laminitos com estruturas em caixa de ovos (Fig 16m), grandes cones complexos (Fig 16j) e cúspedes (Fig 16g) que gradam na vertical para pequenas cristas cônicas (Fig 16d). O terceiro ciclo do M2 é relativamente uniforme, sendo formado por um grande pacote de laminito ondulado (Fig 16p) de inframaré com brechas no topo.

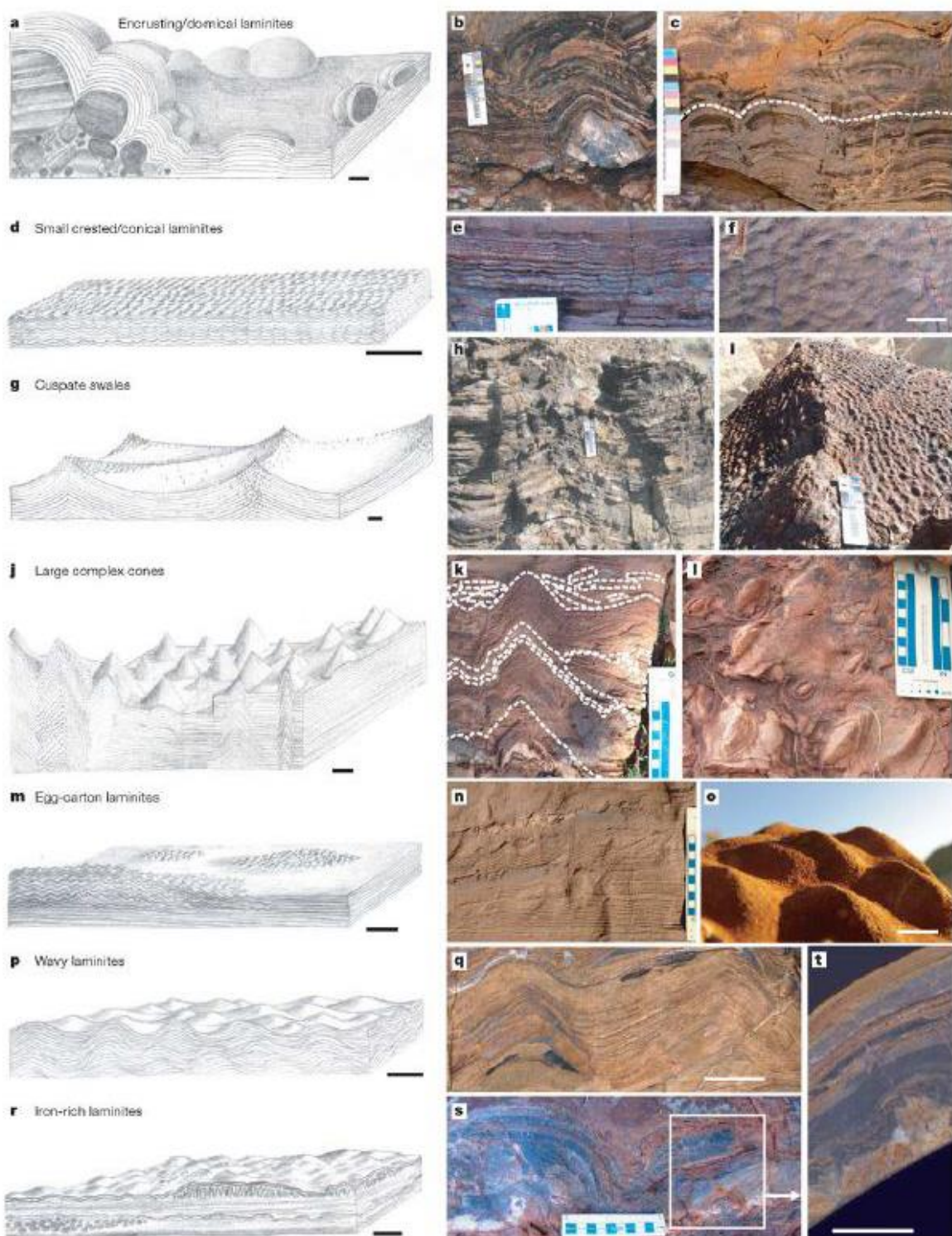


Figura 16. Fácies estromatolíticas de Strelley Pool Chert, com a reconstrução 3-D e fotografias de afloramento. Escalas: b, h – 18 cm; c, e, k, l, n, s – 1 cm cada incremento; blocos diagramas – 5 cm. Retirado de Allwood et al. (2006).

Labaj e Pratt (2016) detalharam a dinâmica deposicional de um sistema misto carbonático/siliciclástico do Cambriano superior da Formação Abrigo, Sudoeste do Arizona, EUA. Esses depósitos são o registro de um ambiente marinho raso dominado por ondas normais e de tempestade (*wave ripples, hummocky, gutter casts*; Figura 17). As associações de fácies presentes são de *offshore* (inferior, superior e transição) e *shoreface* (inferior, intermediário e superior), e essas associações se empilham verticalmente em função das variações do nível relativo do mar.

No geral, a Formação Abrigo é dominada por sedimentos siliciclásticos finos durante o trato de sistema transgressivo, a sedimentação carbonática domina durante a parte intermediária e final do trato de nível alto que termina com progradação dos arenitos de *shoreface*. A estratigrafia revela que carbonatos se depositam em duas porções distintas desse sistema: na transição do *offshore/shoreface*, e no *offshore* distal (Figura 17A). Porém, os estromatólitos só ocorrem na transição *offshore/shoreface* (Figura 17B), associados com lamitos carbonáticos e *wackestones*.

Os depósitos microbiais formam domos de 3 a 4 cm de diâmetro, lateralmente ligados e localmente formam montes de até 10 cm de espessura. A existência dessas estruturas está vinculada a períodos de “tempo bom”, gerando breves períodos de estabilidade do substrato, baixa taxa de sedimentação e pouco sedimento em suspensão (argila e silte).

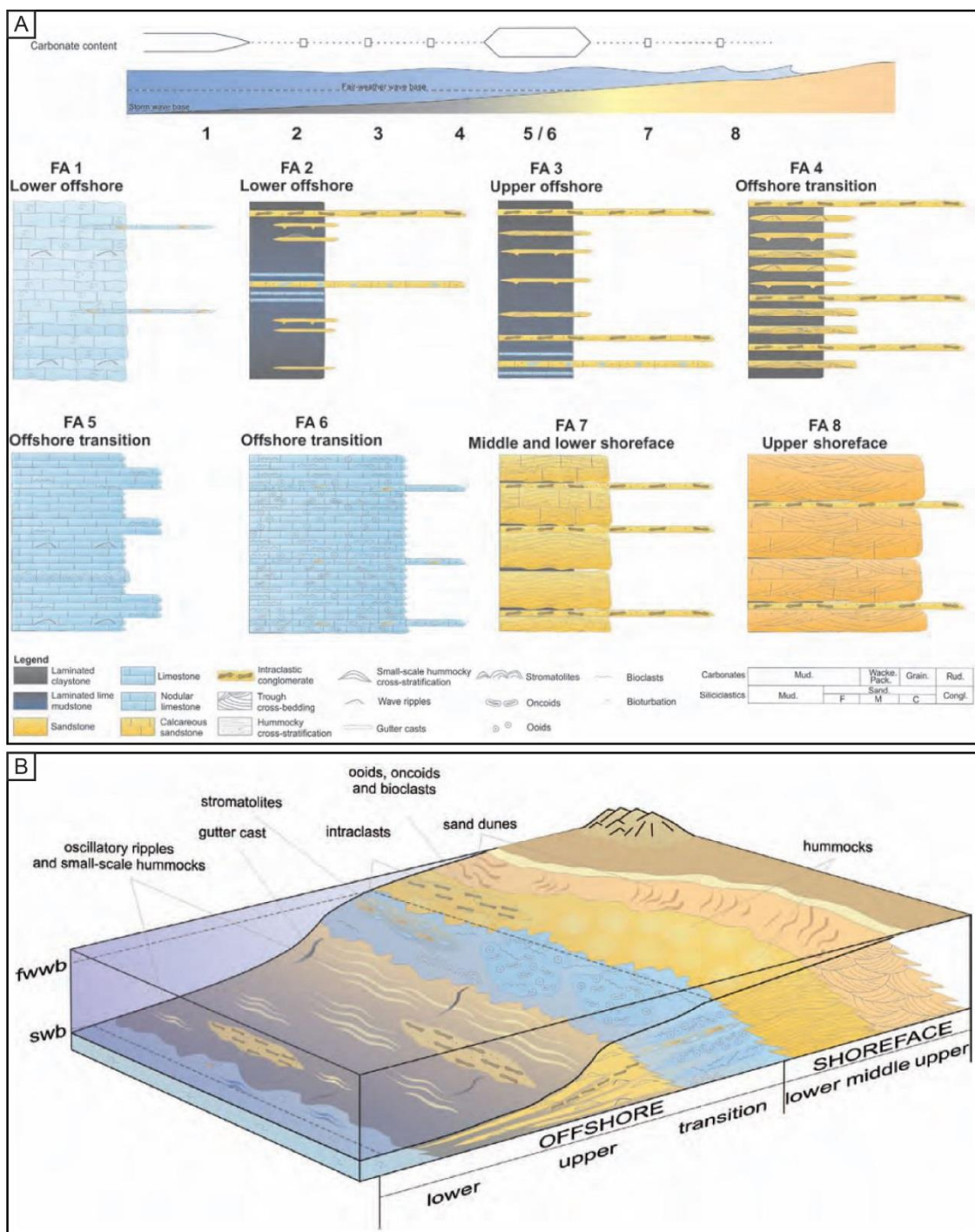


Figura 17. (A) Diagrama ilustrativo idealizado mostrando a distribuição de associações de fácies com relação ao perfil batimétrico. (B) Modelo de fácies para o sistema misto carbonático-siliciclástico mostrando os principais contextos deposicionais da Formação Abrigo. Modificado de Labaj e Pratt (2016).

3.5 Estromatólitos no Proterozóico

Estromatólitos abrangem um grande período da história geológica da terra, tendo seu primeiro registro datado de ~3.45 Ga em depósitos região de Pilbara, oeste da Austrália (Riding, 2011). Atingiram seu ápice durante o Proterozóico, entre 2.8 e 1.0 Ga, sendo esse período reconhecido tanto pela quantidade quanto pela diversidade de morfotipos desses depósitos organosedimentares (Figura 18), que ocorriam em uma ampla diversidade de ambientes. Esse período de acme é possivelmente relacionado à evolução das cianobactérias e ao progressivo desenvolvimento de crátions continentais (Riding, 1991).

No final do Proterozóico/início do Cambriano ocorreu um rápido declínio dessas estruturas. Fischer (1965) sugere que o declínio está relacionado com a redução na saturação de carbonato e pela competição com os eucariontes (Figura 18). Segundo Grotzinger (1990), o principal agente causador da diminuição da quantidade de estromatólitos foi a redução na concentração de carbonato. O autor chega a essa conclusão devido ao fato de existirem evidências desse declínio antes da aparição de organismos mais complexos.

Os diferentes tipos de microfábricas podem ser relacionados com diferentes períodos do tempo geológico (Awramik e Riding, 1988; Riding, 2011; Frantz *et al.*, 2015). Na figura 18 é possível notar a distribuição e diferenças entre as microfábricas que formavam estromatólitos antigos e atuais. A causa dessas diferenças não é bem compreendida, porém registros sugerem essa distribuição ao longo do tempo.

Os primeiros estromatólitos, de idade Arqueana, são formados por microfábrica de crosta cristalina. Durante o Proterozóico aparecem estruturas formadas por grãos finos de micrita e bem laminadas, podendo ser interdigitadas com crostas cristalinas (estromatólitos híbridos). A partir do final do Proterozóico dominam estromatólitos de granulometria fina. Fábrica de grãos grossos só começou a ser incorporados às colônias no final do Fanerozóico, sendo mais comuns do Mioceno até o recente. Esse processo de aprisionamento de grãos grossos, formando laminationes mal desenvolvidas, pode ser relacionado à presença de microrganismos mais evoluídos que não existiam nos primórdios da história da Terra (Gebelein, 1969; Awramik e Riding, 1988; Riding, 1991; Riding, 2011).

Além da microfábrica, existem morfologias típicas, não exclusivas, do Proterozóico. Sendo que, uma notável característica dos estromatólitos do Proterozóico é a grande ocorrência de morfologias colunares ramificadas e estromatólitos cônicos. Estruturas essas não estão presentes em grande quantidade no Arqueano e no Fanerozóico (Riding, 1991; Awramik; 1991). Sendo assim, características micro e macro podem ser utilizadas na identificação estratigráfica dos estromatólitos.

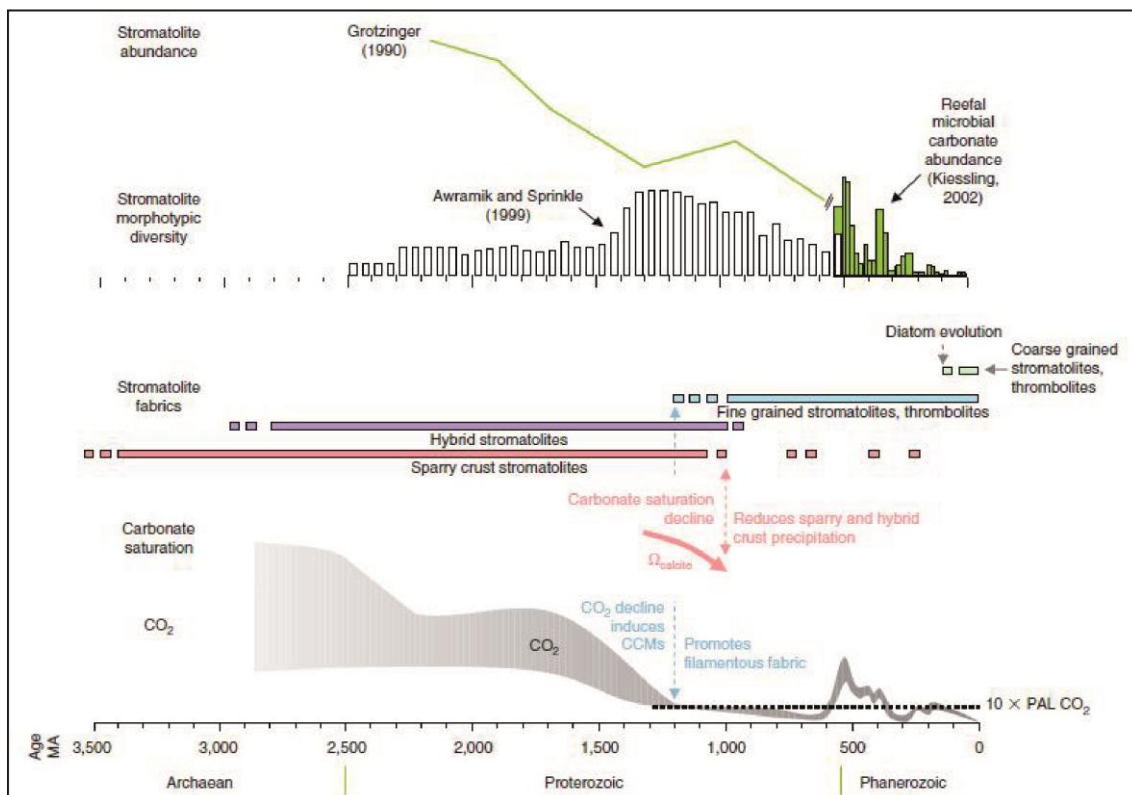


Figura 18. Tendências e possíveis controles sobre o desenvolvimento dos microbiais carbonáticos ao longo do tempo geológico. Esse gráfico mostra um longo período de queda (~1.000 Ma) na abundância de estromatólitos (Grotzinger, 1990) e o auge na diversidade morfológica durante o Mesoproterozóico (Awramik e Sprinkle, 1999). A redução de crosta cristalina (*sparry crust*) e estromatólitos híbridos (*hybrid stromatolites*) pode estar vinculada ao declínio da saturação de carbonato nos oceanos (Grotzinger, 1990). As esporádicas ocorrências de crosta cristalina durante o Fanerozóico estão associadas à bacias evaporíticas (Pope et. al, 2000). CCMs – Mecanismos de Concentração de CO₂. PAL – Nível Atmosférico Atual (Present Atmospheric Level). Níveis de CO₂ do Proterozóico inferidos com base em Sheldon (2006), Kah and Riding (2007), Hyde et al., (2000) e Ridgwell et al., (2003). Níveis de CO₂ do Fanerozóico inferidos com base em Berner e Kothavala (2001, Figura 13). Estromatólitos aglutinadores de grãos grossos e trombolitos no Neógeno podem em parte refletir a incorporação de diatomáceas a esteira microbial e pelos baixos valores de saturação de carbonato nos oceanos. Figura retirada de Riding (2011).

4 DADOS E MÉTODOS

Essa tese foi desenvolvida através de dados coletados de aproximadamente 367 m de perfis colunares de afloramentos. O artigo 1 foi elaborado com base nos 47 m da seção da Gruta do Cristal, afloramento chave da Formação Caboclo que foi descrito em escala 1:20. Para o detalhamento dos estromatólitos do artigo 2 foram analisadas duas seções compostas, paralelas entre si, em escala 1:50. Aproximadamente 150 m de perfil sedimentológico foi levantado no Rio Preto e 170 m no Rio Ventura.

O detalhamento sedimentológico seguiu o método clássico de análise de fácies (Walker, 1992), em que as fácies são reconhecidas com base na sua textura, estrutura sedimentar, geometria do set e continuidade lateral. Fácies geneticamente relacionadas são agrupadas em associações de fácies, representando sub ambientes de um sistema deposicional (Dalrymple, 2010). A descrição dos estromatólitos foi feita em macro, meso e microescala (Hofmann, 1973; Awramik, 1991). Para a descrição em campo foi utilizada a tabela de estruturas estromatolíticas proposta por Preiss (1976). As fácies foram codificadas com base no tamanho de grão (letras maiúsculas; *i.e.*, *sand* 'S', *gravel* 'G') e estruturas sedimentares (letras minúsculas; *i.e.*, *massive* 'm', *low angle* 'l', *wave ripple* 'w'), conforme o modelo proposto por Miall (1996). Para codificar os estromatólitos foi utilizado 'ST', seguido de 'b' para biohermas e 'h' para horizontalmente laminados. O código de fácies foi utilizado apenas no artigo 1.

As lâminas delgadas foram impregnadas com resina epoxy azul, para salientar a porosidade, e tingidas com Alizarina vermelha S e Ferricianeto de Potássio para facilitar a distinção dos carbonatos (Dickson, 1965). A análise petrográfica foi realizada utilizando um microscópio Zeiss AXIO Imager 2 e as fotomicrografias foram obtidas através do programa ZEN 2012. A composição modal dos arenitos foi mensurada qualitativamente através de gráficos de comparação visual e as porcentagens plotadas em um diagrama, seguindo os conceitos de Zuffa (1980), com a intenção de definir quais as amostras são siliciclásticas, híbridas ou carbonáticas. As amostras carbonáticas foram classificadas de acordo com Dunham (1962) e Embry and Klovan (1971).

5 CONTEXTO GEOLÓGICO

A Formação Caboclo (Mesoproterozóico – Steniano), parte do Supergrupo Espinhaço, aflora na região centro-norte do Cráton do São Francisco. Está inserida no domínio morfotectônico do Aulacógeno do Paramirim, na região da Chapada Diamantina (Almeida, 1977).

5.1 Cráton do São Francisco

Durante o Arqueano e o Paleoproterozóico o Cráton do São Francisco juntamente com o Cráton do Congo formavam uma grande massa continental inserida no Supercontinente Rodínia (Brito Neves et al., 1999; Campos Neto, 2000). Esses dois crátons se separaram durante o Mesozóico, ocasionando a abertura do Oceano Atlântico.

O Cráton do São Francisco (Figura 19) é constituído por um núcleo estabilizado no final do Ciclo Transamazônico, sendo ele delimitado por cinturões orogênicos ativos durante o Ciclo Brasiliano (Proterozóico Superior). Na porção sul o limite é marcado pela faixa Brasília, a noroeste pela faixa Rio Preto, a norte pelas faixas Sergipana e Riacho do Pontal e a sudeste pela faixa Araçuaí. O extremo leste do cráton coincide com a margem passiva. O embasamento do Cráton do São Francisco, também conhecido como Pré-Espinhaço, é formado por rochas metamórficas de médio a alto grau e granitoides arqueanos e paleoproterozóicos com coberturas proterozóicas e fanerozóicas.

São reconhecidos dois grandes domínios morfotectônicos para o Cráton do São Francisco, separados pelo Corredor do Paramirim (Schobbenhaus, 1996; Cruz e Alkmim, 2006): Bacia do São Francisco, feição alongada N-S ocupando a porção oeste do cráton, e o Aulacógeno do Paramirim, instalado na região nordeste (Figura 19). Apesar de apresentarem uma separação física, as duas feições apresentam preenchimentos metassedimentares Pré-cambrianos e Fanerozóicos semelhantes.

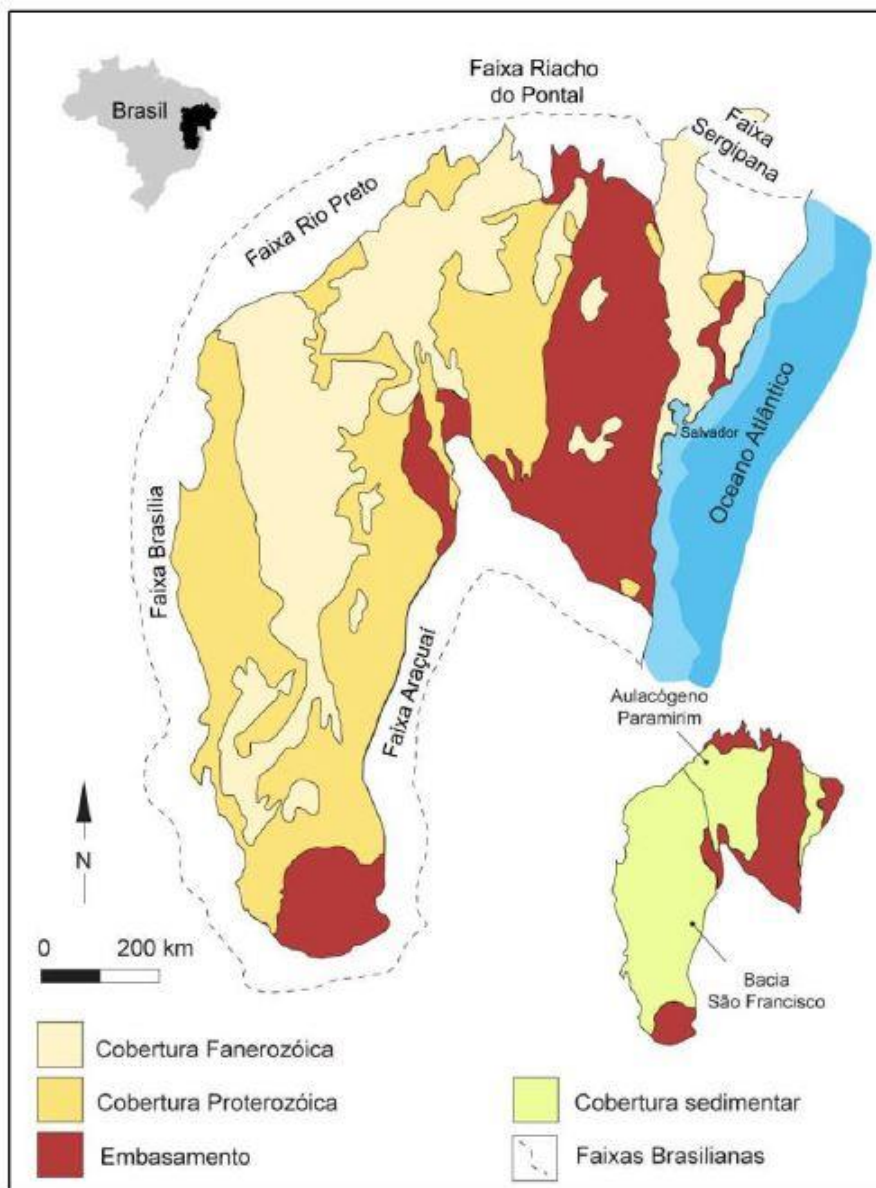


Figura 19. Mapa geológico do Cráton do São Francisco e seus domínios morfotectônicos: Bacia do São Francisco e Aulacógeno do Paramirim (Modificado de Alkmim *et al.*, 1993)

5.2 Supergrupo Espinhaço

É dividido em três domínios: Serra do Espinhaço Meridional, Serra do Espinhaço Setentrional e Chapada Diamantina, cada domínio com nomenclaturas diferentes para suas unidades (Figura 20). As serras do Espinhaço Meridional e Setentrional posicionam-se a oeste do Corredor do Paramirim e as rochas apresentam um grau de metamorfismo e deformação maior que a leste do corredor, onde localiza-se o domínio Chapada Diamantina. No Domínio Chapada Diamantina o Supergrupo Espinhaço é segmentado em três grupos: Rio dos Remédios,

Paraguaçu e Chapada Diamantina (Pedreira, 1988; Dominguez, 1996). Guadagnin *et al.* (2015) subdivide o Supergrupo Espinhaço em três sequências de primeira ordem relacionadas a eventos tectônicos formadores de bacias: inferior (LE), médio (ME) e superior (UE) (Figura 20).

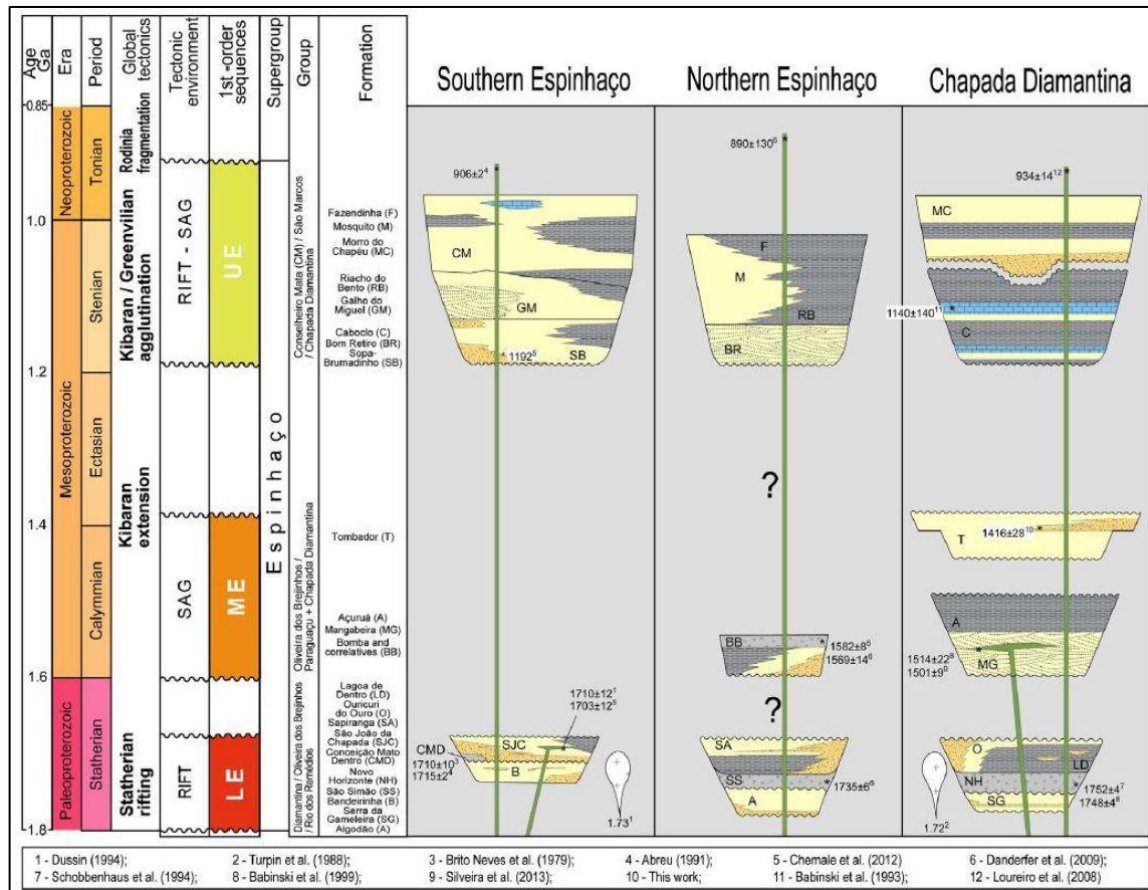


Figura 20. Correlação regional do Supergrupo Espinhaço (Espinhaço Sul, Espinhaço Norte e Chapada Diamantina), indicando características gerais como os eventos e ambientes tectônicos relacionados, sequências deposicionais e datações realizadas por diversos pesquisadores ao longo do supergrupo. Retirado de Guadagnin *et al.*, (2015).

O Grupo Rio dos Remédios compõe a Sequência Inferior (LE; 1.8 – 1.68 Ga). Ocorre em um contexto rifte, sendo formada por depósitos fluviais e eólicos da Fm. Serra da Gameleira, vulcânicos ácidos alcalinos da Fm. Novo Horizonte, sistemas lacustres da Fm. Lagoa de Dentro e aluviais da Fm. Ouricuri do Ouro.

A Sequência Média (ME; 1.6 – 1.4 Ga) corresponde a um evento rifte no Domínio Espinhaço Norte e uma bacia sag na Chapada Diamantina. No Domínio Chapada Diamantina essa sequência compreende o Grupo Paraguaçu (Fm.

Mangabeira e Açuá) e a Fm. Tombador (Grupo Chapada Diamantina). É preenchida na base por sistemas aluviais/fluviais e eólicos da Fm. Mangabeira que são sobrepostos por depósitos transgressivos marinhos rasos e deltaicos da Fm. Açuá. Sobre o Grupo Paraguaçu, em discordância angular, deposita-se a Fm. Tombador como uma nova fase sag.

A Sequência Superior (UE; 1.19 – 0.9 Ga) se formou em um ambiente tectônico rifte-sag. Na Chapada Diamantina, essa fase tectônica é representada pelos depósitos marinhos rasos da Fm. Caboclo e Morro do chapéu. Essa sequência marinha é interpretada como transgressiva e em paraconformidade com a Fm. Tombador (Sequência Média).

5.3 Formação Caboclo

Foi primeiramente definida por Branner (1910) na Serra do Tombador ao descrever uma série denominada *Jacuipe Flints* na base e rochas argilosas, definidas como Folhelho Caboclo, sobre o Arenito Tombador.

Segundo Guimarães e Pedreira (1990), são depósitos marinhos rasos, caracterizados como uma plataforma de idade Mesoproterozóica (1.140 ± 140 Ma - Babinski et al., 1993) com sedimentação siliciclástica e carbonática e dominada por tempestades. Sedimentologicamente é composta principalmente por pelitos e arenitos, subordinadamente ocorrem conglomerados e depósitos carbonáticos biogênicos. Os arenitos são finos a médios bem selecionados, apresentam estratificações de baixo ângulo ou plano-paralelas com marcas onduladas no topo e base com estruturas de carga. Os pelitos são laminados e formam camadas lateralmente contínuas. Os conglomerados são formados por clastos na ordem de 1 cm e apresentam estruturas cruzadas tabulares. Os carbonatos ocorrem na base da formação como calcários silicificados, *Jacuípe flints* de Branner (1910), e no topo são descritos biostromas compostos por estromatólitos colunares. A seção da figura 21, feita por Guimarães e Pedreira (1990) e retirada do trabalho de Doutorado de Pedreira (1994), localiza-se a norte da BR-242, nordeste de Lençóis (BA), e representa a coluna estratigráfica da Formação Caboclo nessa área.

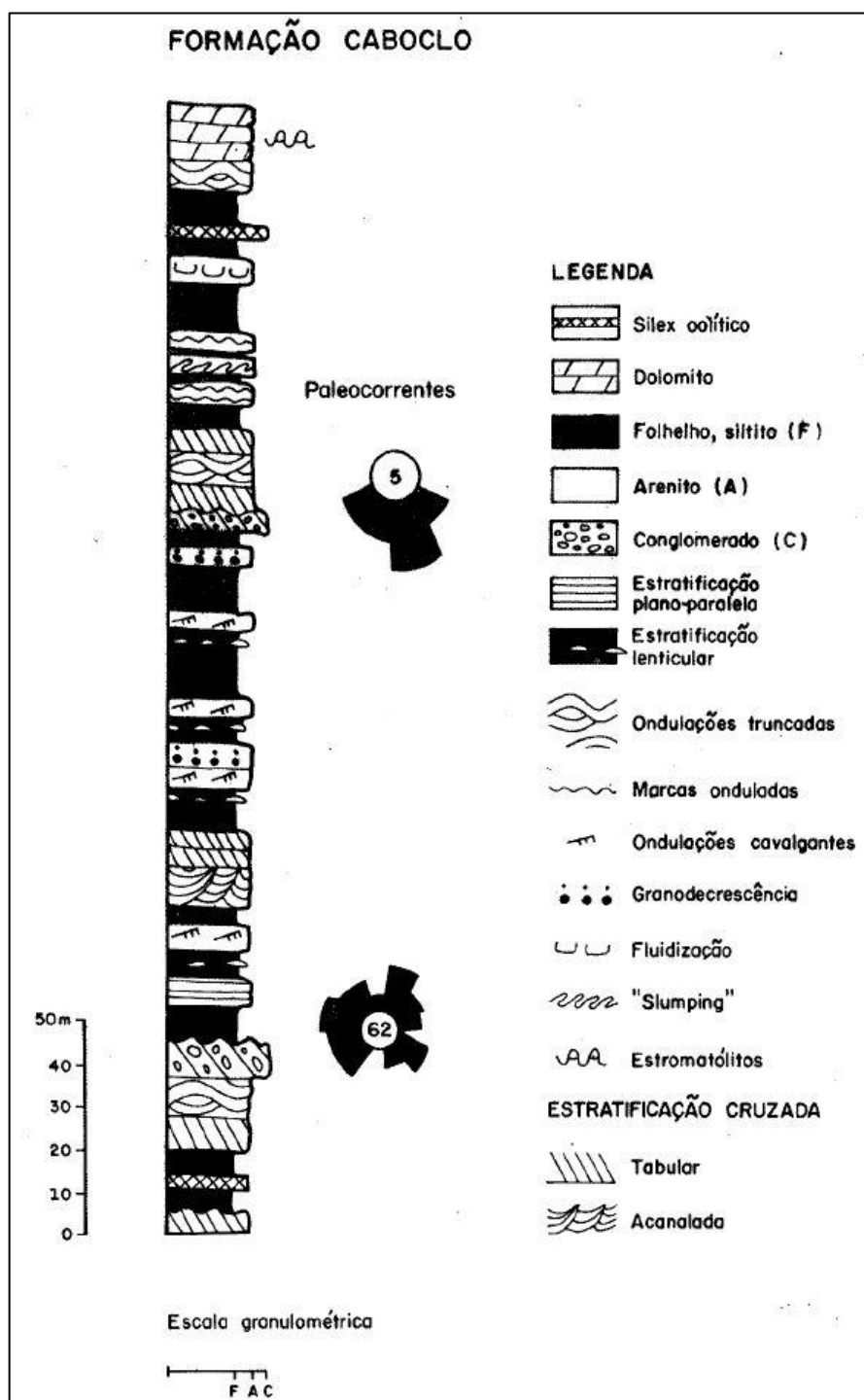


Figura 21. Coluna estratigráfica composta da Formação Caboclo. Modificado de Guimarães e Pedreira (1990), retirada de Pedreira (1994).

6 RESUMO DOS RESULTADOS E DISCUSSÕES

A presente tese focou em dois intervalos estratigráficos da Formação Caboclo. O artigo 1 foca no sistema híbrido carbonático-siliciclástico que compõem a base do intervalo estratigráfico estudado. Através da análise faciológica dos 47 m da Gruta do Cristal, foram reconhecidas 11 litofácies representadas por três composições diferentes: (i) estromatólitos; (ii) arenitos híbridos; (iii) conglomerados híbridos intraformacionais e *rudstones*. A mistura composicional de sedimentos ocorre em todos os grupos litológicos, com pequenas variações na razão carbonáticos/siliciclásticos. Litofácies geneticamente relacionadas foram agrupadas três associações de litofácies, representando diferentes regimes hidrodinâmicos associados ao nível de ação de ondas: (i) *offshore*; (ii) *offshore transition*; (iii) *shoreface*. O conjunto de associações de fácie permite a interpretação de uma rampa mista carbonática-siliciclástica dominada por tempestades, com ampla colonização microbial desde porções rasas a relativamente profundas (abaixo do nível de ação de ondas de tempestade). No *offshore* as esteiras microbiais dominavam o substrato e cobriam longas distâncias com pouca ou nenhuma interferência de correntes. No *offshore transition* as correntes induzidas por tempestades rompiam as esteiras microbianas e moldavam biohermas. Enquanto que no *shoreface* a alta e constante energia das ondas limitava a formação de estromatólitos, restringindo as ocorrências a camadas pouco espessas de esteiras microbiais ou intraclastos. A grande quantidade e distribuição microbial surge em resposta a dois fatores interconectados: (i) ausência de sedimento lamoso; (ii) ausência de predadores. A homogeneidade composicional dos sedimentos é resultado da ampla distribuição e regularidade no aporte de sedimento siliciclástico e a constante formação de aloquímicos ao longo da acumulação sedimentar, associados a correntes constantes de ondas normais e tempestades que permitiam o transporte e mistura desses sedimentos.

O artigo 2 detalha os estromatólitos da porção superior da Formação Caboclo, tendo como base dois perfis compostos (Rio Ventura e Rio Preto). Essas seções consistem predominantemente em pelitos e arenitos acumulados em uma rampa siliciclástica dominada por ondas de tempestades, com intervalos restritos em se desenvolvem estromatólitos siliciclásticos. Nesses intervalos os estromatólitos estão vinculados a duas associações de litofácies distintas: (i) *shoreface* e (ii) *offshore*

transition. Os estromatólitos de *shoreface* são caracterizados pela fábrica siltica e arenosa e laminação mal desenvolvida, enquanto no *offshore transition* os estromatólitos apresentam laminação bem desenvolvida formada pela alternância entre lâminas argilosas e lâminas silticas. De acordo com a morfologia e características composticionais da fábrica os estromatólitos siliciclásticos, foram separados em três tipos distintos, sendo dois de *shoreface* (dômicos rico em ferro e domos arenosos) e um de *offshore transition* (biohermas e biostromas). Em todos os casos são reconhecidas feições que indicam assinatura biológica, tanto em macroescala quanto em microescala. Dois processos foram os responsáveis para a preservação desses estromatólitos: (i) piritização e (ii) litificação por precipitação bioinduzida de carbonatos. As características sedimentológicas indicam um ambiente favorável para o trapeamento e aprisionamento de grãos siliciclásticos por colônias microbiais, marcado por agitação constante e disponibilidade de sedimento siliciclásticos. O ambiente marinho, devido a abundância e diversidade de íons, é favorável para o desenvolvimento de EPS com boa adesividade. Somado a essas características, a idade da Formação Caboclo (1.140 ± 140 Ma) coincide com uma grande queda nas concentrações de CO₂ atmosférico, que é refletida no grau de saturação de CaCO₃ dissolvido nos oceanos. Essa mudança química inibiria a calcificação/litificação muito precoce dessas esteira microbiais, permitindo o trapeamento de grãos.

7 CONCLUSÕES

Esse trabalho detalhou dois intervalos específicos e independentes da Formação Caboclo em que foram identificadas características importantes que ainda não haviam sido discutidas. Essas peculiaridades são importantes não só para o contexto regional, mas também para o entendimento dos controles ambientais e sedimentológicos no desenvolvimento e distribuição dos estromatólitos no Proterozóico.

Comparando os dois intervalos é possível concluir:

- Os dois modelos são distintos quanto a composição sedimentar. Um misto siliciclástico-carbonático, com ampla colonização microbial na base da formação (artigo 1 – Gruta do Cristal), e outro siliciclástico no topo (artigo 2 – Rio Preto e Rio Ventura).
- A composição sedimentar é diferente nos dois intervalos, mas o ambiente deposicional é o mesmo: uma rampa dominada por ondas normais e de tempestade.

Quanto ao intervalo basal da Formação Caboclo (artigo 1), pode-se concluir:

- Todas as litofácies descritas na Gruta do Cristal apresentam mistura de sedimentos em escala composicional. Essa homogeneidade ocorre em todas as regiões da rampa (escala espacial) e não se modificava com as movimentações da linha de costa (escala temporal).
- O aporte siliciclástico não inibia a precipitação carbonática. O suprimento terrígeno e a precipitação carbonática ocorriam simultaneamente ou quase simultaneamente.
- A morfologia dos estromatólitos presentes em cada associação de litofácies é controladas por parâmetros físicos relacionados aos níveis de ação de ondas normais e de tempestades. No *offshore* as esteiras microbiais se espalhavam lateralmente por longas distâncias, formando espessos pacotes de estromatólitos horizontalmente laminados que, por vezes, embrionavam pequenos domos. Em porções de *offshore transition* a morfologia dos biohermas era moldada pelas correntes induzidas pelas ondas. Por sua vez, a alta energia de ondas no *shoreface* inibia a formação de estromatólitos,

restringindo as ocorrências a carpetes microbiais pouco espessos ou *lags* intraclásticos.

- A ausência de lama deixava a coluna d'água com baixa turbidez e consequentemente alta luminosidade, gerando condições ideais para a colonização do substrato por organismos microbiais até em porções relativamente profundas do sistema. Além do mais, a ausência de predadores permitia que os carpetes microbiais se instalassem indiscriminadamente ao longo da rampa sem que tivessem competição.

A respeito da porção superior da Formação Caboclo (artigo 2), é possível concluir:

- É uma rampa dominada por ondas de tempestade, de composição siliciclástica, com desenvolvimento ocasional de estromatólitos aglutinadores de partículas siliciclásticas no *shoreface* e no *offshore transition*.
- De acordo com a morfologia e a composição da fábrica, os estromatólitos de *shoreface* podem ser separados em dois tipos: (i) estromatólitos dômicos ricos em ferro e (ii) montes arenosos. Os estromatólitos de *offshore transition* ocorrem como biohermas e biostromes compostos internamente por pequenas colunas e domos.
- Os processos que permitiram a preservação desses estromatólitos foram a piritização e a precipitação bioinduzida de carbonatos.
- Estruturas indicando assinatura microbial podem ser identificadas tanto na macro quanto na microescala.
- As características sedimentológicas, hidrodinâmicas e químicas do ambiente, associadas a queda abrupta da saturação de CaCO₃ dissolvido nos oceanos durante o Mesoproterozóico, formaram um ambiente propício para o desenvolvimento de esteiras microbiais capazes de aglutinar sedimentos siliciclásticos.

8 REFERÊNCIAS BIBLIOGRÁFICAS

- Alkmim, F.F., Brito-Neves, B.B., Alves, J.A.C., 1993. Arcabouço tectônico do Cráton do São Francisco – uma revisão. In: Dominguez, J.M.L., Misi, A. (Eds.), O Cráton do São Francisco, SBG, SGM, CNPq, Salvador, pp. 45-62.
- Allwood, A.C., Walter, M.R., Kamber, B.S., Marshall, C.P., Burch, I.W., 2006. Stromatolite reef from the early Archean era of Australia. *Nature*, 441, 714-718.
- Almeida, F.F.M., 1977. O Cráton do São Francisco. *Revista Brasileira de Geociências*, 7, 349-364.
- Andres, M.S., Reid, R.P., 2006. Growth morphologies of modern marine stromatolites: A case study from Highborne Cay, Bahamas. *Sedimentary Geology*, 185, 319-328.
- Awramik, S.M., Margulis, L., 1974. *Stromatolite Newsletter*, 2, 5.
- Awramik, S.M., Riding, R., 1988. Role of algal eukaryotes in subtidal columnar stromatolite formation. *Proc. Natl. Acad. Sci. USA*, 85, 1327-1329.
- Awramik, S.M., 1991. Archean and Proterozoic stromatolites. In: Riding, R. (Ed.) *Calcareous Algae and Stromatolites*, Springer-Verlag, Berlin, pp. 289-304.
- Awramik, S. M., Sprinkle, J., 1999. Proterozoic stromatolites: the first marine evolutionary biota. *Historical Biology*, 13, 241–253.
- Babinski, M., Van Schums, W.R., Chemale Jr., F., Brito-Neves, B.B., Rocha, A.J.D., 1993. Idade isocrônica Pb/Pb em rochas carbonáticas da Formação Caboclo, em Morro do Chapéu, BA. In: Simpósio do Cráton do São Francisco, Salvador. Anais...Salvador, 160-163.
- Berner, R. A., Kothavala, Z., 2001. GEOCARB III. A revised model of atmospheric CO₂ over Phanerozoic time. *American Journal of Science*, 301, 182-204.
- Beukes, N.J., 1987. Facies relations, depositional environments and diagenesis in a major early Proterozoic stromatolitic carbonate platform to basinal sequence, Campbellrand Subgroup, Transvaal Supergroup, Southern Africa. *Sedimentary Geology*, 54, 1-46.

- Beukes, N.J., Lowe, D.R., 1989. Environmental control on diverse stromatolite morphologies in the 3000 Myr Pongolo Supergroup, South Africa. *Sedimentology*, 36, 383-397.
- Branner, J.C., 1910. The Tombador Escarpment in the State of Bahia, Brazil. *American Journal of Science*, 335-343.
- Brito-Neves, B.B., Campos Neto, M.C., Fuck, R.A., 1999. From Rodinia to Western Gondwana: na approach to the Brasiliano-Pan African cycle and orogenic collage. *Episodes*, 22, 155-166.
- Burne, R.V., Moore, L.S., 1987. Microbialites: organosedimentary deposits of benthic microbial communities. *Palaios*, 2, 241-254.
- Campos Neto, M.C., 2000. Orogenic systems from southwester Gondwana. In: Cordani, U.G., Milani, E.J Thomaz Filho, A., Campos, D.A. (Eds.) *Tectonic Evolution of South America*, 31th International Geological Congress, Rio de Janeiro, Brasil, 335-365.
- Cruz, S.C.P, Alkmim, F.F., 2006. The tectonic interaction between the Paramirim Aulacogen and the Araçuaí Belt, São Francisco craton region, Eastern Brazil. *Anais da Academia Brasileira de Ciências*, 78, 151-610.
- Dickson, J.A.D., 1965. A modified staining technique for carbonates in thin section. *Nature* 205, 587.
- Dalrymple, M., 2010. Interpreting sedimentary successions: facies, facies analysis and facies models. In: James, N.P., Dalrymple, R.W. (Eds.), *Facies models 4*, Geological Association of Canada. St. John's, Newfoundland, GEO text 6, pp. 3-18.
- Dominguez, J.M.L., 1996. As coberturas plataformais do Proterozóico Médio e Superior. In: Barbosa, J.S.F., Dominguez, J.M.L. (coords.) *Geologia da Bahia: texto explicativo para o mapa geológico ao milionésimo*. Salvador: Secretaria da Indústria, Comércio e Mineração/Superintendência de Geologia e Recursos Minerais, 400 pp.

- Dunham, R.J., 1962. Classification of carbonate rocks according to depositional texture. In: Ham, W.E. (Ed.), *Classification of Carbonate Rocks*. American Association of Petroleum Geologists Memoir 1, pp. 108-121.
- Embry, A.F., Klovan, J.E., 1971. A Late Devonian reef tract on Northeastern Banks Island, NWT. *Canadian Petroleum Geology Bulletin* 19, 730-781.
- Fischer, A.G., 1965. Fossils, early life, and atmospheric history. *Proceedings of the National Academy of Sciences*, 53, 1205-1215.
- Frantz, C.M., Petryshyn, V.A., Corsetti, F.A., 2015. Grain trapping by filamentous cyanobacterial and algal mats: implications for stromatolite microfabrics through time *Geobiology*, 13 (5), 409-423
- Gebelein, C.D., 1969. Distribution, morphology, and accretion rate of recent subtidal algal stromatolites, Bermuda. *J. Sedim. Petrol.*, 39, 49-69.
- Ginsburg, R.N., 1991. Controversies about stromatolites: vices and virtues. In: Müller, D.W., McKenzie, J.A., Weissert, H. (Eds.), *Controversies in Modern Geology*. Academic Press, London, pp. 25-36.
- Grotzinger, J.P., 1990. Geochemical model for Proterozoic stromatolite decline. *American Journal of Science*, 290-A, 80-103.
- Grotzinger, J.P., Rothman, D.R., 1996. An abiotic model for stromatolite morphogenesis. *Nature*, 383, 423-425.
- Grotzinger, J.P., Knoll, A.H., 1999. Stromatolites in Precambrian carbonates: evolutionary mileposts or environmental dipsticks? *Annu. Rev. Earth Planet. Sci.*, 27, 313-358.
- Guadagnin, F., Chemale, Jr.F., Magalhães, A.J.C., Santana, A., Dussin, I., Takehara, L., 2015. Age constrains on crystal-tuff from the Espinhaço Supergroup – Insight into the Paleoproterozoic to Mesoproterozoic intracratonic basin cycles of the Congo-São Francisco Craton *Gondwana Research*, 27, 363-376.
- Guimarães, J.T., Pedreira, A.J., 1990, Programa de Levantamentos Geológicos Básicos do Brasil – PLGB. Utinga – Folha SD.24-V-A-II, Estado da Bahia, Escala 1:100.000. Texto explicativo. Brasília: DNPM.

- Haines, P.W., 1988. Storm-dominated mixed carbonate/siliciclastic shelf sequence displaying cycles of hummocky cross-stratification, late Proterozoic Wonoka Formation, South Australia. *Sedimentary Geology*, 58, 237-254.
- Hofmann, H. J., 1973. Stromatolites: characteristics and utility. *Earth-Science Reviews*, 9, 339-373.
- Hoffman, P., 1974. Shallow an deepwater stromatolites in lower Proterozoic platform – to – basin facies change, Great Slave Lake, Canada. *The American Association of Petroleum Geologists Bulletin*, 58(5), 856-867.
- Hyde, W. T., Crowley, T. J., Baum, S. K., Peltier, W. R., 2000. Neoproterozoic ‘snowball Earth’ simulations with a coupled climate/ice-sheet model. *Nature*, 405, 425-429.
- Kah, L. C., Riding, R., 2007. Mesoproterozoic carbon dioxide levels inferred from calcified cyanobacteria. *Geology*, 35, 799-802.
- Kalkowsky, E., 1908. Oolith und Stromatolith im norddeutschen Buntsandstein. *Z. Deutsch. Geol. Gesellschaft*, 60, 68–125. pls 4-11.
- Knoll, A.H., Semikhatov, M.A., 1998. The genesis and time distribution of two distinctive Proterozoic stromatolite microstructures. *Palaios* 13, 408-422.
- Labaj, M.A., Pratt, B.R., 2016. Depositional dynamics in a mix carbonate-siliciclastic system: middle-upper Cambrian Abrigo Formation, Southeaster Arizona, U.S.A. *Journal of Sedimentary Research*, 86, 11-37.
- Logan, B.W., 1961. Cryptozoon and associate stromatolites from the Recent, Shark Bay, Western Australia. *The Journal of Geology* 69, 517-533.
- Logan, B.W., Rezak, R., Ginsburg, R.N., 1964. Classification and environmental significance of algal stromatolites. *The Journal of Geology*, 72, 68-83.
- Miall, A.D., 1996. *The Geology of Fluvial Deposits: Sedimentary Facies, Basin Analysis and Ptroleum Geology*, Springer, Heidelberg, 582 pp.
- Paul, J., Peryt, T.M., 2000. Kalkowsky’s stromatolites revisited (Lower Triassic Buntsandstein, Harz Mountains, Germany). *Palaeogeography, Palaeoclimatology, Palaeoecology*, 161, 435-458.

- Pedreira, A.J., 1988. Sequências deposicionais no Precambriano: exemplo da Chapada Diamantina Oriental. In: Congresso Brasileiro de Geologia, Goiânia. Anais do ... Belém, SBG, 2, p. 648-659.
- Pedreira, A.J., 1994. O Supergrupo Espinhaço na Chapada Diamantina Centro-Oriental, Bahia: Sedimentação, Estratigrafia e Tectônica. Tese de Doutorado, Instituto de Geociências, Universidade de São Paulo, Brasil.
- Pope, M. C., Grotzinger, J. P., Schreiber, B. C., 2000. Evaporitic subtidal stromatolites produced by *in situ* precipitation: textures, facies associations, and temporal significance. *Journal of Sedimentary Research*, 70, 1139-1151.
- Pratt, B.R., 1982. Stromatolite decline – A reconsideration. *Geology* 10, 512-515.
- Preiss, W.V., 1976. Basic field and laboratory methods for the study of stromatolites. In: *Stromatolites* (ed. M. R. Walter), *Developments in Sedimentology*, Elsevier, Amsterdam, 20, pp. 5-13.
- Reid, R.P., Visscher, P.T., Decho, A.W., Stolz, J.F., Bebout, B.M., Dupraz, C., Macintyre, I.G., Paerl, H.W., Pinckney, J.L., Prufert-Bebout, L., Steppe, T.F., DesMarais, D.J., 2000. The role of microbes in accretion, lamination and early lithification of modern marine stromatolites. *Nature* 406, 989-992.
- Ridgwell, A. J., Kennedy, M. J., Caldeira, K., 2003. Carbonate deposition, climate stability, and Neoproterozoic ice ages. *Science*, 302, 859-862.
- Riding, R., 1991. Classification of microbial carbonates. In: Riding, R. (Ed.), *Calcareous Algae and Stromatolites*, Springer-Verlag, Berlin, pp. 21-51.
- Riding, R., 1999. The term stromatolite: towards an essential definition. *Lethaia*, 32, 321-330.
- Riding, R., 2000. Microbial carbonates: the geological record of calcified bacterial-algal mats and biofilms. *Sedimentology*, 47, 179-214.
- Riding, R., 2008. Abiogenic, microbial and hybrid authigenic carbonate crusts: components of Precambrian stromatolites. *Geologija Croatica*, 61, 73-103.

- Riding, R., 2011. Microbialites, stromatolites, and thrombolites. In: Reitner, J., Thiel, V. (Eds.), Encyclopedia of Geobiology. In: Encyclopedia of Earth Science Series. Springer, Heidelberg, pp.635-654.
- Rocha, A.J., Pereira, C.P., Srivastava, N.K., 1992. Carbonatos da Formação Caboclo (Proterozoico médio) na região de Morro do Chapéu - Estado da Bahia. Revista Brasileira de Geociências 22, 389-398.
- Schobbenhaus, C., 1996. As tafrogêneses superpostas Espinhaço e Santo Onofre, Estado da Bahia. Revisão e novas propostas. Revista Brasileira de Geociências 4, 265-276.
- Semikhatov, M.A., Gebelein, C.D., Cloud, P., Awramik, S.M., Beninore, W.C., 1979. Strontiatolite morphogenesis – progress and problems. Canadian Journal of Earth Sciences 16, 992-1015.
- Schobbenhaus, C., 1996. As tafrogêneses superpostas Espinhaço e Santo Onofre, estado da Bahia: revisão e novas propostas. Revista Brasileira de Geociências, 4, 265-276.
- Sheldon, N. D., 2006. Precambrian paleosols and atmospheric CO₂levels. Precambrian Research, 147, 148-155.
- Srivastava, N.K., 1988. Estromatólitos da Formação Caboclo na Região de Morro do Chapéu: relatório de consultoria I. Salvador: CPRM.
- Trompette, R., 1982. Upper Proterozoic (1800–570 Ma) stratigraphy: a survey of lithostratigraphic, paleontological, radiochronological and magnetic correlations. Precambrian Res. 18, 27-52.
- Walker, R.G., 1992. Facies, facies models and modern stratigraphic concepts. In: Walker, R.G., James, N.P. (Eds). Facies models: response to sea-level change. Geological Association of Canada, 409 pp.
- Walter, M.R., 1976. Introduction. In: Stromatolites (ed. M.R. Walter), Developments in Sedimentology, Elsevier, Amsterdam, 20, pp.1-3.
- Walter, M.R., 1977. Interpreting stromatolites. American Scientist, 65, 563-571.

Zuffa, G.G., 1980. Hybrid arenites; their composition and classification. *Journal of Sedimentary Research* 50, 21-29.

9 ARTIGOS

9.1 ARTIGO 1 - Mixed carbonate-siliciclastic sedimentation in a Mesoproterozoic storm-dominated ramp: depositional processes and stromatolite development.

João Pedro Formolo Ferronatto¹, Claiton Marlon dos Santos Scherer¹, Gabriel Barbosa Drago¹, Amanda Goulart Rodrigues¹, Ezequiel Galvão de Souza², Adriano Domingos dos Reis¹, Manoela Bettarel Bállico³, Carrel Kifumbi¹, Caroline Lessio Cazarin⁴

¹Instituto de Geociências, Universidade Federal do Rio Grande do Sul, Campus do Vale, Av. Bento Gonçalves, 9500; 91509-900, Porto Alegre/RS, Brazil.

²Universidade Federal do Pampa (Unipampa), Campus Caçapava do Sul. Av. Pedro Anunciação, 111 - Vila Batista, 96570-000, Caçapava do Sul/RS, Brazil.

³Departamento de Geociências, Universidade Federal de Santa Catarina, Campus Universitário, 88040-900, Florianópolis/SC, Brazil.

⁴CENPES – Petróleo Brasileiro S.A. (PETROBRAS), 21941-915, Rio de Janeiro/RJ, Brazil.

ABSTRACT

Records of shallow-marine ramps with the mixing of carbonate and siliciclastic sediments are common throughout the geological time. All these records have pure carbonate and pure siliciclastic deposits as end members, occurring contemporaneously in distinct depositional regions along the ramp, and transitional hybrid facies between them. The two end member can mix in different scales and can alternate in time due to climatic changes and regressions and transgressions. This work presents a detailed reconstruction of a Mesoproterozoic storm-dominated mixed carbonate-siliciclastic ramp composed of hybrid sediments and without the presence of pure siliciclastic or carbonate deposits, a rare example in the geological record. Based on a high resolution logged section (in 1:20 scale) and qualitative thin sections, eleven lithofacies were identified and grouped into three lithofacies associations (offshore, offshore transition and shoreface), which are stacked vertically forming a transgressive-regressive cycle. This faciological distribution indicates a low relief ramp with wide microbial colonization from shallow to relatively deep waters (below storm-wave base level). In offshore low-energy distal areas, microbial mats spread laterally over large distances with little or no interference from currents, while in the offshore transition the morphology of the bioherms is shaped by currents induced by waves. In turn, the high wave energy in the shoreface inhibits the formation of stromatolites, restricting their occurrence to thin layers of microbial carpets or intraclastic lags. The mixing occurs in compositional scale and is relatively homogeneous along the whole logged interval, independent of the shifts in lithofacies or lithofacies associations. This compositional homogeneity is linked to the wide distribution and regularity in the input of siliciclastic sediments during the sedimentary accumulation. Strong currents induced by storms allow the transport and mixing of siliciclastic sediments with carbonate grains generated in the basin during fair-weather periods.

Keywords: Proterozoic; Caboclo Formation; Sediment mixing; Hybrid sediments; Precambrian stromatolites

1. INTRODUCTION

Mixed carbonate-siliciclastic shallow-marine systems are quite common throughout the geological history. These environments display variable mixing and resultant heterogeneity of different scales (stratigraphic, stratic and compositional - Mount, 1984; Chiarella et al., 2017). The reported examples cover several ages (e.g., Neoproterozoic – Haines, 1988; Saylor, 2003; Dibenedeto and Grotzinger, 2005; Paleozoic – Barnaby and Ward, 2007; Gomez and Astini, 2015; Labaj and Pratt, 2016; Mesozoic – Spalletti et al., 2000; Sanders and Höfling, 2000; Schwarz et al., 2016; Cenozoic – Tucker, 2003; Scheibner et al., 2003; Thrana and Talbot, 2006). The major characteristic shared with all the examples is represented by the presence of pure carbonate and pure siliciclastic end member deposits occurring contemporaneously in distinct depositional environments of the ramp, and the hybrid sedimentation (Zuffa, 1980) dominating in a transitional zone between the two end members (Schwarz et al., 2018). The sedimentary composition of the mixed system is intimately associated to the processes responsible for carbonate production (skeletal and non-skeletal) and the source area of siliciclastic input in the basin. The mixture depends on the hydrodynamic processes acting on the coast and how the sediments are distributed.

The microbialites are common in Proterozoic successions. Their distribution and spatial evolution are influenced by detrital input and the depositional settings. Although several studies have illustrated the widespread occurrence of stromatolites (Logan et al., 1964; Walter, 1977; Awramik and Riding, 1988; Riding, 1991, 2000; Frantz et al., 2015), few studies demonstrate how the influx of different sediments (i.e., siliciclastic or carbonate) and sedimentary process related to normal and/or storm waves control the morphology, distribution and preservation of stromatolites in Proterozoic mixed carbonate-siliciclastic ramp (Hoffman, 1974; Beukes, 1987; Haines, 1988; Saylor, 2003).

This study focuses on a portion of the Caboclo Formation, Mesoproterozoic of Chapada Diamantina, Brazil. Based on a high-resolution section (logged in 1:20 scale), and on the qualitative thin section, a mixed carbonate-siliciclastic system with a wide distribution of stromatolites was possibly classified via petrographic analysis. The mixing occurs in compositional scale and is relatively homogeneous along the whole logged interval, independent of the shifts in lithofacies or lithofacies

associations. This makes the Caboclo Formation a rather unique example in the geological record, since, in most cases, the degree of mixing of carbonate and siliciclastic grains is usually considered to vary laterally within the same depositional context (Schwarz et al., 2018).

This paper provide a detailed reconstruction of a Mesoproterozoic mixed carbonate-siliciclastic storm-dominated ramp composed entirely of hybrid sediments. The specific goals include (i) to define the different processes controlling the ramp morphology and the stromatolite distribution; (ii) to classify the relationship between the distribution of carbonate and siliciclastic grains and the process of mixing; (iii) to construct a depositional model.

2. GEOLOGICAL SETTING

The Mesoproterozoic Stenian Caboclo Formation, part of Espinhaço Supergroup, crops out in central-northern region of São Francisco Craton, in physiographic region of Chapada Diamantina Domain on Paramirim Aulacogen (Fig. 1A). During Arquean and Paleoproterozoic, São Francisco Craton and Congo Craton belonged to the Rodinia Supercontinent (Brito Neves et al 1999; Campos Neto, 2000). The Espinhaço Supergroup was deposited after the amalgamation of these two cratons at 1.8 Ga and before partial break-up at 0.9 Ga, and is interpreted as being formed in intracontinental rift-sag basins (Brito Neves et al., 1979; Chemale et al., 1993; Martins-Neto, 2000; Alkmim and Martins-Neto, 2012; Guadagnin et al., 2015). During the Neoproterozoic Brasiliano event, the basin suffered a partial inversion, leading to the development of a series of NNW-trending folds and thrust faults (Marshak and Alkmim, 1989; Cruz and Alkmim, 2006).

According to Chemale et al. (2012) and Guadagnin et al. (2015), the Espinhaço Supergroup is divided into three 1st-order megasequences, i.e., Lower, Middle and Upper Espinhaço (Fig. 1A). Of these, the Upper Espinhaço (1.19 to 0.9 Ga) consists of the Caboclo Formation and Morro do Chapéu Formation at Chapada Diamantina domain. The Caboclo Formation, unconformably overlain by the Morro do Chapéu Formation, is paraconformably underlain by alluvial/aeolian deposits of Tombador Formation (Middle Espinhaço megasequence). Thus, the Caboclo and Morro do Chapéu formations are distinct 2nd-order sequences nested in the Upper 1st-order megasequence (Guadagnin et al., 2015).

The Mesoproterozoic Caboclo Formation was interpreted as a mixed siliciclastic-carbonate storm-dominated ramp (Branner, 1910; Pedreira, 1994) situated at low latitude (Pesonen et al., 2012; Pisarevsky et al., 2014). This formation consists mainly of siliciclastic (mudstones and sandstones) and carbonate to siliciclastic-carbonate deposits named as Jacuipe Flint by Branner (1910) and classified as the carbonate interval of Caboclo Formation by various authors (e.g., Srivastava, 1988; Rocha et al., 1992; Babinski et al., 1993; Souza et al., 2021). Depositional age of Caboclo Formation carbonates was dated by radiometric Pb-Pb method at 1140 ± 140 Ma (Babinski et al., 1993).

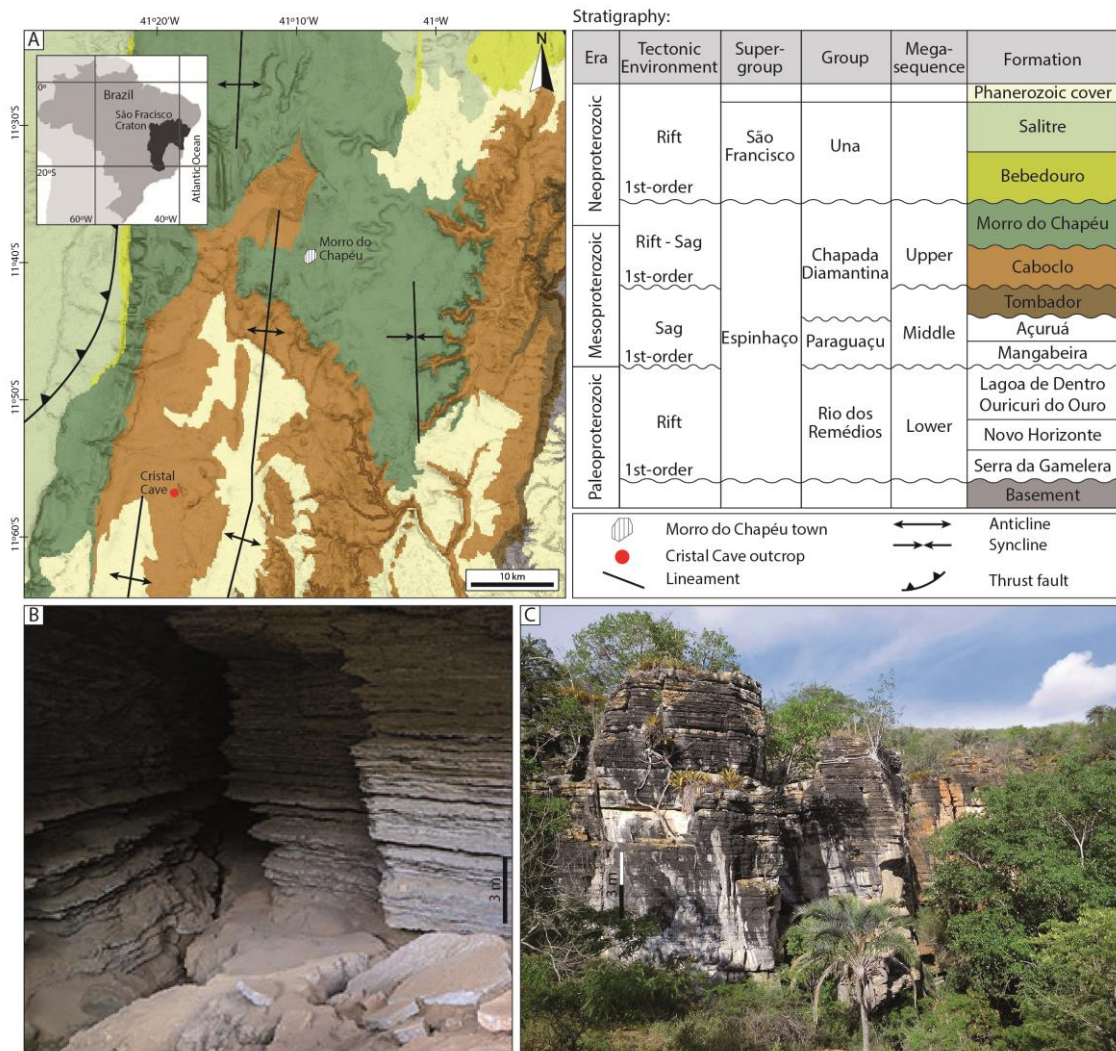


Fig. 1. (A) Simplified geological map based on data from Brazilian Geological Survey (CPRM/CBPM, 2003) and key chart with the stratigraphy of Chapada Diamantina modified from Guadagnin et al. (2015). The map shows the location of Morro do Chapéu town and Cristal Cave outcrop. The inset shows location of São Francisco Craton in Brazil (in black). (B) Inside the cave. The lower portion of the outcrop. (C)

Scarp where the upper portion of the outcrop was logged. In B and C it's possible to observe the tabular geometry of the sedimentary packages.

3. STUDY AREA AND METHODS

The Cristal Cave section is one key natural outcrop that was analyzed in detail in this paper, in which the Caboclo Formation presents an excellent exposure. The section is located approximately 30 km SW from Morro do Chapéu city in a region with many dolines and caves (Fig. 1A). The lower half of the outcrop is inside the cave and the upper half is a scarp on the surface (Fig 1B and C). A 47 m thick sedimentological log (Fig. 2) was measured and described bed-by-bed at 1:20 scale. The lithofacies were identified via the classical methods of facies analysis (Walker and James, 1992), according to their texture, sedimentary structures, set geometry and lateral transitions. The lithofacies code was based on grain-size (capital letters; i.e., sand 'S', gravel 'G') and sedimentary structures (small letters; i.e., massive 'm', low angle 'l', wave ripples 'w'), following the scheme proposed by Miall (1996). To code the stromatolites was used 'ST', followed by 'b' if they are bioherms or 'h' if they are horizontally laminated. Genetically related lithofacies are grouped into lithofacies associations (or belts) that represent sub-environments of a depositional system.

Sixteen thin sections were prepared from representative samples of the lithofacies associations in order to characterize the main features (sedimentary structure, texture, fabric, primary and diagenetic composition) (Fig. 2). In exception, the sampling of conglomerates not represent the heterogeneous composition observed in the entire layer. Since they present normal grading that command the grain size and composition variations. The thin sections were impregnated with blue dyed epoxy and stained with a solution of Alizarin Red S and potassium ferricyanide to distinguish the carbonate species (Dickson, 1965). Qualitative petrography analysis was performed using a Zeiss AXIO Imager 2 microscope and the photomicrographs were taken using the ZEN 2012 program. The modal composition of arenites was qualitatively measured with comparative visual charts and was plotted in a first order diagram following the concepts of Zuffa (1980) to define which samples are siliciclastic, hybrid or carbonates. The carbonate samples were classified according to Dunham (1962) and Embry and Klovan (1971).

Stromatolites analysis was made in macro-, meso and micro-scale (Hofmann, 1973; Awramik, 1991). Field description was based on chart of stromatolites structures proposed by Preiss (1976). Petrological descriptions were applied to define a detailed genetic classification for stromatolites and thrombolites (Riding, 2011).

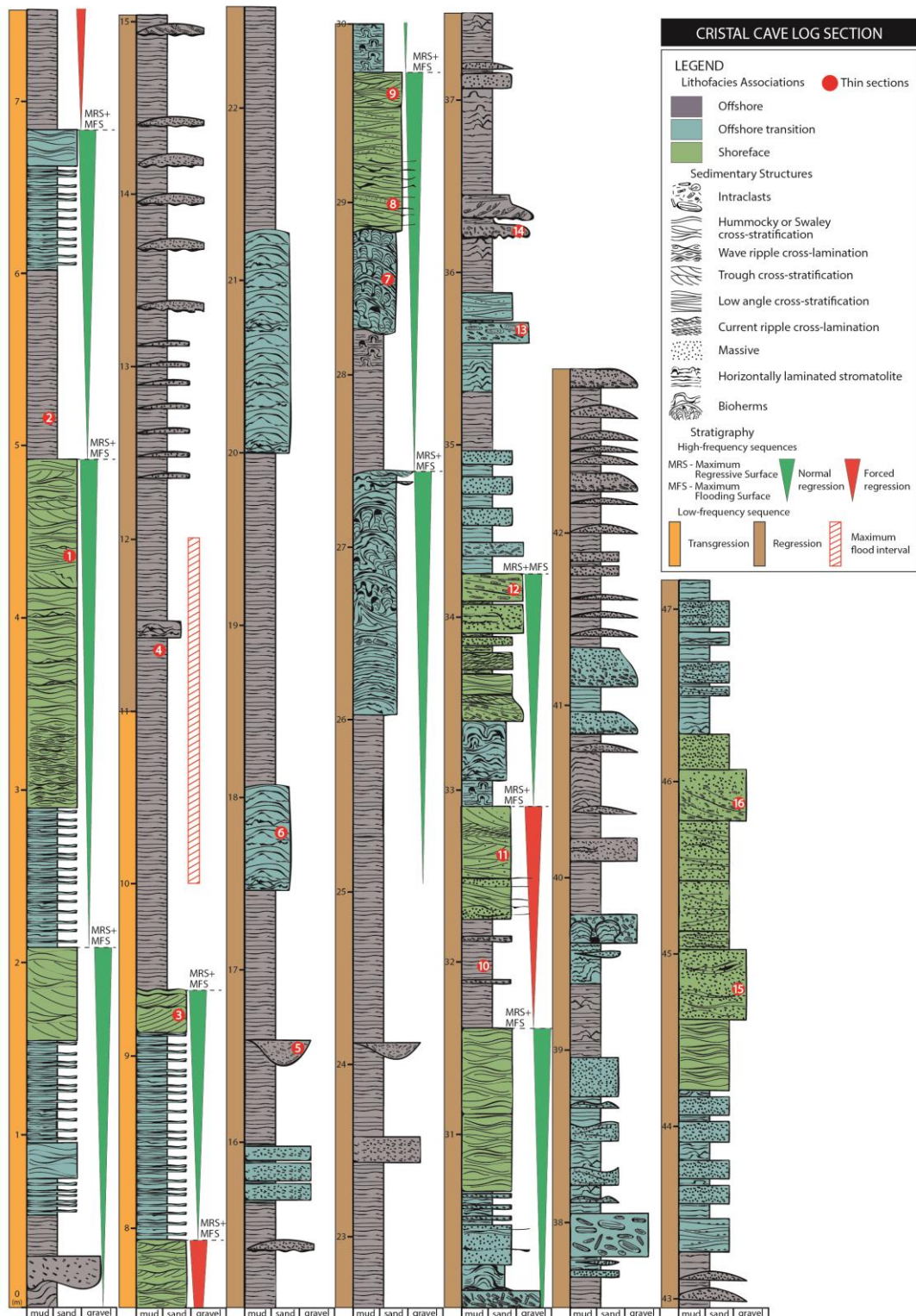


Fig. 2. Cristal Cave log section with stratigraphic interpretation. The base interval of the section represents the transgressive systems tract (TST), followed by a long regressive systems tract (RST), separated by a maximum flood interval.

4. LITHOFACIES

Eleven lithofacies were recognized for the studied interval (Table 1; Figs. 3 and 4). The carbonate-siliciclastic compositions of the lithofacies were determined by qualitative petrographic descriptions. Compositional mixing is present in all lithological groups, with slightly variable siliciclastic/carbonate concentrations. Siliciclastic grains occur as: (i) nuclei for oolites; (ii) particles trapped by microorganisms; (iii) free in the rock fabric; (iv) constituent of intraclasts (Fig. 3). The lithofacies are represented by three different compositions: (i) stromatolites; (ii) hybrid arenites; (iii) intraformational hybrid conglomerates and rudstones. The main petrographic characteristics of each lithology are detailed below.

4.1. Stromatolites

The stromatolites are represented by two lithofacies: bioherms (STb) and horizontally laminated stromatolites (STh) (non-columnar stromatolites sensu Preiss, 1976). They both have carbonate-siliciclastic compositions and similar textures in optical microscopy, being better distinguished by macroscopical morphology, as can be seen in the lithofacies description (Table 1).

The horizontally laminated stromatolites (Fig. 3A and B) are formed by millimetric to centimetric laminations composed mainly of carbonate peloids (coalescing to form a clotted texture), siliciclastics, hybrid and carbonate intraclasts (oolitic – peloidal grainstones and dolomitized mudstones), and rare carbonate ooids. Together with sparry crust (Fig. 3B), these laminations create incipient columnar forms, within which clotted micrite ghosts are locally present. The siliciclastic phases are comprised of monocrystalline quartz, microcline, orthoclase, rare undifferentiated rock fragments (low-grade metamorphic rocks or chert), tourmaline, muscovite and epidote. Stylolites generally develop where the siliciclastic content is relatively high (Fig. 3B) and bordering the sparry crusts. The main diagenetic processes include overgrowth of continuous and discontinuous quartz and K-feldspar, replacement of ooids and carbonate intraclasts by monocrystalline silica, pervasive dolomitization modifying

primary and diagenetic constituents, as well as the cementation of intergranular pores and replacement of heavy minerals by diagenetic titanium oxides. According to Dunham (1962) and Embry and Klovan (1971), these stromatolites can be classified as boundstones. According to Riding (2011), the horizontal stromatolites can be classified as sparry crust with grains. In contrast to horizontal stromatolites, the bioherms present a pervasive replacement of primary phases by dolomite and microcrystalline silica, obliterating the original fabric. Parallel and wavy lamina (Fig. 3C and D), delineated by horizontal stylolites and associated sulfides, are composed by siliciclastic (quartz, orthoclase, microcline and muscovite) and undifferentiated constituents intensely replaced by dolomite.

4.2. Hybrid arenites

The hybrid arenites comprise the Sm, Sl, St, Sr, Sscs, Shcs and Sw lithofacies. The arenites are very fine- to fine-grained (Fig. 3E, F, G and H), moderately to poorly-sorted, with a grain-supported texture and a normal packing pattern. The visualization of the original roundness of the siliciclastics (subangular to subrounded) is hindered by the continuous and discontinuous quartz and K-feldspar overgrowths (Fig. 3H). The primary constituents are composed of carbonate ooid (with quartz as nuclei) and peloids, carbonate and hybrid intraclasts, monocrystalline quartz, orthoclase, microcline and plagioclase. In contrast, heavy minerals such as tourmaline, monazite, epidote, rutile, staurolite, zircon and titanite, and undifferentiated rock fragments (chert and low-grade metamorphic rocks) are rare in the analyzed samples. The proportion of primary constituents varies from 30 to 70% of siliciclastics when compared to carbonate particles. According to Zuffa (1980), these percentages allow to classify the samples as hybrid arenites. The main diagenetic processes are the overgrowth of quartz and K-feldspar, pervasive dolomitization and later silicification that replaces the primary constituents and fills the primary and secondary porosity (Fig. 3H). Selective dissolution in the ooids, horizontal discontinuous stylolites with blocky pyrite and titanium diagenetic mineral replacing heavy minerals are rare.

4.3. Intraformational hybrid conglomerates and rudstones

The intraformational hybrid conglomerates and rudstones compose the Gm and Gt lithofacies (Fig. 3I, J, K and L). These lithotypes are very poorly sorted, with grain-to cement-supported textures and highly variable composition, ranging from 2 to 60% of siliciclastics compared to carbonate sediments. In some samples, the dominance of carbonate and hybrid intraclasts does not represent the heterogeneous composition observed in the entire layer. The intraclasts range in size from very coarse sand to pebble, rounded, and compositionally consist of oolitic grainstones, laminated or massive hybrid arenites, sparry crust and microbial in texture. Sometimes, the intraclasts are fractured, replaced by dolomite and/or bordered by stylolites. The arenaceous portion of the conglomerates are composed of mono- and polycrystalline quartz, orthoclase, microcline, plagioclase, chert fragments, rutile, zircon, tourmaline, monazite, epidote, biotite, and carbonate ooid and peloid. The siliciclastic grains are very fine- to fine-grained and subangular to subrounded. As in the case of the hybrid arenites, continuous and discontinuous quartz and K-feldspar overgrowths make it difficult to visualize the original roundness of the grains. Carbonate ooids (Fig. 3J) and peloids are fine to medium-grained in size, intensely recrystallized and replaced by dolomite.

The diagenetic processes and products are very similar to the hybrid arenites, consisting of quartz and K-feldspar overgrowths, intense dolomitization and silicification that replaced primary and diagenetic constituents and filled pores. Stylolites without preferential orientation is common, bordering carbonate and hybrid intraclasts and being replaced by blocky pyrite.

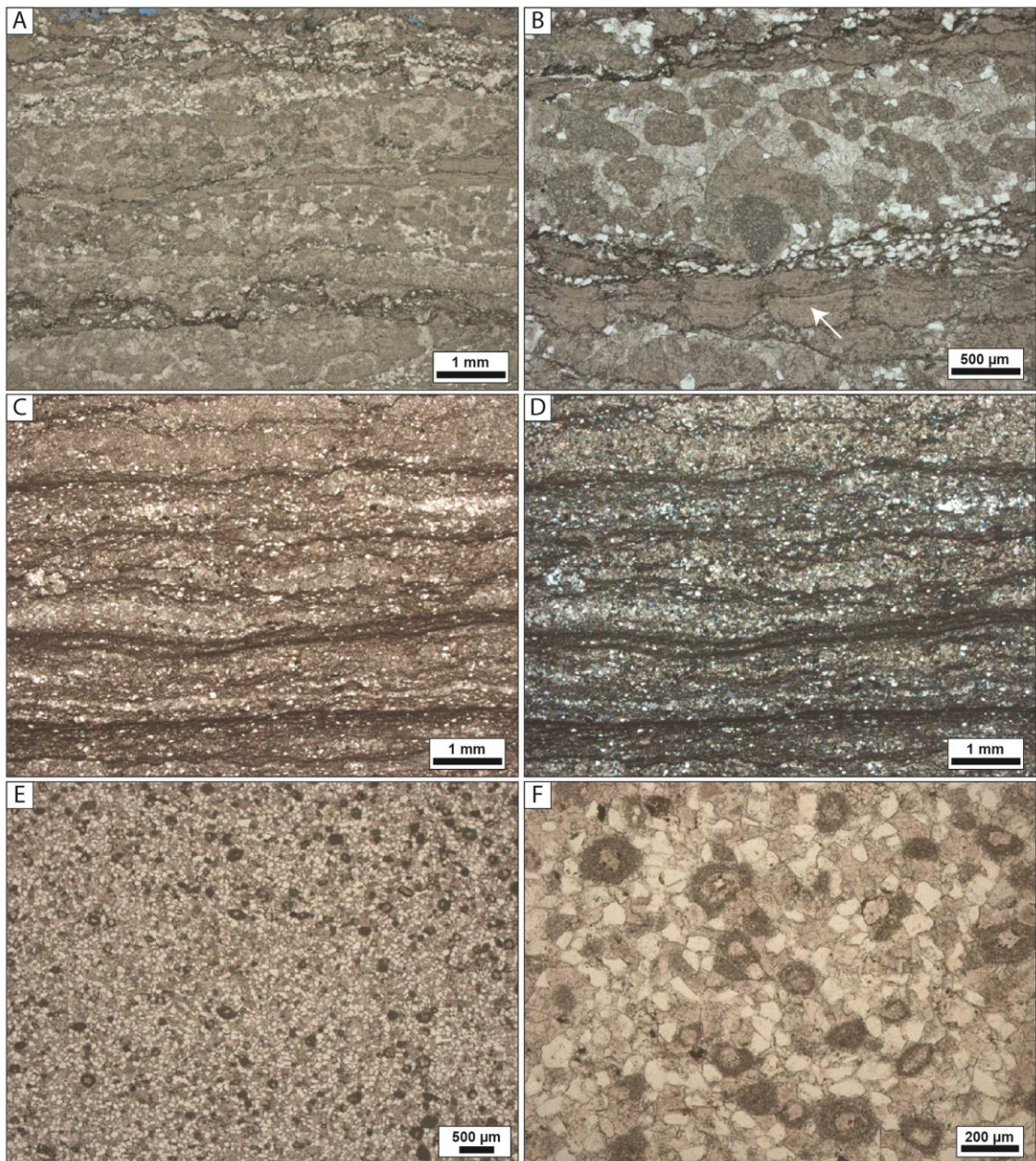


Fig. 3. Continued.

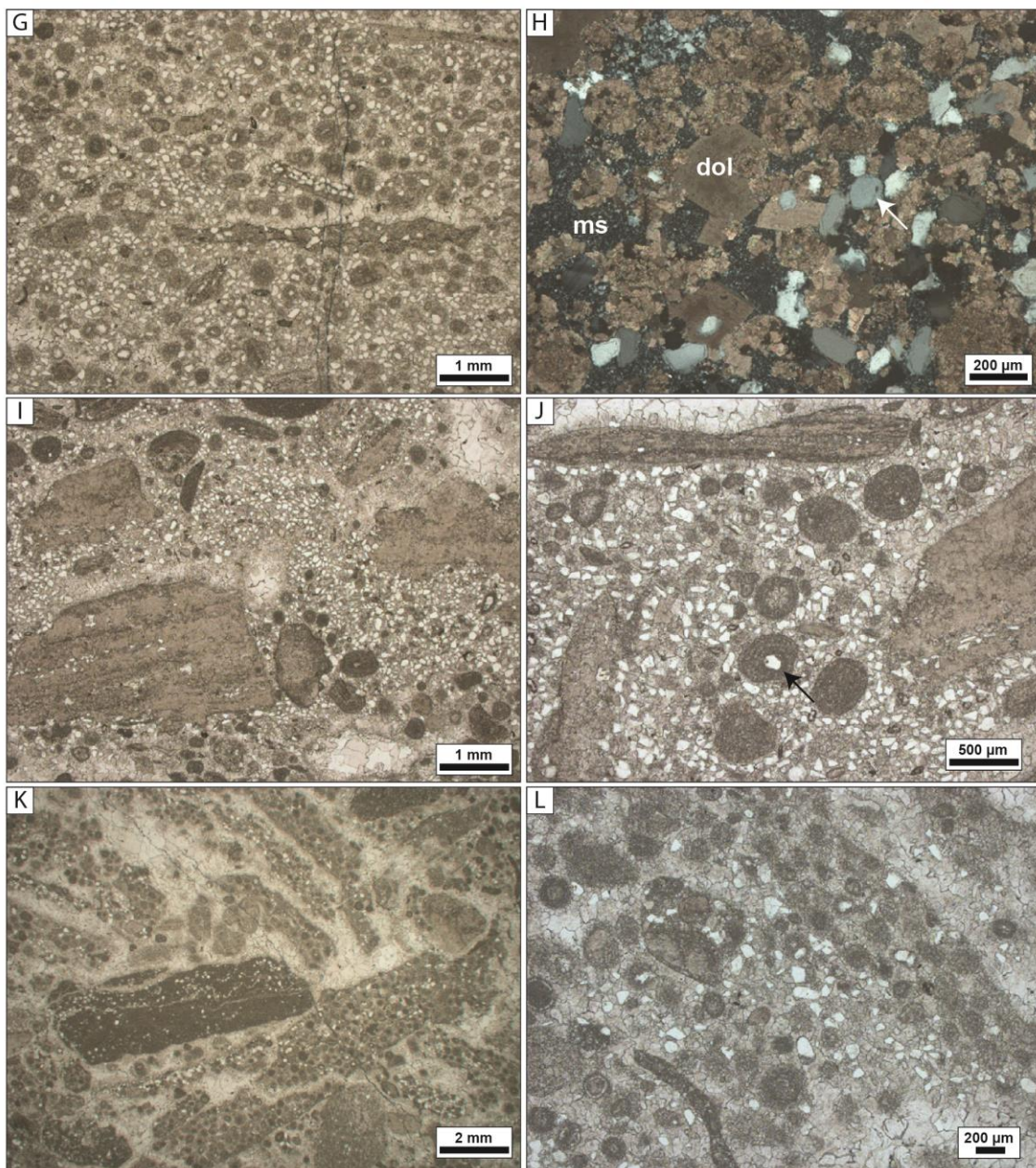


Fig. 3. Textural characteristics, primary constituents and diagenetic aspects of the main lithological groups. (A) Laminations composed by segregated levels of carbonate peloids, ooids, hybrid and carbonate intraclasts, siliciclastics and sparry crusts in the horizontal stromatolites. (B) Sparry crust (arrow) is overlaid by a subsequent siliciclastic level with stylolites. Carbonate intraclasts and peloids are concentrated in levels with minor dispersed siliciclastic content. (C - D) Parallel and wavy laminations preserved in the bioherms. (E) Very fine to fine-grained hybrid arenites, moderately sorted, composed mainly by quartz, feldspar and carbonate ooids. (F) Slightly deformed carbonate ooids are replaced by microcrystalline dolomite. Siliciclastic grains are partially replaced by macrocrystalline dolomite in the hybrid arenites. (G) Incipient horizontal lamination is marked by carbonate and hybrid

intraclasts orientation in the oolitic hybrid arenites. (H) Discontinuous quartz overgrowths covering detrital quartz grains (arrow) are common. Siliciclastic and carbonate grains are intensely replaced by blocky dolomite (dol) and microcrystalline silica (ms). (I) and (J) Sparry crust and micritic intraclasts, carbonate ooids and siliciclastics are the main components of hybrid conglomerates and intraclastic rudstone. Siliciclastic grains also occur as ooid nucleus (arrow). (K) and (L) Granules and pebbles of oolitic, micritic and hybrid intraclasts, and carbonate ooids are the main components in the hybrid conglomerates and intraclastic rudstone. Subrounded siliciclastic grains (mainly quartz and feldspars) occur dispersed in the fabric and inside the intraclasts. All photomicrographs are taken in parallel-polarized light, except D and H.

Table 1: Lithofacies summary.

Facies	Code	Description	Interpretation
Massive hybrid conglomerate/rudstone	Gm	Matrix- or clast-supported, poorly sorted, massive intraformational sandy conglomerate to conglomerate. Sandy matrix composed of fine- to medium-grained allochemic grains and subangular to subrounded, very fine- to fine-grained siliciclastic particles. Intraclasts vary from granule to cobble (< 10 cm), subangular to rounded, usually with elongated tabular shape. Oncolites up to 10 cm. The beds are continuous or lenticular, < 30 cm thick, sometimes with normal gradation and erosive base (Fig. 4A and B).	Rapid sedimentation of coarse sediments from turbulent flows. Hyper-concentrated gravity flows. Post-depositional fluidization processes obliterating the depositional stratification.
Trough cross-stratified hybrid conglomerate/rudstone	Gt	Matrix- or clast-supported, poorly sorted, trough cross-stratified, intraformational, sandy conglomerate. Sandy matrix composed of fine- to medium-grained allochemic grains and subangular to subrounded, very fine- to fine-grained siliciclastic particles.	Migration of subaqueous, sinuous-crested gravel dunes under unidirectional flow.

		Trough cross-stratification forming sets ranging from 20 to 30 cm. Intraclasts vary from granule to cobble (< 15 cm), subangular to rounded, usually with elongated tabular shape oriented parallel to stratification, sometimes imbricated. The beds have lenticular geometry and erosive base (Fig. 4A and C).	
Massive hybrid arenite	Sm	Fine- to coarse-grained, moderate to poorly sorted, massive arenite. Granules and pebbles are frequent, occurring sparsely or concentrated at the base of the bed. Allochemics are fine- to coarse-grained and siliciclastics are subangular to rounded, very fine- to fine-grained. Tabular or lenticular bed < 30 cm thick (Fig. 4D).	Deposition from subaqueous hyper-concentrated gravity flows or resulting from post-depositional fluidization, obliterating the primary depositional structure.
Low angle laminated hybrid arenite	Sl	Fine- to medium-grained, moderately sorted arenite, with low angle lamination (< 15°). Medium-grained allochemic grains and very fine- to fine-grained, subangular to rounded siliciclastic grains. Intraclasts are common. Sets < 15 cm, with erosive base and flat to slightly undulated top (Fig. 4G and H).	Migration of attenuated bedforms under the influence of critical unidirectional currents associated with oscillatory flows (combined flow regime).
Trough cross-stratified hybrid arenite	St	Fine- to medium-grained, moderate to poorly sorted, small-scale trough cross-stratified arenite. Medium-grained allochemic grains and very fine- to fine-grained, subangular to rounded, siliciclastic grains. Amalgamated sets (5 – 30 cm thick) with flat to slightly undulated top (Fig. 4E).	Migration of sinuous-crested subaqueous bedforms under unidirectional to combined flow regime.
Ripple cross-laminated hybrid	Sr	Very fine- to fine-grained, moderately sorted arenite, with small-scale asymmetric ripple cross-lamination (< 4 cm). The	Migration of ripples under unidirectional lower flow regime.

arenite		climbing angle vary from subcritical to critical (Fig. 4F).	
Swaley cross-stratified hybrid arenite	Sscs	Very fine- to medium-grained, moderately to poorly sorted arenite. Allochemic grains are fine- to medium-grained and siliciclastics are subangular to rounded, very fine- to fine-grained. Cut and fill structures with undulated edges, filled by small-scale sets (< 20 cm) of accretionary undulated lamination, low angle lamination and/or trough/sigmoidal cross-stratification. Intraclasts are common at the base of the sets (Fig. 4H).	Migration of symmetric bedforms, isotropic to anisotropic, with high wavelength/amplitude ratio in conditions of combined flows regime. High-intensity storm conditions.
Hummocky cross-stratified hybrid arenite	Shcs	Fine- to medium-grained, moderately to poorly sorted arenite. Allochemic particles are fine- to coarse-grained and siliciclastic grains are very fine- to fine grained. The beds vary from 10 to 40 cm thick and the thickness varies laterally. Top surfaces are undulated (wavelength from 0.4 to 2 m). Internally the lamination can be isotropic undulated, scour and drape or anisotropic trough cross stratification. Wave ripples occur at bedforms limits (Fig. 4I).	Symmetric bedforms, isotropic to anisotropic with a high wavelength/amplitude ratio under high intensity oscillatory to combined flow. Wave ripples represent the attenuation of the flow.
Wave ripple cross-laminated hybrid arenite	Sw	Fine- to medium-grained, moderately sorted arenite with small scale symmetrical to asymmetrical wave ripple cross-lamination. Sets < 5 cm and wavelength from 5 to 30 cm (Fig. 4G).	Migration of wave ripples under oscillatory to combined oscillatory-unidirectional flow.
Bioherm	STb	Isolated bodies, 0.1 to 1.3 m thick and up to 3 m wide, with domal or columnar morphology. Internally the lamination is millimetric, smooth and continuous to wrinkled and disrupted.	Organosedimentary deposits formed from benthic microbial trapping and bidding of siliciclastic and carbonate particles;

		<p>Internal structures of bioherms are laterally continuous, with simple and/or branched columns up to 10 cm high. Microfabric composed of carbonate peloids, oolites and sparry crusts, and very fine- to fine-grained siliciclastic grains. Intraclasts are common at the bases of the bioherms, between domes or columns (Fig. 4J, K, L and N).</p>	<p>and from bioinduced carbonate precipitation. Crusts are formed by inorganic precipitation. The morphology of bioherms suggests deposition in a relatively high energy environment and high water column.</p>
Horizontall y laminated stromatolit e	STh	<p>Centimetric to metric layers, laterally continuous (biostromes) and horizontally laminated. Sparse small domes (< 5 cm) can occur. Smooth to wrinkle millimetric lamination. In thin section, crudely to well-defined micro lamination characterized by the alternation of sparry crusts, fine-grained allochemic particles and very fine- to fine-grained siliciclastic grains. Intraclasts are common (Fig. 4M).</p>	<p>Organosedimentary deposits formed from benthic microbial trapping and bidding of siliciclastic and carbonate particles; and of bioinduced carbonate precipitation. Crusts are formed by inorganic precipitation.</p>

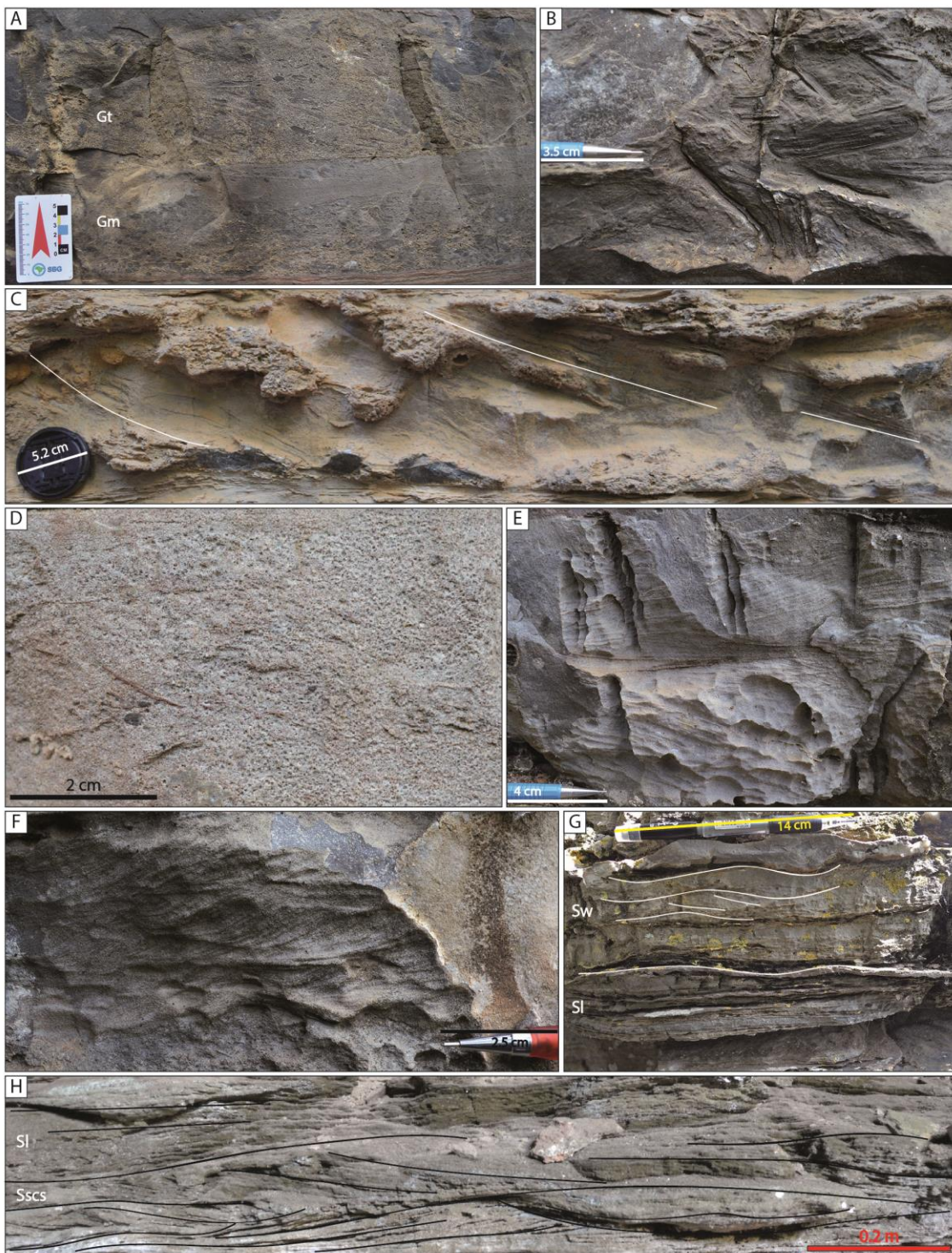


Fig. 4. Continued.

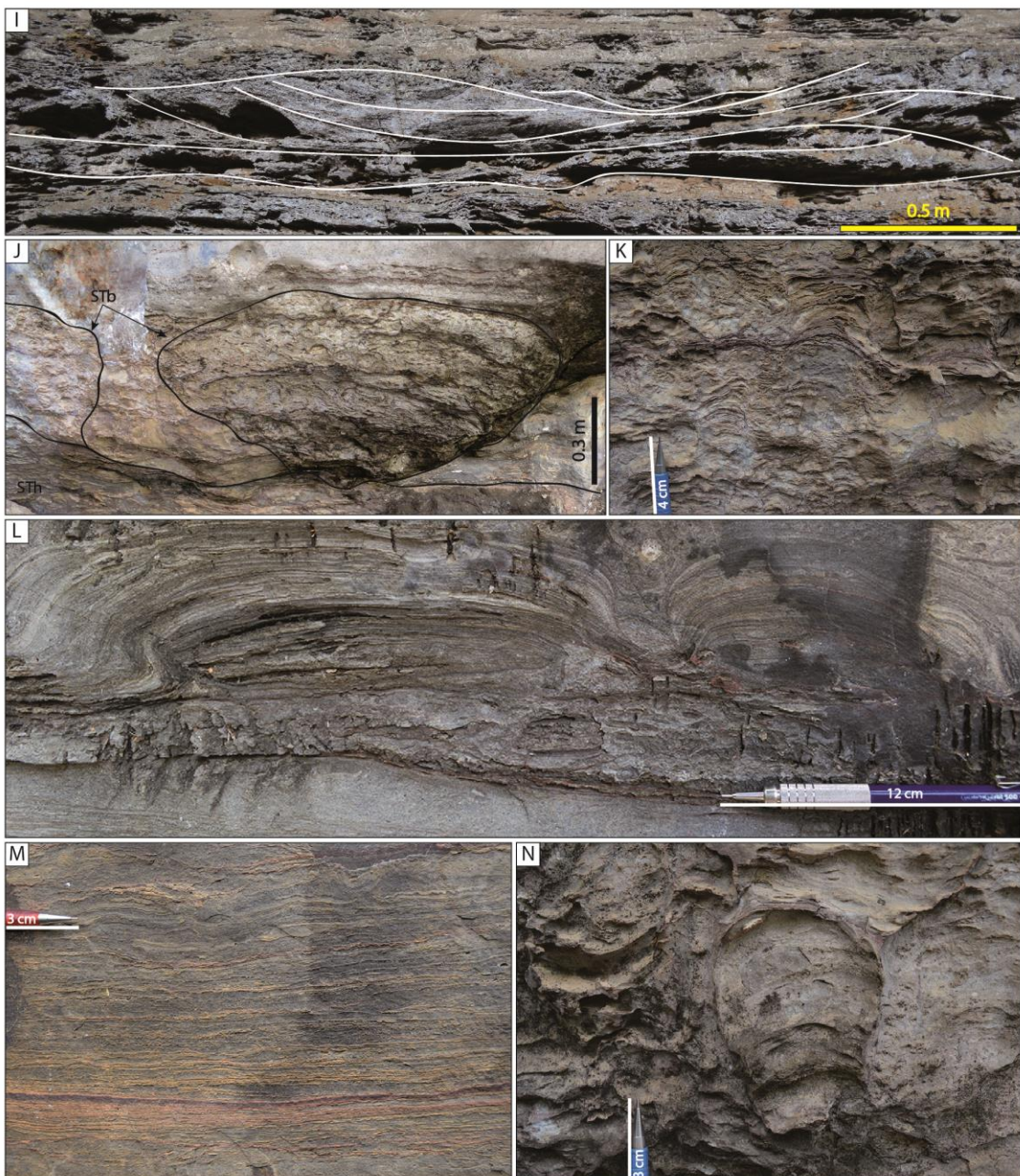


Fig. 4. Examples of lithofacies (see table 1). (A) Gm - massive hybrid conglomerate with normal gradation; Gt - Trough cross-stratified hybrid conglomerate. (B) Gm - massive hybrid conglomerate; rounded and tabular shaped intraclasts, internally laminated, composing a chaotic fabric. (C) Gt - Trough cross-stratified hybrid conglomerate; stratification marked by the axis orientation of the intraclasts (white lines). (D) Sm - massive hybrid arenite with sparse and chaotic intraclasts. (E) St - two sets of trough cross-stratified hybrid arenite. (F) Sr - Ripple cross-laminated hybrid arenite; note the critical angle of climb. (G) Sl - low angle laminated hybrid arenite; Sw - wave ripple cross-laminated hybrid arenite. (H) Sscs - Swaley cross-stratified hybrid arenite; Si - low angle laminated hybrid arenite. (I) Shcs - hummocky

cross-stratified hybrid arenite. (J) STb - columnar and dome-shaped bioherms. (K) STb - detail of small branched columns composing a bioherm. (L) STb - small dome-shaped bioherms with laterally continuous lamination; massive conglomerate filling the inter-bioherms zone and burying them. (M) STh - horizontally laminated stromatolite. Toward the top lamination becomes wavy. (N) STb - detail of a small, simple bioherm column; note on the left side of the column the disrupted lamination and the intraclasts.

5. LITHOFACIES ASSOCIATIONS

The Caboclo Formation in the study area comprises three lithofacies associations identified by distinct proportions between lithofacies (Fig. 5): (1) Offshore; (2) Offshore transition and (3) Shoreface.

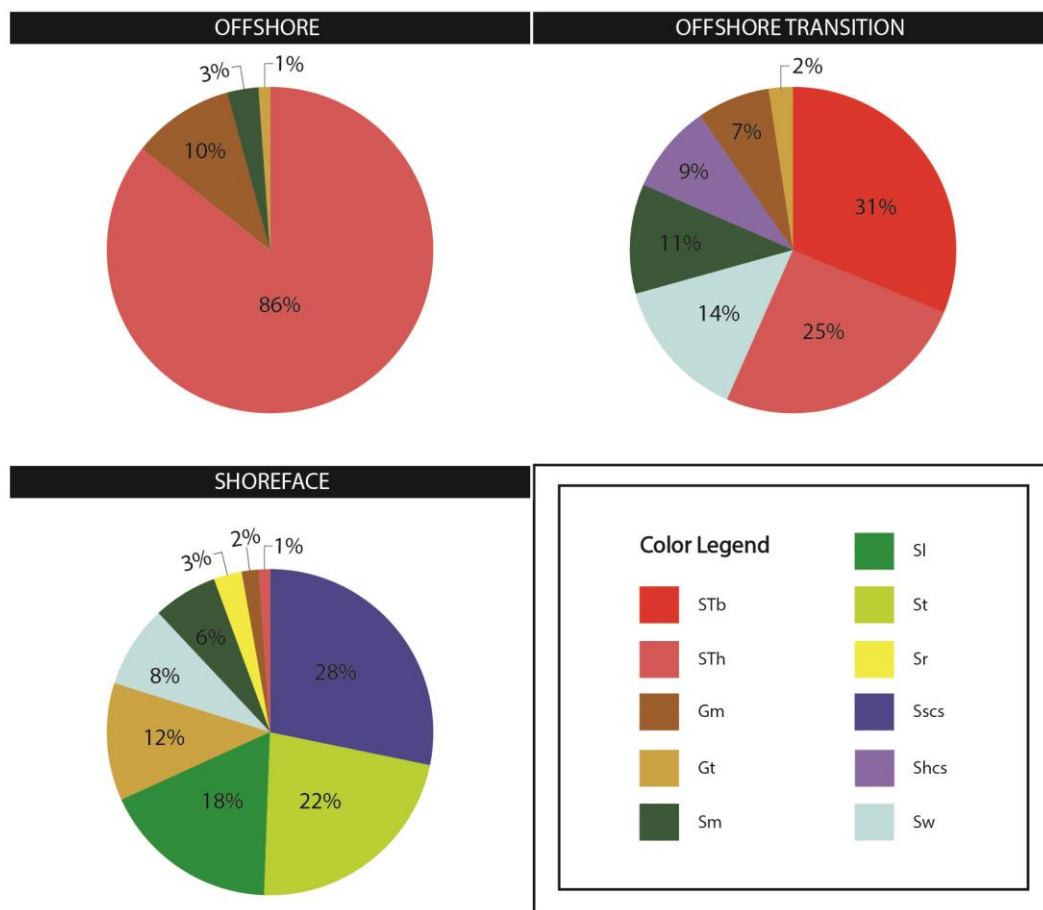


Fig. 5. Diagrams showing the percentage of lithofacies in each lithofacies association.

5.1. Offshore

Facies (Fig. 5) – STh (86%); Gm (10%); Sm (3%); Gt (1%).

Description

This lithofacies association forms tabular packages up to 5 m thick (Fig. 6A and B). It is composed mainly of horizontally laminated stromatolite (STh), and subordinately of massive hybrid conglomerates (Gm), massive hybrid arenites (Sm) or cross-stratification hybrid conglomerates (Gt). The conglomerates and arenites beds are lenticular and 0.1 to 0.3 m thick. They intercalate with stromatolites and locally fill small erosive structures (Fig. 6C, D, E and F).

Interpretation

The dominant presence of horizontally laminated stromatolites formed by the trapping of very fine to fine-grained siliciclastic particles and sparry crusts with great lateral continuity indicates a low energy condition, probably below the storm-weather wave-base, at a depth corresponding to the offshore (Reading and Collinson, 1996) or the external ramp (Burchette and Wright, 1992). Under fair-weather conditions (Fig. 7A and C), microbial mats dominated the seabed. Proximal areas were occasionally affected by storm waves (Fig. 7B and D) generating resuspension and transport of sediment to the distal portion (Aigner, 1982; Tucker, 1982; Myrow and Southard, 1996; Badenas e Aurell, 2001; Myrow et al., 2002; Basilici et al., 2012; Pérez-López e Pérez-Valera, 2012; Brady and Bowie, 2017; Collins et al., 2017). Lenticular beds of massive arenites and/or massive conglomerates (Sm and Gm) are related to hyperconcentrated gravitational flows (storm-generated turbidity currents). Besides, storm surge flows carry larger volumes of sediments, generating conglomerates bedforms (Gt) under combined to unidirectional tractive high-velocity flows (Myrow et al., 2002; Brady and Bowie, 2017). The alternation between periods of fair-weather and storm events (Fig. 7) resulted in the deposition of different lithofacies in the offshore sub-environment. Horizontally laminated stromatolites accumulated in low-energy periods interspersed with reworked sediments deposited by high-energy storm-induced currents. The absence of sub-aerial exposure features in horizontal stromatolites, such as karstic features and paleosols, is indicative of a permanently submerged area, reinforcing the interpretation of an offshore context.

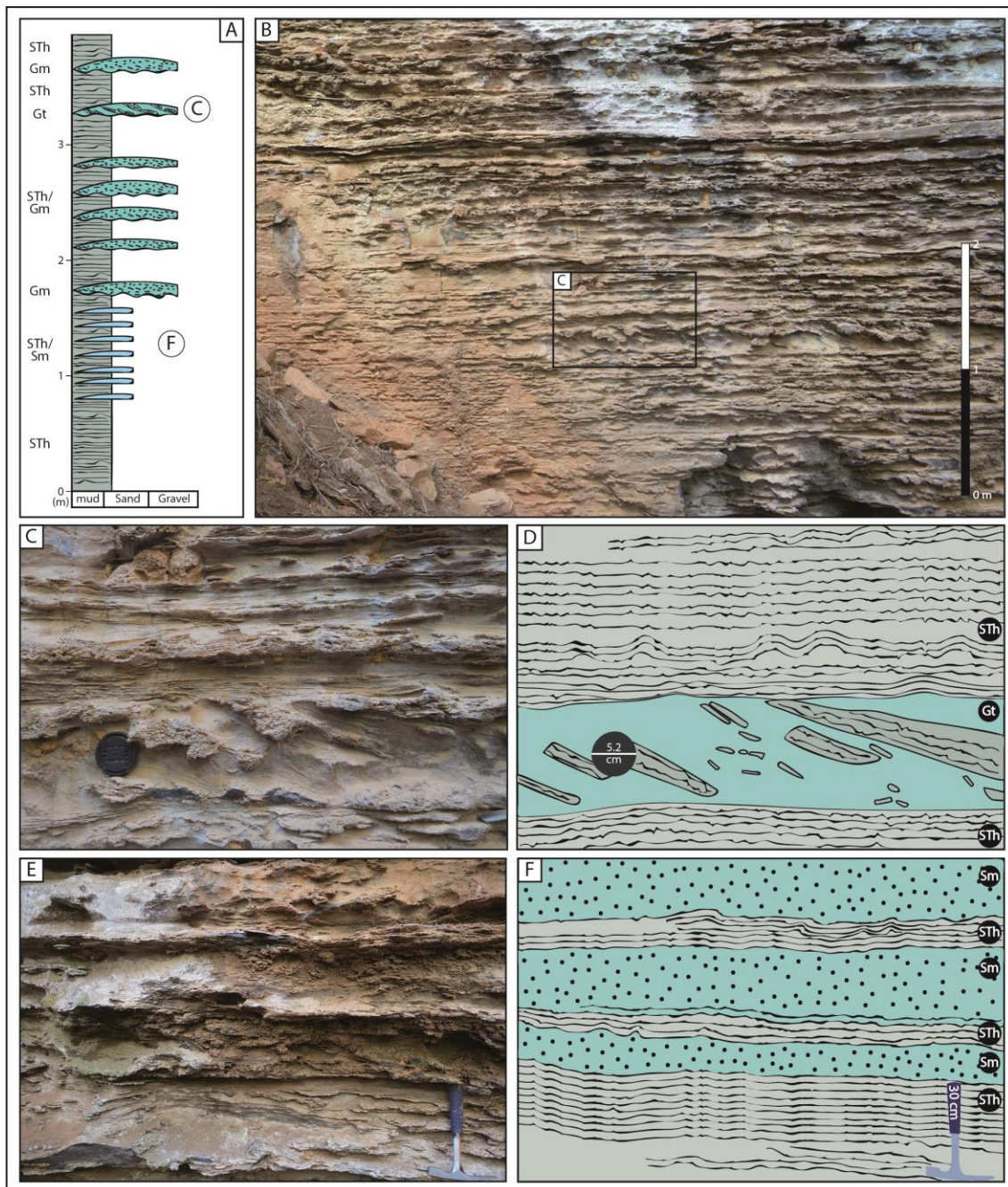


Fig. 6. (A) Typical stacking pattern of the offshore lithofacies association. (B) Outcrop showing the stacking of offshore layers; note the lateral continuity of the STh layers and the lenticular geometry of the arenites and conglomerates. (C - D) Photograph and interpretation of an interval in which occurs the overlap of horizontally laminated stromatolites (STh) with small domes, and trough cross-stratified conglomerate (Gt). (E - F) Photograph and interpretation showing the overlap of horizontally laminated stromatolites (STh) and massive arenites (Sm).

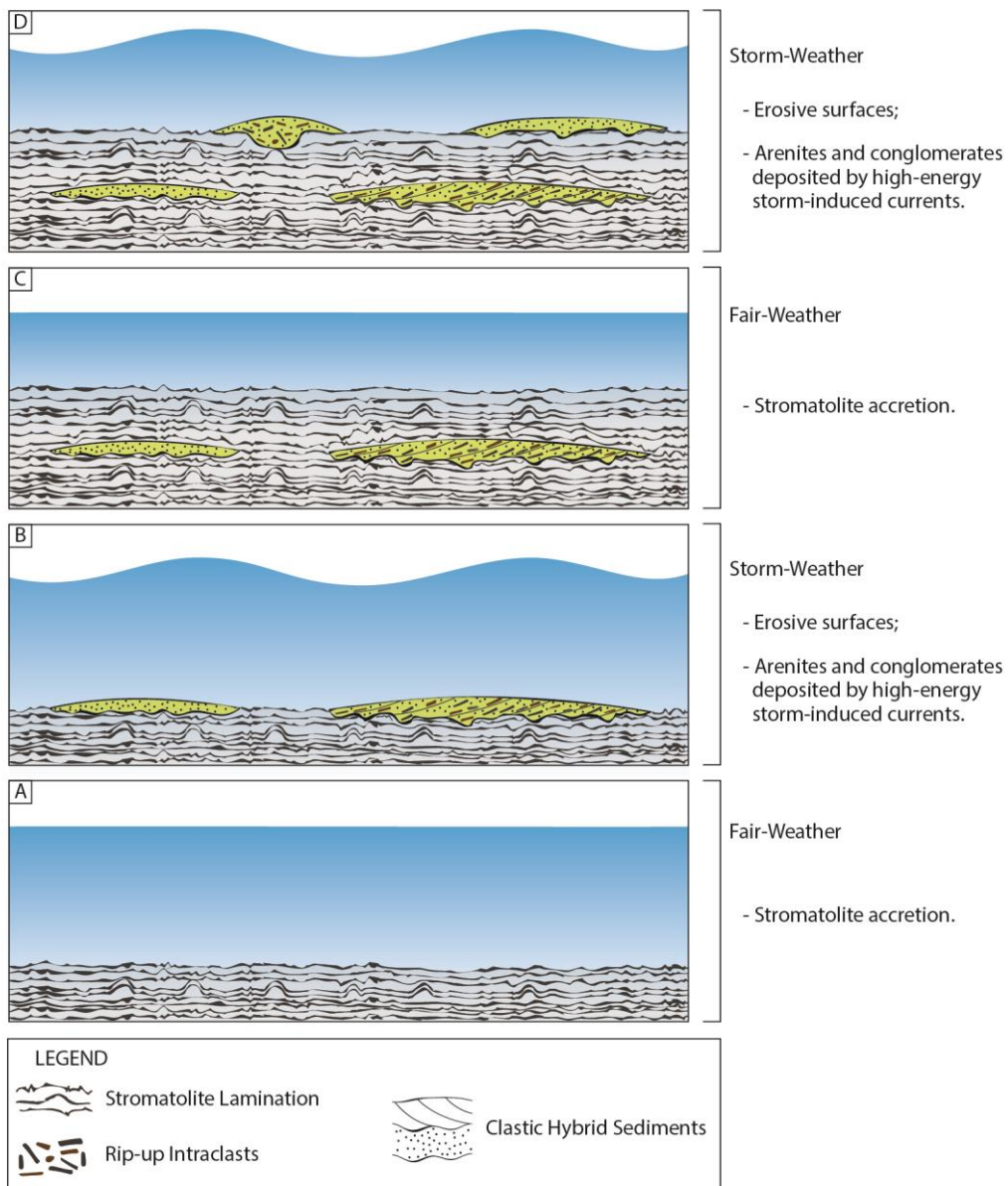


Fig. 7. Successions of events (A to D) showing the alternation of fair- and storm-weather periods and its associated deposits in the offshore zone.

5.2. Offshore Transition

Facies (Fig. 5) – STb (31%); STh (25%); Sw (14%); Sm (11%); Shcs (9%); Gm (7%); Gt (2%).

Description

This lithofacies association consists of tabular packages up to 2 m thick (Fig. 8 and 9). It is composed of bioherms (STb), horizontally laminated stromatolites (STh), hybrid arenites with hummocky cross-stratification (Shcs), wave ripples (Sw) or massive (Sm), massive hybrid conglomerates (Gm) and with trough cross-

stratification (Gt). Arenite beds with wave ripple lamination usually occurs overlying trough cross-bedded conglomerates or hummocky cross-stratified arenites. Sw lithofacies can also occur intercalated with horizontally laminated stromatolites. Some layers of conglomerates and arenites have great lateral continuity, and can be traced for more than a dozen of meters.

Bioherms are exclusive to this lithofacies association, making up columns and domes from 0.1 to 1.3 m thick and lateral extension lesser than 3 m, which are built from horizontally laminated stromatolite pavement. Morphologically they are simple domes with laterally continuous lamination or with more complex shapes composed of branched or not-branched columnar structures. Internally to bioherms, concentration of intraclasts are common (Fig. 8F). The bioherms occur as isolated constructions (Fig. 8G) or as laterally connected domes, which are built from the same depositional horizon (Fig. 8B, C, D and E). The interdome areas were filled by hybrid conglomerates (Gm and Gt) and/or arenites (Sw, Sm and Shcs) separated by millimetric or centimetric levels of horizontal stromatolites (STh). In some cases, horizontal stromatolites are eroded, forming millimetric levels of microbial intraclasts at the base of arenites and conglomerates. Typically, arenites and conglomerates fill the inter-bioherms depressions zone, burying the stromatolite buildups and flattening the relief (Fig. 8B, C, D and E).

Interpretation

This lithofacies association is typical of a context in which rapid and intense variations in energy occur in the system. This alternation of energetic periods suggests that these deposits were formed in the offshore transition (Dott and Bourgeois, 1982; Reading and Collinson, 1996) or middle ramp (Burchette e Wright, 1992), between the fair-weather wave-base and the storm-weather wave-base.

Hybrid arenites and conglomerates were deposited by storm-related flows. The aggradational, isotropic to anisotropic hummocky arenite beds (Shcs) are related to oscillatory to combined flow, while trough cross-stratified conglomerates (Gt) are deposited as a result of strong unidirectional currents developed during storm events (Dott and Bourgeois, 1982; Molina, 1997; Dumas and Arnott, 2006; Chen, 2014). The massive hybrid conglomerates and arenites deposits (Gm and Sm respectively) are related to hyperconcentrated gravitational flows, interpreted as storm-generated turbidity currents (Aigner, 1982; Myrow and Southard, 1996; Bádenas and Aurell, 2001; Myrow et al., 2002; Brady and Bowie, 2017).

The arenites with wave ripples cross-lamination (Sw) overlying trough cross-stratified conglomerates (Gt) and hummocky arenite (Shcs) deposits represent the attenuation of the intensity of the storm. The storm's peak energy generates unidirectional or combined flows, resuspending sandy sediments, rip-up and transporting clasts from the (semi)consolidated substrate, generating erosive surfaces. The decrease in storm intensity results in pure oscillatory to slightly combined flows, initially depositing Gt or Shcs followed by Sw, representing the waning flow stage of a storm (Collins et al., 2017).

The development of bioherms responds to the dynamics of shallow marine depositional processes, growing in a context of relatively high water depth and moderate to high wave energy (Andres and Reid, 2006). In the present case, the bioherms were established over a hardground formed by horizontal stromatolites developed during relatively long fair-weather periods (Fig. 10A and B). During storm events (Fig. 10C and E), the oscillatory flows and storm-induced currents shape the stromatolitic morphology and increase the grain availability to be trapped by the microbial colony (Logan et al., 1964; Gebelein, 1969; Hofmann, 1973; Walter, 1977; Grotzinger and Knoll, 1999; Andres and Reid, 2006; Dupraz et al., 2006). The relief between the bioherms was filled during storm events until the sedimentation rate exceeds the microbial accretion rate, burying the bioconstructions (Fig. 10E). The burial of bioherms can occur by a single storm event or by the stacking of multiples events. In cases of multi-events (Fig. 10), periods of fair-weather are recorded by the development of thin levels of horizontally laminated stromatolites, which separate layers of hybrid arenites and conglomerates deposited during storm events (Shcs, Sw, Sm, Gm and Gt). STh layers were often eroded during the early stages of storm events, leaving only intraclastic lags. These multiple events are recorded in the bioherms as internal erosive surfaces covered by clastic sediments and intraclasts added to the colony and by the disruption and deformation of the laminations.

When the storms were very intense and/or frequent, there was no time and conditions to establish a stable substrate through the early cementation of microbial mats (hardground), and consequently, bioherms do not form. Therefore, in these periods, the offshore transition was formed by the high-frequency intercalations of hybrid arenites, conglomerates and thin layers of horizontally laminated stromatolite (Fig. 9). The presence of STh layers with maximum thickness of 0.15 m suggests periods of a few years between storm events (Dibenedetto and Grotzinger, 2005).

The occurrence of bioherms could also be linked to open or sheltered areas on the coast. In sheltered portions, the intensity with which storms hit the coast was lower compared to open areas. This energy difference could result in offshore transition sheltered zones with bioherms and open areas without bioherms coexisting laterally.

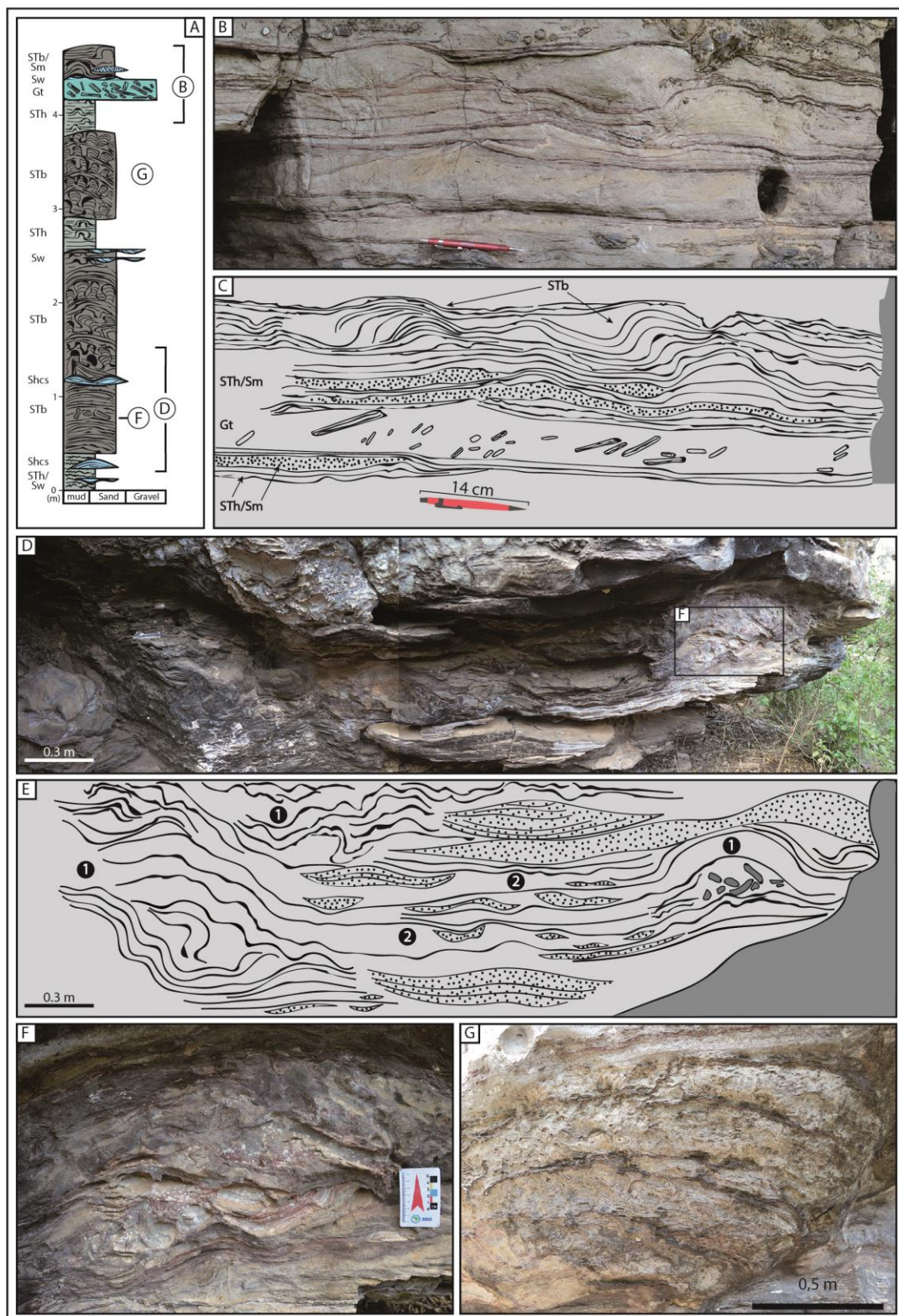


Fig. 8. (A) Typical stacking pattern of the offshore transition with bioherms. (B – C) Photograph and interpretation. Interval with overlap of trough cross-stratified conglomerate (Gt), horizontally laminated stromatolites (STh), massive arenites (Sm) and bioherms (STb). The lateral transition of detrital and microbial lithofacies indicates contemporaneous deposition between them. (D – E) Photograph and interpretation. Bioherms (STb – 1) and the space between them (2) filled by horizontally laminated stromatolites (STh) and arenites (dotted layers) with wave ripples (Sw) and hummocky cross-stratification (Shcs). (F) Detail of the concentration of intraclasts within a bioherm. (G) Isolated dome-shaped bioherm.

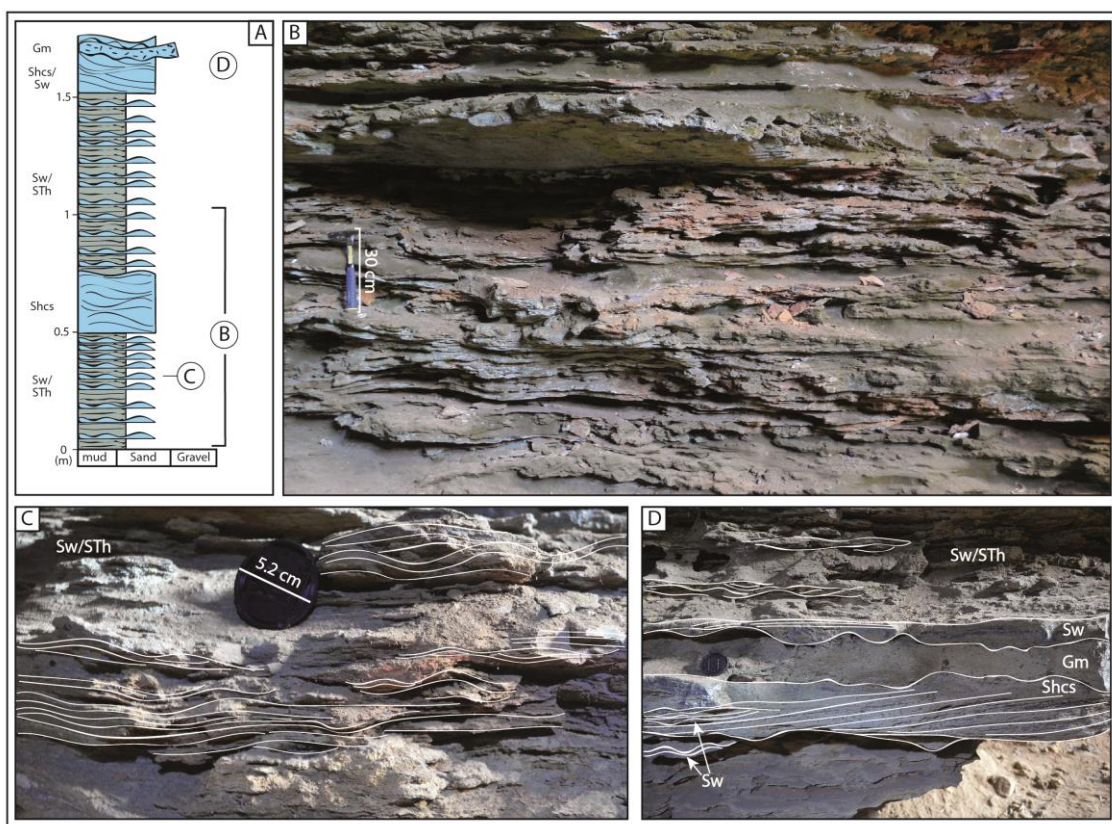


Fig. 9. (A) Stacking pattern of the offshore transition without the development of bioherms. (B) Outcrop showing the stacking of offshore transition deposits; note the abrupt transition of a high-frequency intercalation of small wave ripples (Sw) and horizontally laminated stromatolites (STh) to a hummocky (Shcs). (C) Detail of the high-frequency intercalations of wave ripples cross-laminated arenite (Sw – white lines) and horizontally laminated stromatolites (STh). (D) Anisotropic hummocky cross-stratification arenite (Shcs) transitioning laterally to wave ripples arenites (Sw) and overlapped by massive conglomerate (Gm) with wave ripples (Sw) on the top.

Sw/STh - High-frequency intercalations of wave ripples cross-laminated arenite and horizontally laminated stromatolites.

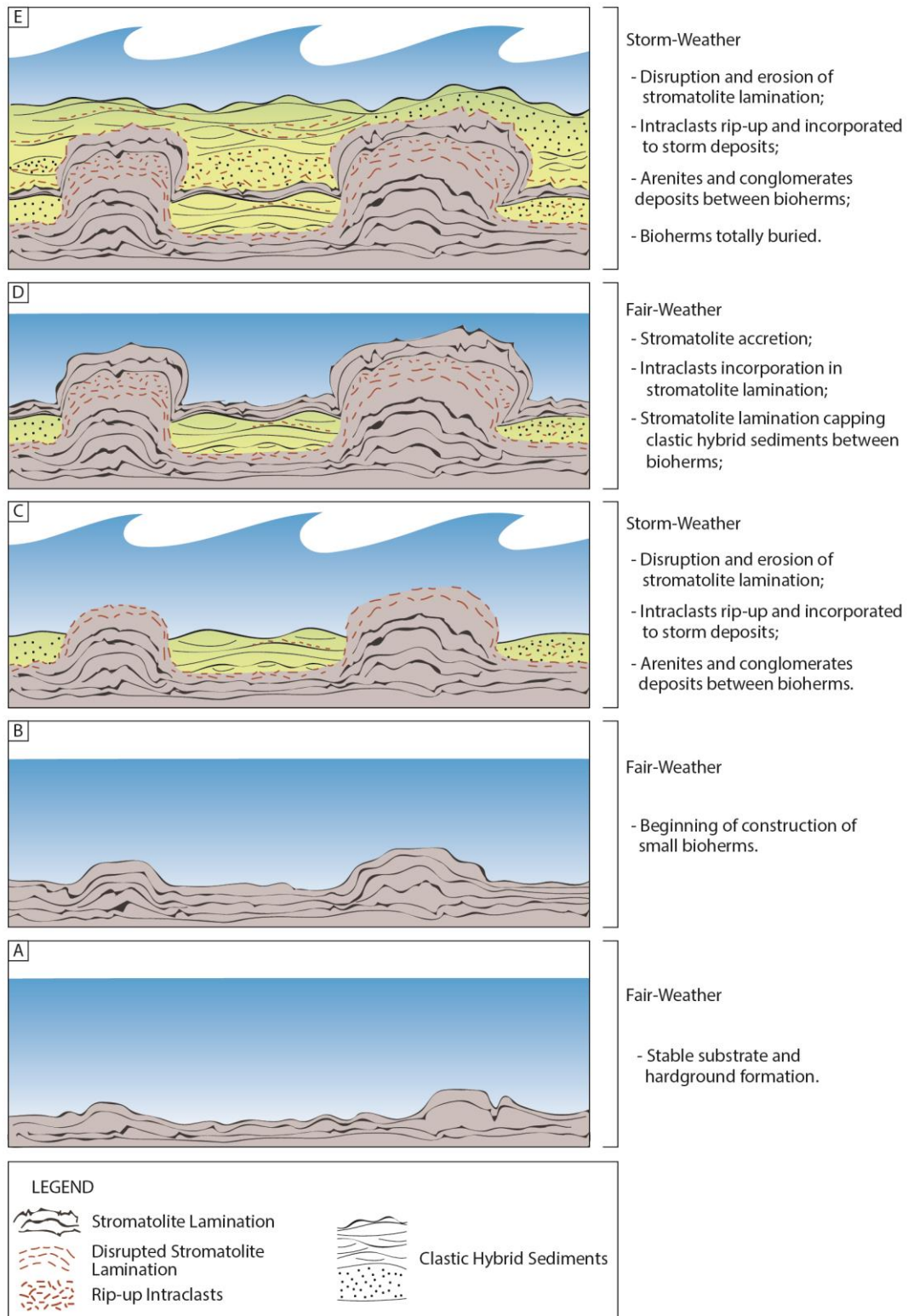


Fig. 10. Successions of events (A to E) showing the alternation of fair- and storm-weather periods and its associated deposits in the offshore transition zone with bioherms.

5.3. Shoreface

Facies (Fig. 5) – Sscs (28%); St (22%); SI (18%); Gt (12%); Sw (8%); Sm (6%); Sr (3%); Gm (2%); STh (1%).

Description

This lithofacies association forms tabular packages up to 2 m thick (Fig. 11), composed of amalgamated sets (< 0.3 m thick) of hybrid arenites with through cross-stratification (St), low angle cross-stratification (SI), swaley cross-stratification (Sscs), wave ripples (Sw) and, less frequently, current ripples (Sr). Massive hybrid arenites and conglomerates (Sm and Gm) are subordinated, and in most cases, it is possible to identify an indistinct lamination (faint lamination). Horizontally laminated stromatolites (STh), up to 4 cm thick, can occur interlayered with hybrid arenites and conglomerate lithofacies (Fig. 11D and E). However, stromatolitic levels may have been partially or totally eroded, being incorporated as intraclasts at the base of the overlapping layers of arenites and conglomerates.

Interpretation

The occurrence of amalgamated arenite beds composed mainly of oscillatory and combined flows structures suggests a high energy shoreface or inner ramp environment, above the fair-weather wave-base (Dott and Bourgeois, 1982; Burchette and Wright, 1992; Reading and Collinson, 1996). Swaley cross-stratification arenites (Sscs) are related to storm-generated combined flows in nearshore areas (Dumas and Arnott, 2006). However, relatively permanent subcritical to supercritical unidirectional currents occurred in the surf zone, forming subaqueous dunes (St and SI) probably associated to rip or longshore currents (Fig. 12A and C) (Dott and Bourgeois, 1982; Leckie and Walker, 1982). In periods of low energy, microbial carpets colonized the seabed. According to Bose et al. (2012), microbial mats can develop in short periods of time (8-12 hours), probably linked to intervals of low intensity of fair-whether waves (Fig. 12B and D). Increasing the intensity of fair-whether waves or during storm events these microbial deposits could be partially or totally eroded.

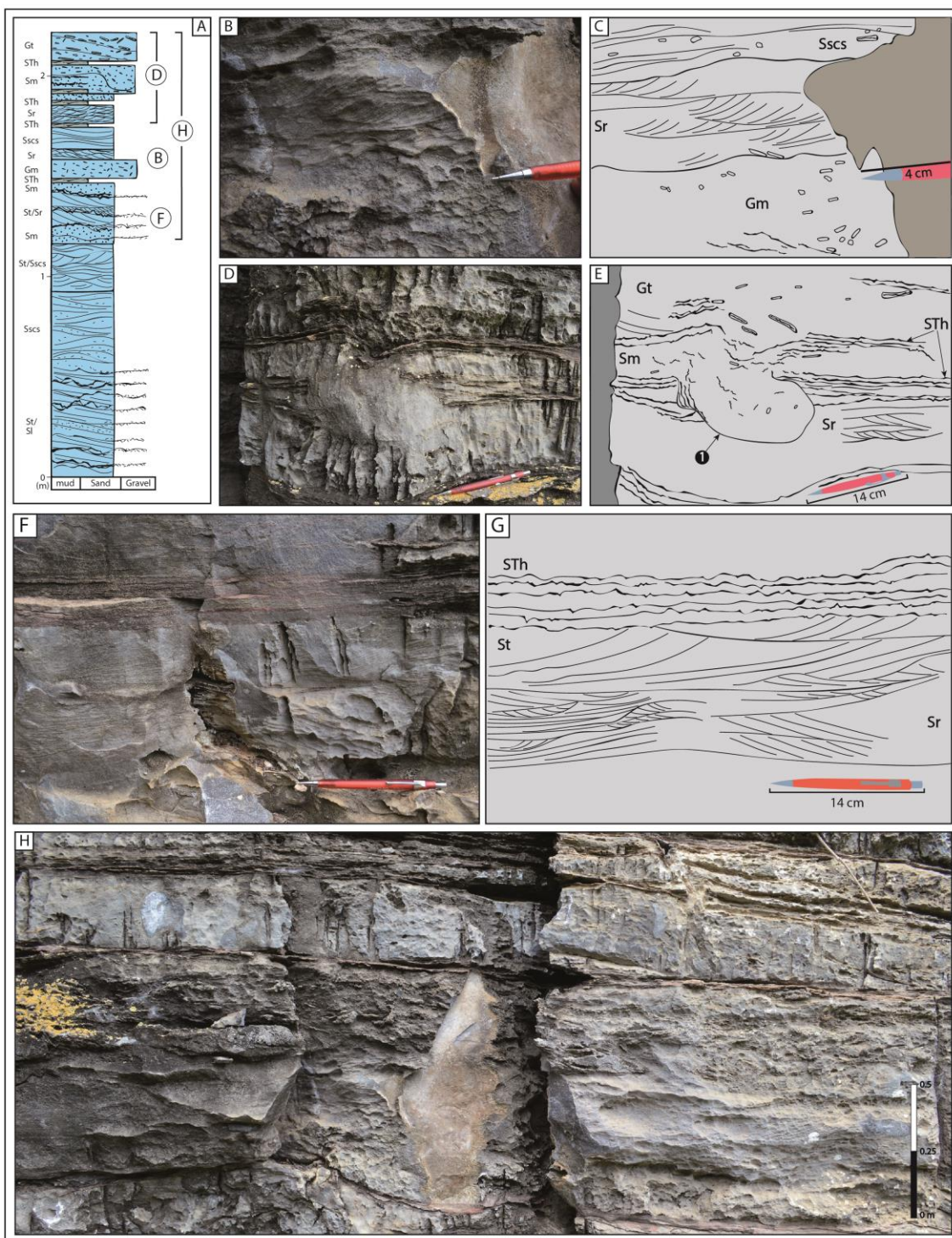


Fig. 11. (A) Typical stacking pattern of the shoreface lithofacies association. (B - C) Photograph and interpretation of an interval with overlapping of massive conglomerate (Gm), ripples cross-lamination arenite (Sr) and swaley cross-stratification arenites (Sscs). Note the irregular contact between lithofacies, and the change in the angle of climb of the ripples (Sr) from subcritical to critical. (D – E) Photograph and interpretation of an interval with ripple cross-lamination arenite (Sr), horizontally laminated stromatolites (STh), massive arenites (Sm) and trough cross-

stratified conglomerate (Gt). Erosive structure (1) filled with massive arenite. (F – G) Ripple cross-lamination arenite (Sr) passing upward to trough cross-stratification arenite (St). Horizontally laminated stromatolite (STh). (H) Interval showing shoreface stacking layers.

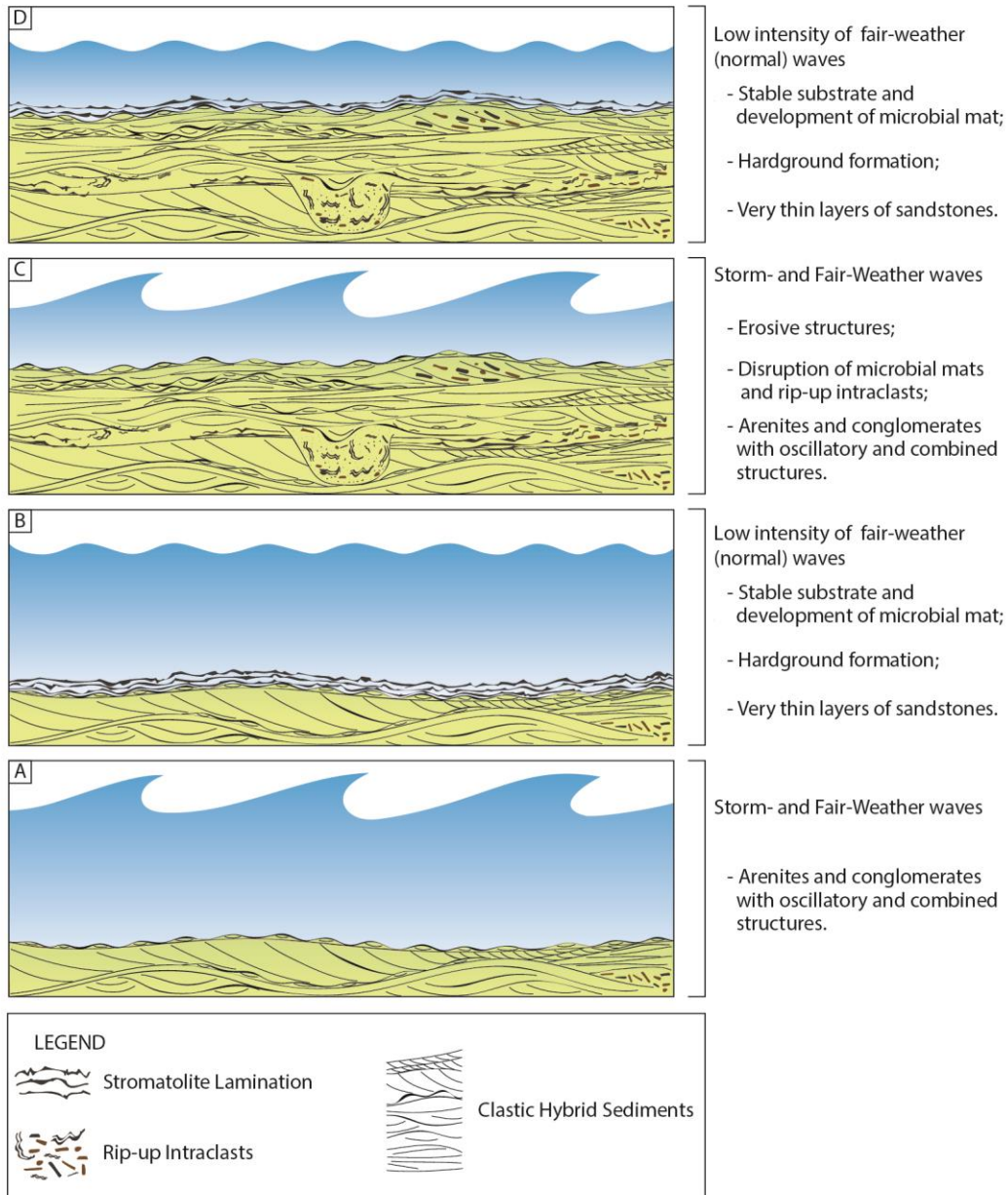


Fig. 12. Successions of events (A to D) representing the alternation of fair-/storm-weather periods and low intensity of fair-weather waves; and its associated deposits in the shoreface zone.

6. STRATIGRAPHIC CYCLES

A large-scale transgressive-regressive cycle was identified in the Caboclo Formation in the study area (TR - Johnson and Murphy, 1984; Catuneanu et al.,

2009), which is characterized by a retrogradational stacking pattern at the base and a progradational stacking pattern to the top (Fig. 2). The retrogradational trend is represented by an upward increase in the proportion of lithologic packages of offshore transition and offshore lithofacies associations relative to the shoreface lithofacies associations; whereas, the reverse trend occurs in the progradational part. The maximum flooding surface (MFS - Posamentier et al., 1988) is marked by a 3-meter-thick aggradational interval that consists essentially of offshore deposits. Although the precise position of MFS is not defined, the interval displays the inversion of retrogradational to progradational stacking pattern.

In the log section intervals between 0 – 9.5 m and 25 – 34 m (Fig. 2), the large T-R cycle can be subdivided into 10 high-frequency meter-scale cycles. The high-frequency sequences are composed essentially by progradational asymmetrical cycles, with gradual or abrupt stacking of lithofacies and bounded by maximum regression surfaces (MRS). In this study, the MRS are consistently defined as those that represent an abrupt flooding, marked by a vertical shift of lithofacies associations from shoreface to offshore or offshore transition and from offshore transition to offshore. In cases in which progradational cycles are stacked, the MFS coincides with the MRS. Eight of the ten high-frequency sequences record a gradual lithofacies successions, consisting of 1 to 3 meters thick cycles characterized by the overlying of laterally adjacent lithofacies associations. A complete cycle records the shallowing from offshore to shoreface. However, incomplete cycles showing vertical transition from offshore transition to shoreface or offshore to offshore transition may also occur. Two high-frequency sequences, up to 1.5 m thick, document abrupt lithofacies successions. These cycles are composed by the overlying of lithofacies associations that are not laterally adjacent, passing sharply from offshore to shoreface deposits, without the offshore transition deposits between them.

The presence of different scales of transgressive-regressive cycles in the Caboclo Formation indicates that, similarly to the Phanerozoic, the Proterozoic record is also organized in different stratigraphic orders (Magalhães et al., 2015). The large-scale transgressive-regressive cycle represents long-term variation of the accommodation/sediment supply (A/S) ratio, generating a symmetric sequence with equivalent development of retrogradational and progradational interval. High-frequency cycles respond to high-frequency variations in the A/S ratio (Zecchin, 2007; Catuneanu et al., 2009; Catuneanu and Zecchin, 2013; Magalhães et al.,

2015). Gradual, high-frequency progradational sequences occur in periods of relative sea-level rise or stabilization (normal regression), when the A/S ratio is positive, between 0 and 1. Incomplete and abrupt, high-frequency progradational sequences, took place in periods when the coastline regression occurred in response to a drop in relative sea level (forced regression), when A/S ratio < 0. The asymmetric anatomy of the cycles, essentially composed of regressive intervals, indicates a low-gradient topography of the Caboclo ramp associated with the relatively low sedimentary supply during transgressive phases (Cattaneo and Steel, 2003; Zechin, 2007; Catuneanu and Zecchin, 2013). This interpretation based on the anatomy of the cycles is compatible with the depositional model of the mixed storm-dominated ramp proposed for the Caboclo Formation, which will be discussed in detail in Section 7.2.

7. DISCUSSION

7.1. Carbonate-Siliciclastic Mixing

The hybrid deposits of the Caboclo Formation present compositional mixing that occurs in all layers, with slightly variable siliciclastic/carbonate concentrations. Siliciclastic sediments occur as: (i) nuclei for oolites; (ii) particles trapped by microorganisms; (iii) free in the rock fabric; (iv) constituent of intraclasts (Fig. 3). The persistent and homogeneous composition of the sediments indicates that the terrigenous input was relatively constant and that the carbonate precipitation occurred simultaneously or almost simultaneously with the continental input. Faciological analysis (Fig. 2 and Table 1) suggests fair-weather waves and storm events as the dominant processes during deposition.

The lack of records of continental and coastal deposits does not allow the construction of the precise source of the siliciclastic sedimentary supply to the basin. However, sedimentological features (sorting and roundness of terrigenous grains) allow some inferences about the supply of terrigenous sediments (Folk and Ward, 1957; Flemming, 2007, 2017). The siliciclastic grains are well-sorted and sub-angular to rounded (Fig. 3), indicating selective transport and reworking during long distances. These characteristics suggest a sedimentary supply from terminal portions of alluvial systems. Siliciclastic input can be linked to transport processes in storm periods. Through these events, two mechanisms can contribute to the terrigenous sediment input: (i) alluvial and (ii) storm-surge ebb. During storms, alluvial systems would have higher discharge, increasing the sedimentary supply at the river mouth along the coastline. In addition, with the increase in the coastal setup, the siliciclastic

sediments accumulated in the river mouths were reworked and transported to offshore zones.

During fair-weather periods, siliciclastic grains served as nuclei for the formation of ooids and oncoids, under moderate and constant action of normal waves. During storms, these allochems were mixed with new siliciclastic sediments added to the shoreface, generating hybrid deposits by the mixture of siliciclastic and carbonate grains. It is important to observe that in the studied deposits the size of siliciclastic grains is always one or two granulometric classes smaller than the carbonate allochems. These deposits with different grain sizes, under the same hydrodynamic regime, can be explained by the difference in the density of the particles (Allen, 1984; Flemming, 2017; Garzanti, 2017). In the hybrid arenites from the Caboclo Formation, the grain size difference is promoted by the difference in density between the denser siliciclastic sediments with silt to fine sand size and less denser, fine to coarse sand size carbonate ooids and oncoids. The lower density of the carbonate sediments is linked to their microporosity (Flügel, 2004; Hashim and Kaczmarek, 2019). According to Sellwood and Beckett (1991), microporosity within ooids can vary from 30% (pristine radial) to 50% (micritized). This caused the deposition of coarser carbonate particles together with finer siliciclastic grains. A clear grain-size segregation is recorded only with the gravel fraction (intraclasts), which presents a significantly larger weight than the siliciclastic, ooid and oncoid grains, concentrating at the base of the normally-graded beds. This does not apply to sediments deposited by non-selective processes (i.e. hyperconcentrated flows), in which grain segregation cannot occur.

7.2. Depositional Model

The absence of rimmed shelves deposits (e.g., carbonate sand shoal or reefs and fore-reef talus) and the well-defined offshore, offshore transition and shoreface lithofacies associations, indicates that the studied interval can be interpreted as a very low-gradient ramp with carbonate-siliciclastic sedimentation (Fig. 13). The offshore distal areas are represented mainly by horizontally laminated stromatolites (Fig. 6 and 7). Offshore transition deposits are characterized by the presence of bioherms and horizontal stromatolites intercalated with hybrid lithofacies generated by the action of storm waves (Fig. 8, 9 and 10). In turn, the shoreface portion consists of amalgamated hybrid arenites, with combined flow structures, intercalated

with thin and discontinuous layers of horizontal stromatolites (Fig. 11 and 12). This faciological distribution indicates a storm-dominated carbonate-siliciclastic ramp, with wide microbial colonization from shallow to relatively deep waters (below storm-wave base level).

The ramp morphology of the Caboclo Formation is the result of the balance between the growth and development of stromatolites and the input and distribution of sediments. Stromatolites growth generates morphological differences of the substrate, forming millimetric roughness at lamina scale and bioherms at macro-scale. In both situations, these irregularities are smoothed due to the high rate of sediment mobility induced by normal and storm waves, redistributing the sediments along the coast. The intense wave actions inhibit the development of a platform edge and prevent the ramp from evolving into a rimmed shelf (Dibenedetto and Grotzinger, 2005).

Stromatolites occur from the shoreface to the offshore zones of the mixed carbonate-siliciclastic Caboclo ramp (Fig. 13). The wide distribution and abundance of stromatolites seems to be a feature of the Precambrian (Hofmann, 1973; Knoll and Semikhatov, 1998; Grotzinger and Knoll, 1999; Grotzinger and James, 2000; Riding, 2000; Allwood et al., 2006). The occurrence of stromatolitic deposits of the Caboclo Formation is similar to the Early Proterozoic stromatolitic carbonate platform of Campbellrand subgroup (Beukes, 1987), the Lower Proterozoic Pethei Group carbonate platform (Hoffman, 1974) and the 2.72 Ga stromatolite biofacies of Tumbiana Formation (Coffey et al., 2013). In these units stromatolitic deposits form thick successions (1,500 m in Campbellrand Subgroup; 350 m in Pethei Group) across the entire carbonate platform, from shallower to deeper waters environments. In the Phanerozoic, stromatolites had a more restricted living environment, were less abundant and had less diversity of morphological types (Yancen, 1991; Gomez and Astini, 2015; Brady and Bowie, 2017). Modern stromatolites are present in extreme environments (i.e., springs, hot springs, hypersaline lagoons, alkaline lakes). Exuma Cays in Bahamas is the only current example analogous to the Precambrian coast stromatolites, whereas they are restricted to a proximal narrow belt of the platform (Reid et al., 1995, 2000, 2003; Dupraz et al., 2009; Reid et al., 2011; Bowlin et al., 2012).

The large microbial amount and wide distribution observed in Caboclo Formation (Fig. 13), as well as in other Proterozoic successions, can be linked to two interconnected factors: (i) detrital mud and (ii) predators. The absence of mud reduces water turbidity and increases the luminosity, generating optimal conditions for the substrate colonization by microbial even in relatively deep waters. In addition, microbes were the only life in the middle Proterozoic, with no predators that could inhibit the development of microbial colonies, allowing the stromatolite to occur in different depositional zones of the ramp, as long as there was mineral matter and enough light for photosynthesis (Hofmann, 1973; Walter, 1977; Awramik, 1991; Riding, 2000, 2011).

The characteristic morphologies of stromatolites present in each lithofacies association in the detailed section of the Caboclo Formation are controlled by specific physical parameters (water column, currents - e.g., Logan et al., 1964; Walter, 1977; Andres and Reid, 2006; Dupraz et al., 2006, Varejão et al., 2019). In offshore low-energy distal areas, microbial mats spread laterally over large distances with little or no interference from currents (Fig. 7). In the offshore transition, the morphology of the bioherms is shaped by currents induced by waves (Fig. 10). In times of low energy microbial carpets were established, while during storm events these carpets were disrupted and moulded for tens to hundreds of years, forming isolated buildings. In turn, the constant wave energy on the shoreface inhibits the formation of stromatolites, restricting their occurrence to thin layers of microbial carpets, which in most cases were broken, being incorporated as intraclasts in arenites and conglomerates (Fig. 12).

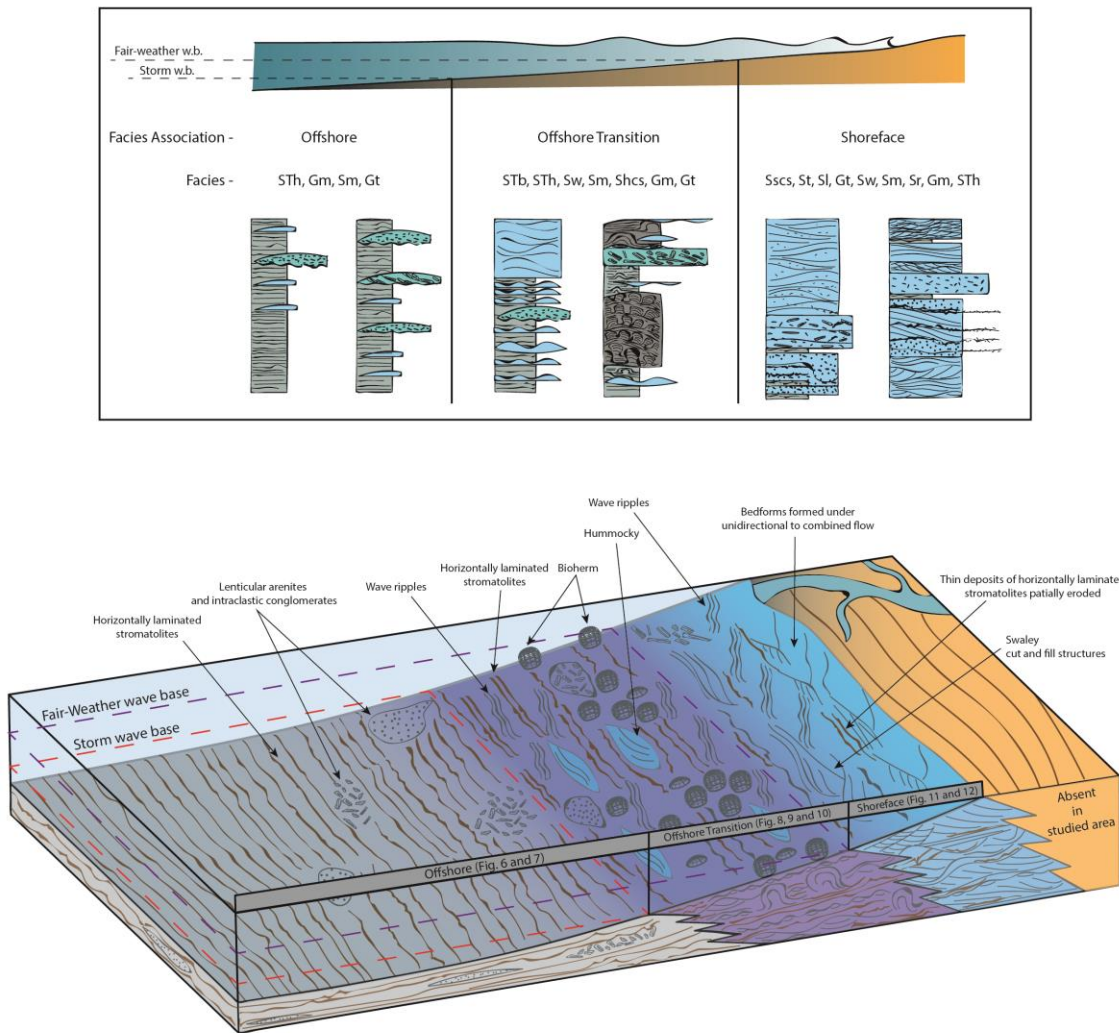


Fig. 13. Distribution of lithofacies and lithofacies associations for the bathymetric profile and the storm and fair-weather wave base limits.

7.3. Compositional Homogeneity in Stratigraphic Succession

Mixed carbonate-siliciclastic ramp models indicate variations in the degree of mixing in facies scale or on specific facies associations, coexisting laterally with purely carbonate or siliciclastic deposits (e.g., Mount, 1984; Sanders and Höfling, 2000; Chiarella, 2017; Gomez and Astini, 2015; Labaj and Pratt, 2016; Schwarz et al., 2018). This variation in the degree of mixing reflects a set of controlling factors related to the processes responsible for the production and deposition of carbonate grains and to the processes linked to the input of siliciclastic sediments. These processes are variable not only in the dip direction, but also in the strike direction, generating depositional models with different trends of spatial distribution of facies (Coffey and Sunde, 2014; Labaj and Pratt, 2016; Schwarz et al., 2016; Schwarz et al., 2018). The Caboclo Formation in the study area differs from other recent and

ancient carbonate-siliciclastic ramps, being characterized by the homogeneity of hybrid deposits throughout the stratigraphic succession (Fig. 2). This compositional homogeneity is linked to the wide distribution and regularity of the siliciclastic input during the sedimentary accumulation. That is, during the interval studied the Caboclo Formation coastal region is characterized by wide alluvial plain with multiple points of sedimentary input that allowed a homogeneous distribution of sandy siliciclastic sediments. During storms there is an increase in fluvial discharge and, consequently, in sediment load transported to the coast. In addition, strong currents induced by storms allow the transport and mixing of siliciclastic sediments stored in the river mouth bars with carbonate grains generated in the basin during fair-weather periods. The very limited presence of silt and clay particles allowed carbonate production was not interrupted in different sectors of the ramp. That is, a high sedimentary supply, mobility and distribution of siliciclastic sandy sediments on a ramp with contemporary carbonate production generates the indiscriminate mixture of sediments, making the deposit homogeneously hybrid.

8. CONCLUSIONS

- Eleven lithofacies are grouped in three lithofacies associations: offshore, offshore transition and shoreface. All lithofacies are compositionally carbonate-siliciclastic and stromatolites occur in all lithofacies associations.
- The faciological analysis indicates a low gradient carbonate-siliciclastic ramp dominated by the action of normal and storm waves, with wide microbial colonization from shallow to relatively deep waters environments.
- The siliciclastic input does not inhibit the carbonate precipitation. The terrigenous input and the carbonate precipitation occurred simultaneously or almost simultaneously.
- The large microbial amount and wide distribution is associated with the absence of detrital mud and the absence of predators. The absence of mud would have reduced the turbidity of water column and increased the luminosity, generating optimal conditions for the substrate colonization even in the deepest portions of the system. In addition, the absence of predators would have allowed the stromatolite to occur in different depositional zones of the ramp without competition.

ACKNOWLEDGMENTS

This paper is part of the PhD thesis carried out by the first author at the Universidade Federal do Rio Grande do Sul (UFRGS) and fully sponsored by Petrobras. JPFF thank Francisco Barbosa for the assistance, dedication and friendship during the fieldwork. L. F. De Ros and G. K. L. Orita are acknowledged for their helpful with the petrographic analysis and constructive comments. The authors thank the editor Professor Wilson Teixeira, and the constructive comments made by Giorgio Basilici and an anonymous reviewer.

REFERENCES

- Aigner, T., 1982. Calcareous tempestites: storm-dominated stratification in Upper Muschelkalk limestones (Middle Trias, SW-Germany). In: Einsele, G., Seilacher, A. (Eds.), Cyclic and event stratification. Springer-Verlag, Heidelberg, Heidelberg, pp. 180-198.
- Alkmim, F.F., Martins-Neto, M.A., 2012. Proterozoic first-order sedimentary sequences of the São Francisco craton, eastern Brazil. *Marine and Petroleum Geology* 33, 127-139.
- Allen, J.R.L., 1984. Wrinkle marks: an intertidal sedimentary structure due to aseismic soft-sediment loading. *Sedimentary Geology* 41, 75-95.
- Allwood, A.C., Walter, M.R., Kamber, B.S., Marshall, C.P., Burch, I.W., 2006. Stromatolite reef from the Early Archean of Australia. *Nature* 441, 714-718.
- Andres, M.S., Reid, R.P., 2006. Growth morphologies of modern marine stromatolites: a case study from Highborne Cay, Bahamas. *Sedimentary Geology* 185, 319-328.
- Awramik, S.M., Riding, R., 1988. Role of algal eukaryotes in subtidal columnar stromatolite formation. *Proceeding of National Academy of Science, USA*, 85, 1327-1329.
- Awramik, S.M., 1991. Archaean and Proterozoic stromatolites. In: Riding, R. (Ed.), *Calcareous algae and stromatolites*. Springer-Verlag, Heidelberg, pp. 289-304.
- Babinski, M., Van Schmus, W.R., Chemale Jr, F., Brito Neves, B.B., Rocha, A.J. D., 1993. Idade isocrônica Pb/Pb em rochas carbonáticas da Formação Caboclo, em Morro do Chapéu, BA. Simpósio sobre o Cráton do São Francisco 2, 160-163.

- Bádenas, B., Aurell, M., 2001. Proximal-distal facies relationships and sedimentary processes in a storm dominated carbonate ramp (Kimmeridgian, northwest of the Iberian Ranges, Spain). *Sedimentary Geology* 139, 319-340.
- Barnaby, R.J., Ward, W.B., 2007. Outcrop analog for mixed siliciclastic–carbonate ramp reservoirs - stratigraphic hierarchy, facies architecture, and geologic heterogeneity: Grayburg Formation, Permian Basin, USA. *Journal of Sedimentary Research* 77, 34-58.
- Basilici, G., de Luca, P.H.V., Poiré, D.G., 2012. Hummocky cross-stratification-like structures and combined-flow ripples in the Punta Negra Formation (Lower-Middle Devonian, Argentine Precordillera): a turbiditic deep-water or storm-dominated prodelta inner-shelf system? *Sedimentary Geology* 267, 73-92.
- Beukes, N.J., 1987. Facies relations, depositional environments and diagenesis in a major early Proterozoic stromatolitic carbonate platform to basinal sequence, Campbellrand Subgroup, Transvaal Supergroup, Southern Africa. *Sedimentary Geology* 54, 1-46.
- Bose, P.K., Eriksson, P.G., Sarkar, S., Wright, D.T., Samanta, P., Mukhopadhyay, S., Mandal, S., Banerjee, S., Altermann, W., 2012. Sedimentation patterns during the Precambrian: a unique record? *Marine Petroleum Geology* 33, 34 – 68.
- Bowlin, E.M., Klaus, J.S., Foster, J.S., Andres, M.S., Custals, L., Reid, R.P., 2012. Environmental controls on microbial community cycling in modern marine stromatolites. *Sedimentary Geology* 263, 45-55.
- Brady, M., Bowie, C., 2017. Discontinuity surfaces and microfacies in a storm-dominated shallow Epeiric Sea, Devonian Cedar Valley Group, Iowa. *The Depositional Record* 3, 136-160.
- Branner, J.C., 1910. The Tombador Escarpment in the State of Bahia, Brazil. *American Journal of Science* 30, 335-343.
- Brito Neves, B.B., Kawashita, K., Delhal, J., 1979. A evolução geocronológica da Cordilheira do Espinhaço; dados novos e integração. *Revista Brasileira de Geociências* 9, 71-85.
- Brito Neves, B.B., Campos Neto, M.D.C., Fuck, R.A., 1999. From Rodinia to Western Gondwana: an approach to the Brasiliano-Pan African Cycle and orogenic collage. *Episodes-Newsmagazine of the International Union of Geological Sciences* 22, 155-166.
- Burchette, T.P., Wright, V.P., 1992. Carbonate ramp depositional systems. *Sedimentary geology* 79, 3-57.

- Campos Neto, M.C., 2000. Orogenic systems from southwester Gondwana. In: Cordani, U.G., Milani, E.J Thomaz Filho, A., Campos, D.A. (Eds.), Tectonic Evolution of South America, 31th International Geological Congress. Rio de Janeiro, Brasil, pp. 335-365.
- Cattaneo, A., Steel, R.J., 2003. Transgressive deposits: a review of their variability. *Earth-Science Reviews* 62, 187-228.
- Catuneanu, O., 2006. Principles of sequence stratigraphy. Amsterda: Elsevier, 375 p.
- Catuneanu, O., 2019. Scale in sequence stratigraphy. *Marine and Petroleum Geology* 106, 128-159.
- Catuneanu, O., Zecchin, M., 2013. High-resolution sequence stratigraphy of clastic shelves II: controls on sequence development. *Marine and Petroleum Geology* 39, 26-38.
- Catuneanu, O., Abreu, V., Bhattacharya, J.P., Blum, M.D., Dalrymple, R.W., Eriksson, P.G., Fielding, C.R., Fisher, W.L., Galloway, W.E., Gibling, M.R., Giles, K.A., Holbrook, J.M., Jordan, R., Kendall, C.G.St.C., Macurda, B., Martinsen, O.J., Miall, A.D., Neal, J.E., Nummedal, D., Pomar, L., Posamentier, H.W., Pratt, B.R., Sarg, J.F., Shanley, K.W., Steel, R.J., Strasser, A., Tucker, M.E., Winker, C., 2009. Towards the standardization of sequence stratigraphy. *Earth-Science Reviews* 92, 1-33.
- Chemale Jr., F., Alkmim, F.F., Endo, I., 1993. Late Proterozoic tectonism in the interior of the São Francisco craton. In: Findlay, R.H., Uhrug, R., Banks, M.R., Veevers, J.J. (Eds.), *Gondwana eight: assembly, evolution and dispersal*. Balkema, Rotterdam, pp. 29-41.
- Chemale Jr., F., Dussin, I.A., Alkmim, F.F., Martins, M.S., Queiroga, G., Armstrong, R., Santos, M.N., 2012. Unravelling a Proterozoic basin history through detrital zircon geochronology: The case of the Espinhaço Supergroup, Minas Gerais, Brazil. *Gondwana Research* 22, 200-206.
- Chen, J., 2014. Surface and subsurface reworking by storms on a Cambrian carbonate platform: evidence from limestone breccias and conglomerates. *Geologos* 20, 13-23.
- Chiarella, D., Longhitano, S.G., Tropeano, M., 2017. Types of mixing and heterogeneities in siliciclastic-carbonate sediments. *Marine and Petroleum Geology* 88, 617-627.
- Coffey, J.M., Flannery, D.T., Walter, M.R., George, S.C., 2013. Sedimentology, stratigraphy and geochemistry of a stromatolite biofacies in the 2.72 Ga

- Tumbiana Formation, Fortescue Group, Western Australia. Precambrian Research 236, 282-296.
- Coffey, B.P., Sunde, R.F., 2014. Lithology-based sequence-stratigraphic framework of a mixed carbonate-siliciclastic succession, Lower Cretaceous, Atlantic coastal plain. AAPG Bulletin 98, 1599-1630.
- Collins, D.S., Johnson, H.D., Allison, P.A., Guilpain, P., Damit, A.R., 2017. Coupled 'storm-flood' depositional model: Application to the Miocene–Modern Baram Delta Province, north-west Borneo. Sedimentology 64, 1203-1235.
- CPRM – SERVIÇO GEOLÓGICO DO BRASIL; 2003. Geologia e recursos minerais do Estado da Bahia: Sistema de Informações Geográficas – SIG. Versão 1.1. Salvador: CPRM, 1 CD-ROM. Convênio CPRM-CBPM.
- Cruz, S.C., Alkmim, F.F., 2006. The tectonic interaction between the Paramirim aulacogen and the Araçuaí belt, São Francisco craton region, Eastern Brazil. Anais da Academia Brasileira de Ciências 78, 151-173.
- Dibenedetto, S., Grotzinger, J., 2005. Geomorphic evolution of a storm-dominated carbonate ramp (c. 549 Ma), Nama Group, Namibia. Geological Magazine 142, 583-604.
- Dickson, J.A.D., 1965. A modified staining technique for carbonates in thin section. Nature 205, 587.
- Dott Jr, R.H., Bourgeois, J., 1982. Hummocky stratification: significance of its variable bedding sequences. Geological Society of America Bulletin 93, 663-680.
- Dumas, S., Arnott, R.W.C., 2006. Origin of hummocky and swaley cross-stratification. The controlling influence of unidirectional current strength and aggradation rate. Geology 34, 1073-1076.
- Dunham, R.J., 1962. Classification of carbonate rocks according to depositional texture. In: Ham, W.E. (Ed.), Classification of Carbonate Rocks. American Association of Petroleum Geologists Memoir 1, pp. 108-121.
- Dupraz, C., Pattison, R., Verrecchia, E.P., 2006. Translation of energy into morphology: Simulation of stromatolite morphospace using a stochastic model. Sedimentary Geology 185, 185-203.
- Dupraz, C., Reid, R.P., Braissant, O., Decho, A.W., Norman, R.S., Visscher, P.T., 2009. Processes of carbonate precipitation in modern microbial mats. Earth-Science Reviews 96, 141-162.
- Embry, A.F., Klovan, J.E., 1971. A Late Devonian reef tract on Northeastern Banks Island, NWT. Canadian Petroleum Geology Bulletin 19, 730-781.

- Flemming, B.W., 2007. The influence of grain-size analysis methods and sediment mixing on curve shape and textural parameters: Implications for sediment trend analysis. *Sedimentary Geology* 202, 425-435.
- Flemming, B.W., 2017. Particle shape-controlled sorting and transport behavior of mixed siliciclastic/bioclastic sediments in a mesotidal lagoon, South Africa. *Geo-Marine Letters* 37, 397-410.
- Flügel, E., 2004. Microfacies of carbonate rocks, analysis, interpretation and application. Springer Verlag, Berlin, Heidelberg, New York, 976 p.
- Folk, R.L., Ward, W.C., 1957. Brazos River bar: a study in the significance of grain size parameters. *Journal of Sedimentary Petrology* 27, 3-26.
- Frantz, C.M., Petryshyn, V.A., Corsetti, F.A., 2015. Grain trapping by filamentous cyanobacterial and algal mats: implications for stromatolite microfabrics through time. *Geobiology* 13, 409-423
- Garzanti, E., 2017. The Maturity Myth In Sedimentology and Provenance Analysis. *Journal of Sedimentary Research* 87, 353-365.
- Gebelein, C.D., 1969. Distribution, morphology, and accretion rate of recent subtidal algal stromatolites, Bermuda. *Journal of Sedimentary Research* 39, 49-69.
- Gomez, F.J., Astini, R.A., 2015. Sedimentology and sequence stratigraphy from a mixed (carbonate–siliciclastic) rift to passive margin transition: the Early to Middle Cambrian of the Argentine Precordillera. *Sedimentary Geology* 316, 39-61.
- Grotzinger, J.P., Knoll, A.H., 1999. Stromatolites in Precambrian carbonates: evolutionary mileposts or environmental dipsticks? *Annual review of earth and planetary sciences* 27, 313-358.
- Grotzinger, J.P., James, N.P., 2000. Precambrian carbonates: evolution of understanding. In: Grotzinger, J.P., James, N.P. (Eds.), *Carbonate Sedimentation and Diagenesis in the Evolving Precambrian World*. SEPM Special Publication 67, pp. 3–20.
- Guadagnin, F., Chemale Jr, F., Magalhães, A.J.C., Santana, A., Dussin, I., Takehara, L., 2015. Age constrains on crystal-tuff from the Espinhaço Supergroup – Insight into the Paleoproterozoic to Mesoproterozoic intracratonic basin cycles of the Congo-São Francisco Craton. *Gondwana Research* 27, 363-376.
- Haines, P.W., 1988. Storm-dominated mixed carbonate/siliciclastic shelf sequence displaying cycles of hummocky cross-stratification, late Proterozoic Wonoka Formation, South Australia. *Sedimentary Geology* 58, 237-254.

- Hashim, M.S., Kaczmarek, S.E., 2019. A review of the nature and origin of limestone microporosity. *Marine and Petroleum Geology* 107, 527-554.
- Hoffman, P., 1974. Shallow an deepwater stromatolites in lower Proterozoic platform - to - basin facies change, Great Slave Lake, Canada. *The American Association of Petroleum Geologists Bulletin* 58, 856-867.
- Hofmann, H.J., 1973. Stromatolites: characteristics and utility. *Earth-Science Reviews* 9, 339-373.
- Johnson, J.G., Murphy, M.A., 1984. Time-rock model for Siluro-Devonian continental shelf, western United States. *Geological Society of America Bulletin* 95, 1349-1359.
- Knoll, A.H., Semikhatov, M.A., 1998. The genesis and time distribution of two distinctive Proterozoic stromatolite microstructures. *Palaios* 13, 408-422.
- Labaj, M.A., Pratt, B.R., 2016. Depositional dynamics in a mixed carbonate-siliciclastic system: Middle-Upper Cambrian Abrigo Formation, southeastern Arizona, USA. *Journal of Sedimentary Research* 86, 11-37.
- Leckie, D.A., Walker, R.G., 1982. Storm- and tide-dominated shorelines in Cretaceous Moosebar-Lower Gates interval - outcrop equivalents of Deep Basin gas trap in western Canada. *AAPG bulletin* 66, 138-157.
- Logan, B.W., Rezak, R., Ginsburg, R.N., 1964. Classification and environmental significance of algal stromatolites. *The Journal of Geology* 72, 68-83.
- Magalhães, A.J.C., Raja Gabaglia, G.P., Scherer, C.M.S., Bállico, M.B., Guadagnin, F., Bento Freire, E., Silva Born, L.R., Catuneanu, O., 2015. Sequence hierarchy in a Mesoproterozoic interior sag basin: from basin fill to reservoir scale, the Tombador Formation, Chapada Diamantina Basin, Brazil. *Basin Research* 28, 393-432.
- Marshak, S., Alkmim, F.F., 1989. Proterozoic contraction/extension tectonics of the southern São Francisco region, Minas Gerais, Brazil. *Tectonics* 8, 555-571.
- Martins-Neto, M.A., 2000. Tectonics and sedimentation in a paleo/mesoproterozoic rift-sag basin (Espinhaço basin, southeastern Brazil). *Precambrian Research* 103, 147-173.
- Molina, J.M., Ruiz-Ortiz, P.A., Vera, J.A., 1997. Calcareous tempestites in pelagic facies (Jurassic, Betic Cordilleras, southern Spain). *Sedimentary Geology* 109, 95-109.
- Mount, J.F., 1984. Mixing of siliciclastic and carbonate sediments in shallow shelf environments. *Geology* 12, 432-435.

- Myrow, P.M., Southard, J.B., 1996. Tempestite deposition. *Journal of Sedimentary Research* 66, 875-887.
- Myrow, P.M., Fischer, W., Goodge, J.W., 2002. Wave-modified turbidites: combined-flow shoreline and shelf deposits, Cambrian, Antarctica. *Journal of Sedimentary Research* 72, 641-656.
- Pedreira, A.J., 1994. O Supergrupo Espinhaço na Chapada Diamantina centro oriental, Bahia: Sedimentologia, estratigrafia e tectônica. São Paulo, USP, Instituto de Geociências, 126 p.
- Pérez-López, A., Pérez-Valera, F., 2012. Tempestite facies models for the epicontinental Triassic carbonates of the Betic Cordillera (southern Spain). *Sedimentology* 59, 646-678.
- Pesonen, L.J., Mertanen, S., Veikkolainen, T., 2012. Paleo-Mesoproterozoic supercontinents - a paleomagnetic view. *Geophysica* 48, 5-47.
- Pisarevsky, S.A., Elming, S.Å., Pesonen, L.J., Li, Z.X., 2014. Mesoproterozoic paleogeography: supercontinent and beyond. *Precambrian Research* 244, 207-225.
- Posamentier, H., Vail, P., 1988. Eustatic controls on clastic deposition, II: sequence and systems tract models. In: Wilgus, C.K., Hastings, B.S., Kendall, C.G.St.C., Posamentier, H.W., Ross, C.A., Van Wagoner, J.C. (Eds.), *Sea Level Changes: an Integrated Approach*. SEPM Special Publication 42, pp. 125-154.
- Preiss, W.V., 1976. Basic field and laboratory methods for the study of stromatolites. In: Walter, M.R. (Ed.), *Stromatolites. Developments in Sedimentology*, Vol. 20. Elsevier, Amsterdam, pp. 5-13.
- Reading, H.G., Collinson, J.D., 1996. Clastic Coasts. In: Reading, H.G. (Ed.), *Sedimentary Environments: Processes, Facies and Stratigraphy*, 3rd. Edition, pp. 154-231.
- Reid, R.P., Macintyre, I.G., Browne, K.M., Steneck, R.S., Miller, T., 1995. Modern Marine Stromatolites in the Exuma Cays, Bahamas: Uncommonly Common. *Facies* 33, 1-17.
- Reid, R.P., Visscher, P.T., Decho, A.W., Stoltz, J.F., Bebout, B.M., Dupraz, C., Macintyre, I.G., Paerl, H.W., Pinckney, J.L., Prufert-Bebout, L., Steppe, T.F., DesMarais, D.J., 2000. The role of microbes in accretion, lamination and early lithification of modern marine stromatolites. *Nature* 406, 989-992.
- Reid, P., Dupraz, C.D., Visscher, P.T., Sumner, D.Y., 2003. Microbial processes forming marine stromatolites: microbe-mineral interactions with a three-billion-

- year rock record. In: Krumbein, W. E., Paterson, D. M., Zavarzin, G. A. (Eds), *Fossil and Recent Biofilms – A Natural History of Life on Earth*. Springer, Dordrecht, pp. 103-118.
- Reid, R.P., Foster, J.S., Radtke, G., Golubic, S., 2011. Modern marine stromatolites of Little Darby Island, Exuma Archipelago, Bahamas: environmental setting, accretion mechanism and role of euendoliths. In: Reitner, et al. (Ed.), *Advances in Stromatolite Geobiology*. Lecture Notes in Earth Sciences 131, pp. 77–89.
- Riding, R., 1991. Classification of microbial carbonates. In: Riding, R. (Ed.), *Calcareous Algae and Stromatolites*, Springer-Verlag, Berlin, pp. 21–51.
- Riding, R., 2000. Microbial carbonates: the geological record of calcified bacterial-algal mats and biofilms. *Sedimentology* 47, 179-214.
- Riding, R., 2011. Microbialites, stromatolites, and thrombolites. In: Reitner, J., Thiel, V. (Eds.), *Encyclopedia of geobiology, Encyclopedia of Earth Sciences Series*. Springer Netherlands, pp. 635-654.
- Rocha, A.J., Pereira, C.P., Srivastava, N.K., 1992. Carbonatos da Formação Caboclo (Proterozóico médio) na região de Morro do Chapéu - Estado da Bahia. *Revista Brasileira de Geociências* 22, 389-398.
- Sanders, D., Höfling, R., 2000. Carbonate deposition in mixed siliciclastic-carbonate environments on top of an orogenic wedge (Late Cretaceous, Northern Calcareous Alps, Austria). *Sedimentary Geology* 137, 127-146.
- Saylor, B.Z., 2003. Sequence stratigraphy and carbonate-siliciclastic mixing in a terminal Proterozoic foreland basin, Urusis Formation, Nama Group, Namibia. *Journal of Sedimentary Research* 73, 264-279.
- Scheibner, C., Kuss, J., Speijer, R.P., 2003. Stratigraphic modelling of carbonate platform-to-basin sediments (Maastrichtian to Paleocene) in the Eastern Desert, Egypt. *Palaeogeography, Palaeoclimatology, Palaeoecology* 200, 163-185.
- Schwarz, E., Veiga, G.D., Álvarez Trentini, G., Isla, M.F., Spalletti, L.A., 2018. Expanding the spectrum of shallow-marine, mixed carbonate-siliciclastic systems: Processes, facies distribution and depositional controls of a siliciclastic-dominated example. *Sedimentology* 65, 1558-1589.
- Schwarz, E., Veiga, G.D., Trentini, G.Á., Spalletti, L.A., 2016. Climatically versus eustatically controlled, sediment-supply-driven cycles: Carbonate-siliciclastic, high-frequency sequences in the Valanginian of the Neuquén Basin (Argentina). *Journal of Sedimentary Research* 86, 312-335.

- Sellwood, B.W., Beckett, D., 1991. Ooid microfabrics: the origin and distribution of high intra-ooid porosity; Mid-Jurassic reservoirs, S. England. *Sedimentary Geology* 71, 189-193.
- Souza, V.H.P., Bezerra, F.H.R., Vieira, L.C., Cazarin, C.L., Brod, J.A., 2021. Hydrothermal silicification confined to stratigraphic layers: Implications for carbonate reservoirs. *Marine and Petroleum Geology* 124, 104818.
- Spalletti, L.A., Franzese, J.R., Matheos, S.D., Schwarz, E., 2000. Sequence stratigraphy of a tidally dominated carbonate-siliciclastic ramp; the Tithonian–Early Berriasian of the Southern Neuquén Basin, Argentina. *Journal of the Geological Society* 157, 433-446.
- Srivastava, N.K., 1988. Estromatólitos da Formação Caboclo na Região de Morro do Chapéu: relatório de consultoria I. Salvador: CPRM.
- Thrana, C., Talbot, M.R., 2006. High-frequency carbonate-siliciclastic cycles in the Miocene of the Lorca Basin (Western Mediterranean, SE Spain). *Geologica Acta* 4, 343-354.
- Tucker, M., 1982. Storm-surge sandstones and the deposition of interbedded limestone: Late Precambrian, southern Norway. In: Einsele, G., Seilacher, A. (Eds.), *Cyclic and event stratification*. Springer-Verlag, Heidelberg, pp. 363-370.
- Tucker, M.E., 2003. Mixed clastic-carbonate cycles and sequences: Quaternary of Egypt and Carboniferous of England. *Geologia Croatica* 56, 19-37.
- Varejão, F.G., Fürsich, F.T., Warren, L.V., Matos, S.A., Rodrigues, M.G., Assine, M.L., Sales, A.M.F., Simões, M.G., 2019. Microbialite fields developed in a protected rocky coastaline: The shallow carbonate ramp of the Aptian Romualdo Formation (Araripe Basin, NE Brazil). *Sedimentary Geology* 389, 103-120.
- Walker, R.G., James, N.P., 1992. Facies models: response to sea level change. Newfoundland, Canada: Geological Association of Canada 409 p.
- Walter, M.R., 1977. Interpreting stromatolites. *American Scientist* 65, 563-571.
- Yancey, T.E., 1991. Controls on carbonate and siliciclastic sediment deposition on a mixed carbonate-siliciclastic shelf (Pennsylvanian Eastern Shelf of north Texas). *Kansas Geological Survey, Bulletin* 233, 263-272.
- Zecchin, M., 2007. The architectural variability of small-scale cycles in shelf and ramp clastic systems: The controlling factors. *Earth-Science Reviews* 84, 21–55.
- Zuffa, G.G., 1980. Hybrid arenites; their composition and classification. *Journal of Sedimentary Research* 50, 21-29.

The screenshot shows a software interface for managing manuscript submissions. At the top, there's a red header bar with the text 'PRECAMBRIAN RESEARCH'. Below it, a black navigation bar includes links like 'HOME', 'LOGOUT', 'HELP', 'REGISTER', 'UPDATE MY INFORMATION', 'JOURNAL OVERVIEW', 'MAIN MENU', 'CONTACT US', 'SUBMIT A MANUSCRIPT', 'INSTRUCTIONS FOR AUTHORS', and 'PRIVACY'. On the right side of the top bar, it says 'Role: Author' and 'Username: joaopedroformolo@hotmail.com'. There's also a circular arrow icon.

The main area is titled 'Submissions with an Editorial Office Decision for Author João Pedro Formolo Ferronatto'. It displays two rows of submission details:

Action	Manuscript Number	Title	Authorship	Initial Date Submitted	Status	Current Status	Date Final Disposition Set	Final Disposition
Action Links	PRECAM_2018_320	SEQUENCE STRATIGRAPHY OF THE MIXED WAVE-TIDAL-DOMINATED MESOPROTEROZOIC SEDIMENTARY SUCCESSION IN CHAPADA DIAMANTINA BASIN, ESPÍNHAO SUPERGROUP- NE/BRAZIL	Other Author	Jul 18, 2018	Mar 14, 2019	Completed - Accept	Mar 14, 2019	Accept
Action Links	PRECAM-D-20-00067	Mixed carbonate-siliciclastic sedimentation in a Mesoproterozoic storm-dominated ramp: depositional processes and stromatolite development.	Corresponding Author	Sep 01, 2020	Apr 18, 2021	Accept		

Below the table, there are two small text blocks: 'Page: 1 of 1 (2 total completed submissions)' and 'Display 10 results per page.'

Decision on submission to Precambrian Research

Precambrian Research em@editorialmanager.com

Dom, 18/04/2021 09:21

Para: João Pedro Formolo Ferronatto joaopedroformolo@hotmail.com

Manuscript Number: PRECAM-D-20-00067R2

Mixed carbonate-siliciclastic sedimentation in a Mesoproterozoic storm-dominated ramp: depositional processes and stromatolite development.

Dear Dr. Ferronatto,

Thank you for submitting your manuscript to Precambrian Research.

I am pleased to inform you that **your manuscript has been accepted for publication.**

My comments, and any reviewer comments, are below.

Your accepted manuscript will now be transferred to our production department. We will create a proof which you will be asked to check, and you will also be asked to complete a number of online forms required for publication. If we need additional information from you during the production process, we will contact you directly.

We appreciate you submitting your manuscript to Precambrian Research and hope you will consider us again for future submissions.

Kind regards,
Wilson Teixeira, Pd.D.
Editor

Precambrian Research

9.2 ARTIGO 2 – Mesoproterozoic siliciclastic stromatolites of Chapada Diamantina (Brazil): morphological types, genesis and environmental context.

João Pedro Formolo Ferronatto¹, Claiton Marlon dos Santos Scherer¹, Bruno Silverstone Angonese¹, Amanda Goulart Rodrigues¹, Ezequiel Galvão de Souza², Carrel Kifumbi¹, Adriano Domingos dos Reis¹, Felipe Guadagnin², Caroline Lessio Cazarin³

¹Instituto de Geociências, Universidade Federal do Rio Grande do Sul (UFRGS), Campus do Vale, Av. Bento Gonçalves, 9500; 91509-900, Porto Alegre/RS, Brazil.

²Universidade Federal do Pampa (Unipampa), Campus Caçapava do Sul. Av. Pedro Anunciação, 111 - Vila Batista, 96570-000, Caçapava do Sul/RS, Brazil.

³CENPES – Petróleo Brasileiro S.A. (PETROBRAS), 21941-915, Rio de Janeiro/RJ, Brazil.

ABSTRACT

Laminations of organosedimentary constructions can be formed by three distinct processes:(i) bioinduced mineral precipitation, (ii) trapping and binding and (iii) abiotic mineral precipitation, and each of these processes occurs preferentially in a particular geological time interval. Agglutinated stromatolites are rare and seem to form in specific environmental conditions. Siliciclastic stromatolites are an even rarer class of agglutinated stromatolites, which are formed in response to the process of trapping and binding of siliciclastic grains by erect filaments or by extracellular polymers substances (EPS). This research describe and interpret one of the oldest siliciclastic stromatolites of the geological record and discuss the microbial evidences and mechanisms that controlled their accumulation and preservation. Two compound sections were analyzed and ten thin sections were prepared to characterize the siliciclastic stromatolites from the Mesoproterozoic Caboclo Formation. Stromatolites are present in two different lithofacies associations: (i) shoreface and (ii) offshore transition. The shoreface stromatolites are characterized by silty to sandy fabric and poor lamination, and the distal ones by clay, silt grains, relatively less sand and distinct lamination. The volume of siliciclastic grains composing the stromatolites fabric is > 85% in the shoreface and > 30% in offshore transition. These stromatolites were deposited in a favorable environment for trapping and binding of siliciclastic sediments: a wave-dominated siliciclastic ramp with availability of siliciclastic grains and common water column agitation. The marine environment is favorable to forming EPS with good adhesive properties. Besides, the Caboclo Formation age (1.3 – 1.0 Ga) coincides with an abrupt fall in the amount of atmospheric CO₂, reflected in CaCO₃ saturation in the oceans. This change in ocean chemistry may have led to a change in the stromatolite fabric, from sparry crust and fine-grained precipitated to agglutinated.

Keywords: Agglutinated stromatolites; Microbial; Precambrian stromatolites; Espinhaço Supergroup; Proterozoic

1. INTRODUCTION

Stromatolites are the only record of life during 85% of the Earth's geological history. They are found from the Archean to the present, having their acme in the Proterozoic and their decline in the Cambrian (Logan, 1961; Hofmann, 1973; Walter, 1977; Pratt, 1982; Knoll and Semikhatov, 1998; Reid et al., 2000; Allwood et al., 2006). The hypotheses about the decline of microbial deposits are related to the abrupt decrease in CO₂ concentrations in the atmosphere composition and consequently in the CaCO₃ saturation in the oceanic waters, and/or due to the competition generated on the appearance of more evolved organisms (Monty, 1973; Pratt, 1982; Grotzinger, 1990; Riding, 2011). The laminations of these organosedimentary constructions can be formed by three distinct processes: (i) bioinduced mineral precipitation (fine-grained stromatolites), (ii) trapping and binding (agglutinated stromatolites) and (iii) abiotic mineral precipitation (sparry crust stromatolites), and each of these processes occurs preferentially in a particular geological time interval (Awramik e Riding, 1988; Grotzinger, 1990; Riding, 2011; Frantz et al., 2015).

During most of the Archean, the stromatolite fabric was formed exclusively by abiotic mineral precipitation, generating a sparry crust fabric. In the Paleoproterozoic and Mesoproterozoic, the stromatolitic fabric was composed of both abiotic and biotic mineral precipitation (sparry crust and fine-grained hybrid fabric). Throughout the Neoproterozoic and Phanerozoic, fine-grained was the main component of the stromatolite fabrics. In turn, agglutinated textures generated by trapping and binding processes are rare in the stromatolite record, being more common during the Mesozoic and Cenozoic with the oldest record found in the Mesoproterozoic (Table 1; Schieber, 1988). Agglutinated stromatolites seem to form in specific environmental conditions. The examples described in the literature were formed in high-energy shallow marine environments, commonly with tidal influence (see Table 1 and 2 in Suarez-Gonzalez et al., 2019; Riding, 2000). Siliciclastic stromatolites are an even rarer class of agglutinated stromatolites (Table 1), which are formed in response to the process of trapping and binding of siliciclastic grains by erect filaments or by extracellular polymers substances (EPS).

The well-preserved stromatolites from the upper half of Caboclo Formation are one of the oldest examples in the geological record formed by trapping and binding of

siliciclastic silt and sand grains. The main objective of this paper is to describe and interpret these siliciclastic stromatolites and discuss the mechanisms that controlled their accumulation and preservation. The specific objectives are: (i) to characterize the different morphotypes of Mesoproterozoic siliciclastic stromatolites and (ii) to understand the occurrence of these morphotypes in a siliciclastic ramp dominated by normal and storm waves.

1 **Table 1.** Compilation of the siliciclastic stromatolites found in the bibliography.

Bibliography	Age	Formation and Location	Paleoenvironment	Stromatolite Structures	
				Macro and Mesoscale	Microscale
Schwarz et al., 1975	Recent	Saint Jean Bay, Mauritania	Stromatolites occur along the strand line of the inner part of the bay. Their position within the tidal range was found between mean low level and about 0.40 m above it.	Flat stromatolite mat with slight depressions and humps, small islets, cusps, arches, isolated domes, or peninsulas are typical structures.	Nearly horizontal lamination, 2-7 mm thick. Each layer is formed by a film of aragonite. The main part of a layer consists of sand and silt with upwards increasing portions of algal filaments. Quartz sand and faecal pellets are the main constituents of the stromatolites.
Martin et al., 1993; Braga et al., 1995; Braga and Martin, 2000	Miocene	Terminal Complex and Sorbas Member, Sorbas Basin, SE Spain	Mixed siliciclastic-carbonate depositional environment. Beach deposits. Stromatolites formed at the transition from the lowermost beach shoreface to the shelf.	Large microbial domes (dimensions in meters) form thin biostromes and small bioherms. Proximal domes have high synoptic relief with steep sides. Downslope, they grade into large, flattened stromatolites with gentle sides.	Millimetric lamination made up of dense, peloidal, clotted and bushy micrite, interpreted as microbial precipitated, together with siliciclastic particles. Micrite as bundles of vertical filaments.
Marcinowski and Szulczewski, 1972	Cretaceous	Jura Chain, Poland	Carbonate-siliciclastic sequence. High-energy, shallow marine water below the intertidal zone.	Biostrome composed of many small stromatolites up to 3 cm in diameter. Individual stromatolites are dome-shaped to stubby low-cylindrical. Usually they do not branch.	The stromatolites are composed of a partly chemical and partly detrital material, mostly a micritic calcium carbonate. Millimetric lamination formed by the alternation of chemical precipitaton and detrital quartz and glauconite.
Hardwood, 1990	Permian	Yates Fm., New Mexico, USA	Mixed carbonate-siliciclastic shallow marine sequence.	Stromatolite heads reach over 1 m in vertical and lateral dimension.	----
Bertrand-Sarfati,	Carboniferous	Ajjers Basin,	The lower unit was	Lower unit: Domal bioherms, up	Clay and silt size quartz is

1994		Eastern Sahara, Algeria	probably deposited in coastal lakes, protected from marine Waters. The upper unit is deposited in an intertidal lagoon isolated from open sea	to 0,8 to 1 m height and 0,5 - 0,8 m in diameter. They grow first asymmetrically, then laminae type changes and they grow in an upward direction building bulbous columns. Upper unit: Discrete domes (20 cm) coalescing in large domes (1-1.5 m thick and up to 2-2.5 m diameter). Laminae in the domes are pseudo columnar.	present in almost all the laminae (10 to 50 %). The laminae are moderately convex, pseudocolumnar. Stromatolite laminae is a siliciclastic-micritic mat, interpreted as built by non filamentous micro-organisms, probably bactéria. Microbial filaments and bushes.
Draganits and Noffke, 2004	Devonian	Muth Fm., Pin Valley, NW Himalayas, India	Mixed siliciclastic-carbonate wave-dominated barrier-island system. Siliciclastic stromatolites occur in foreshore and shoreface zones.	Stromatolite domes are up to 80 cm in diameter and some 30 cm high. The vertical stacking pattern of the domes is random.	The layers are millimetric, with diffuse, wavy lamination. Detrital grains commonly constitute more than 60% of the layers.
Druschke et al., 2009	Ordovician	Eureka Quartzite, SE California and S Nevada, USA	High-energy shallow marine environments. Stromatolites occur in lower and upper shoreface.	Well-preserved domal stromatolites that increase in size and abundance up-section. Isolated forms in lower shoreface (5 to 15 cm wide and 3 to 8 cm high) grade into larger and more conspicuous stromatolite domes in upper shoreface (30 to 50 cm wide and 30 to 80 cm high).	Laminae 1 to 5 mm thick composed of alternating white and dark-grey layers. Laminae volumetrically consist of >70% very fine-grained to medium-grained quartz sand. Darker layers are commonly enriched in opaque minerals consisting mainly of pyrite and ferric iron oxide.
Davis, 1968	Ordovician	New Richmond Sandstone, Minnesota, USA	Deposition near the boundary between a shallow quartz sand environment and an intertidal carbonate environment.	Domal bioherms with 60 cm diameter.	Obscure layering of well-sorted, medium-grained quartz sand. Thin bands of dolomite parallel to layering.
Soudry and Weissbrod, 1995	Cambrian	Timna Fm., Elat,	Tidal Stromatolites sequence.	The stromatolites have a lateral extension of a few meters. They	Stromatolitic fabric is finely laminated and poorly defined. Quartz grains,

	Southern Israel	within channelled cross-stratified sandstones.	are mostly pseudocolumnar, eventually columnar.	together with small amounts of mica and K-feldspar, make up 70% of the stromatolitic fabric. Detrital grains are cemented by calcite and dolomite spar.
Schieber, 1998	Mesoproterozoic Mt. Shields Fm, Belt Supergroup, Montana, U.S.A.	Shallow nearshore	Large domal stromatolites (< 1 m).	Millimetric alternation of finely crystalline dolomitic laminae and terrigenous laminae that contain abundant detrital quartz grains.

2. GEOLOGICAL SETTING

The Mesoproterozoic Stenian Caboclo Formation, part of Espinhaço Supergroup, crops out in the central-northern region of São Francisco Craton, in the physiographic region of Chapada Diamantina on Paramirim Aulacogen (Fig. 1). During the Archean and Paleoproterozoic, São Francisco Craton and Congo Craton formed part of the Rodinia Supercontinent (Brito Neves et al 1999; Campos Neto, 2000). The Espinhaço Supergroup deposited after the amalgamation of these two cratons at 1.8 Ga and before partial break-up at 0.9 Ga (Brito Neves et al., 1979; Chemale et al., 1993; Martins-Neto, 2000; Alkmim and Martins-Neto, 2012) and is interpreted as a sequence of events of intracontinental rift-sag basins.

The Espinhaço Supergroup can be divided into three 1st order megasequences (Chemale et al., 2012; Guadagnin et al., 2015): Low, Middle and Upper Espinhaço (Fig. 1). At Chapada Diamantina domain, the Caboclo Formation and Morro do Chapéu Formation form the Upper Espinhaço sequence (1.19 to 0.9 Ga). The basal contact of Caboclo Formation with alluvial/aeolian deposits of Tombador Formation (Middle Espinhaço megasequence; 1416 ± 28 Ma – Guadagnin et al., 2015) is transgressive and paraconformable. The upper contact with the Morro do Chapéu Formation (934 ± 14 Ma; Loureiro et al., 2008) is marked by a disconformity. Thus, the Caboclo and Morro do Chapéu formations are distinct 2nd order sequences nested in the Upper Espinhaço 1st order megasequence (Guadagnin et al., 2015).

The Caboclo Formation (Branner, 1910; Srivastava, 1988; Rocha et al., 1992; Babinski et al., 1993; Pedreira, 1994) is interpreted as a mixed siliciclastic-carbonate storm dominated ramp located at low latitude (Pesonen et al., 2012; Pisarevsky et al., 2014). Sedimentation is dominated by siliciclastics (mudstones and sandstones) with subordinate mixed siliciclastic-carbonate deposits. Depositional age of Caboclo Formation carbonates was dated by radiometric Pb-Pb method at 1140 ± 140 Ma (Babinski et al., 1993).

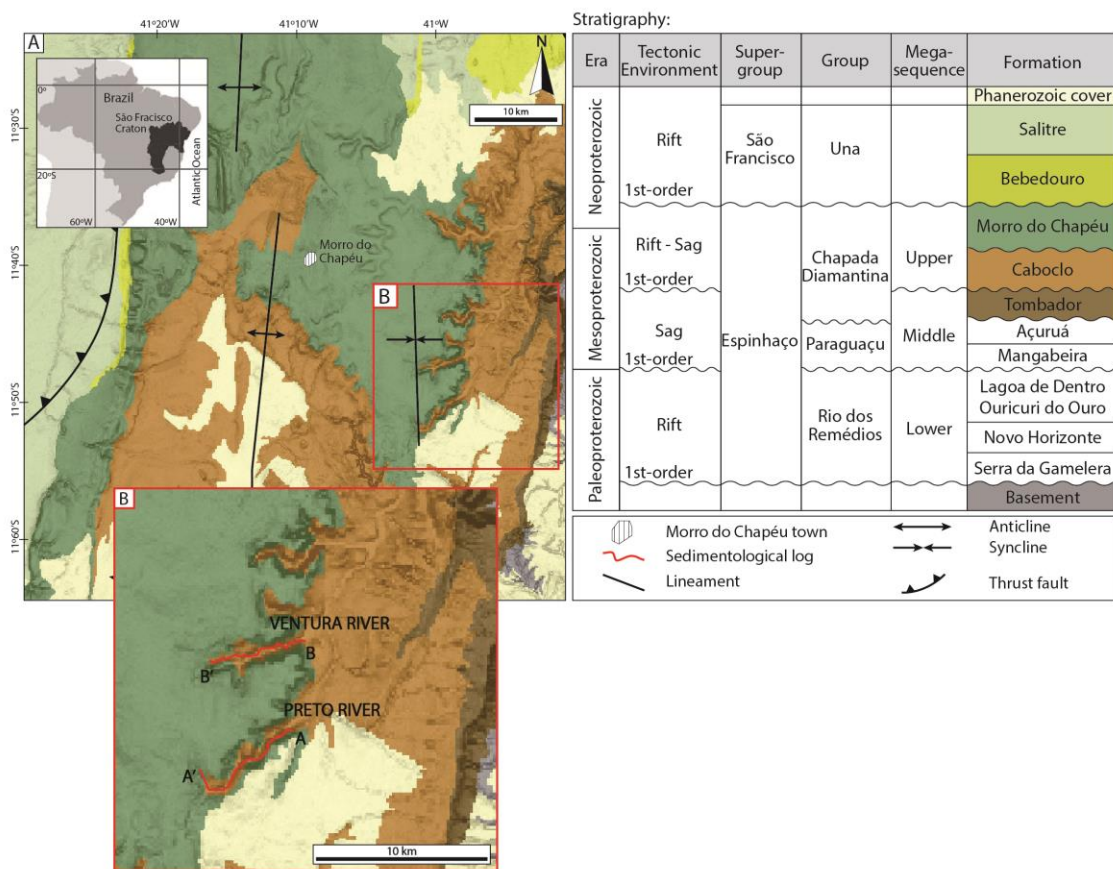


Fig. 1. (A) Simplified geological map based on data from Brazilian Geological Survey (CPRM/CBPM, 2003) and key chart with the stratigraphy of Chapada Diamantina modified from Guadagnin et al. (2015). The inset shows the location of the São Francisco Craton in Brazil (in black). (B) Detail of the area where the Ventura and Preto rivers are located and the beginning (A and B) and the end (A' and B') of the log sections.

3. STUDY AREA AND METHODS

Two compound sections (Ventura River and Preto River) were analyzed to characterize the siliciclastic stromatolites from Caboclo Formation. Ventura River and Preto River are parallel sections located approximately 7 km from each other and 25 km to southeast of Morro do Chapéu city (Fig. 1 and Fig. 2).

The outcrops are escarpments on the edges of rivers or on the dry riverbed. Approximately 150 m of sedimentological log on Preto River and 170 m on Ventura River (Fig. 2) were measured and described bed by bed, recorded at 1:50 scale and interpreted using the classical methods of facies analysis (Walker & James, 1992), in which sedimentary facies are recognized based on their texture, sedimentary

structures, set geometry and lateral transitions. Genetically related facies are grouped in facies associations representing sub-environments of a depositional system (Dalrymple, 2010).

Stromatolite analysis was made in macro, meso and microscale (Hofmann, 1973; Awramik, 1991). For the field descriptions, the chart of stromatolites structures proposed by Preiss (1976) was used. Petrological descriptions of thin sections allowed a detailed genetic classification for stromatolites and thrombolites (Riding, 2011).

Ten thin sections were prepared from representative samples of the stromatolites in order to characterize the main aspects of structure, texture, fabric, primary and diagenetic composition (Fig. 2). The thin sections were impregnated with blue-dyed epoxy and stained with a solution of Alizarin Red S and potassium ferricyanide to distinguish the carbonate species (Dickson, 1965). Qualitative petrography analysis was performed using a Zeiss AXIO Imager 2 microscope and the photomicrographs were taken using the ZEN 2012 program.

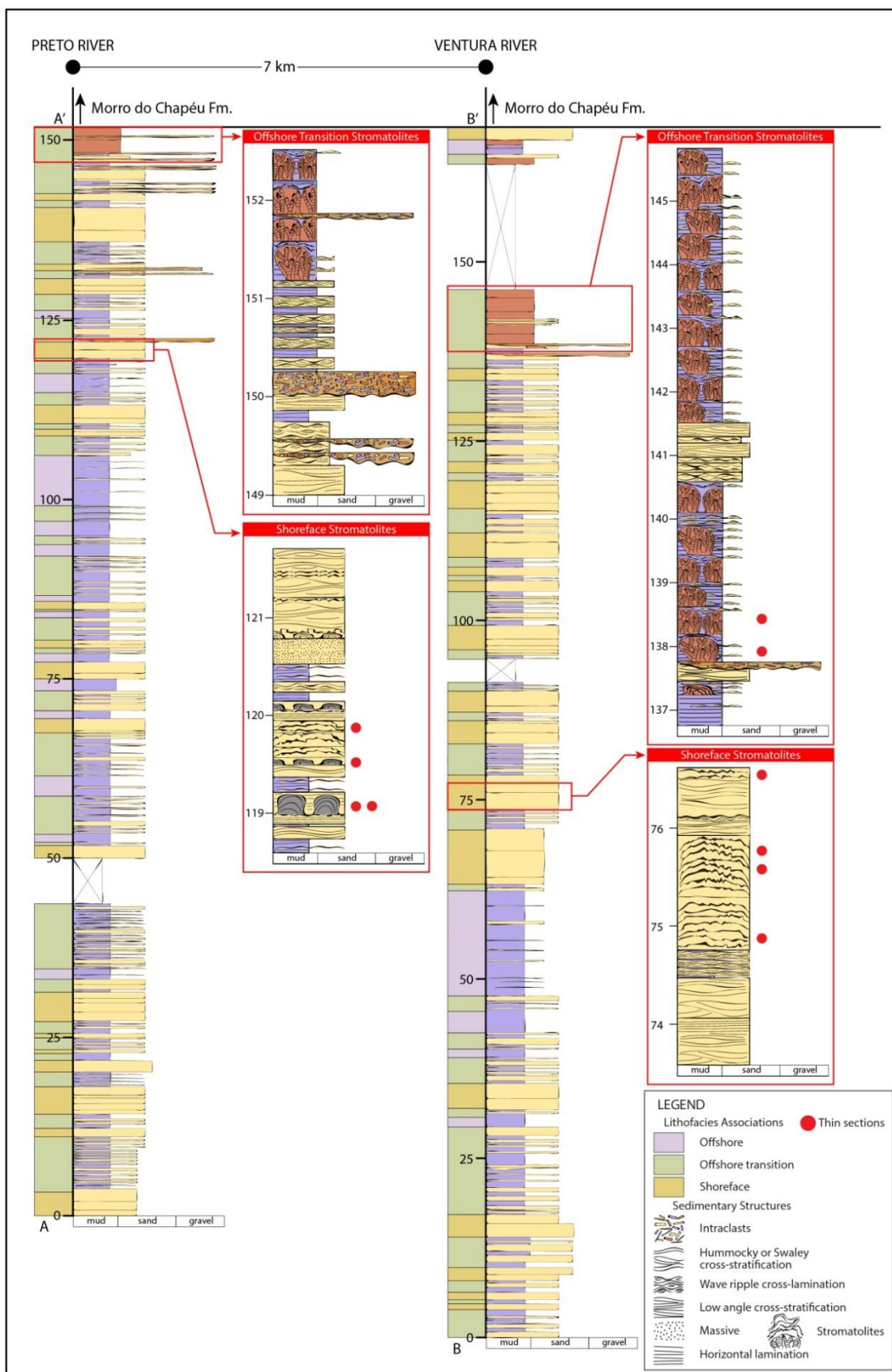


Fig. 2. Preto River and Ventura River log section with lithofacies association interpretation. In the red boxes the intervals in which the stromatolites occur are detailed.

4. RESULTS

The upper part of Caboclo Formation consists of sandstones and mudstones accumulated on a storm wave-dominated siliciclastic ramp, with occasional development of siliciclastic stromatolites. The facies associations present in the upper part of the Caboclo Formation are described and interpreted below: Offshore, Offshore Transition and Shoreface. Siliciclastic stromatolites were described in two stratigraphic intervals of the Ventura River and Preto River, linked to offshore transition and shoreface lithofacies association (Fig. 2). These stromatolites will be described and interpreted in detail in item 4.2.

4.1. Lithofacies Association

4.1.1. Offshore

This lithofacies association is formed by tabular packages up to 13 m composed predominantly of laminated mud, without subaerial exposure features. Thin layers of very fine to fine-grained sandstones occur between laminated mudstones, which are lenticular shaped, up to 10 cm thick and 10 m wide (Fig. 3). The sandstones are composed mainly by hummocky bedforms with isotropic undulated or scour and drape low-angle laminations, and wave ripples. Massive sandstones occur less frequently.

The dominance of clay and silt sedimentation without evidence of sub-aerial exposure suggests that these deposits had their genesis linked to decantation of fine sediments below the storm-weather wave-base. Under intense storm events there was the reworking and transport of sandy sediments from proximal areas to offshore portion by hyperconcentrated gravity flows, what resulted in massive sandstones deposits (Aigner, 1982; Tucker, 1982; Myrow and Southard, 1996; Bádenas e Aurell, 2001; Myrow et al., 2002; Pérez-López e Pérez-Valera, 2012; Basilici et al., 2012; Collins et al., 2017; Brady and Bowie, 2017). During major storm events the storm waves could touch the deep offshore substrate, concentrating sand and generating wave ripple laminated and hummocky cross-stratified sandstones.

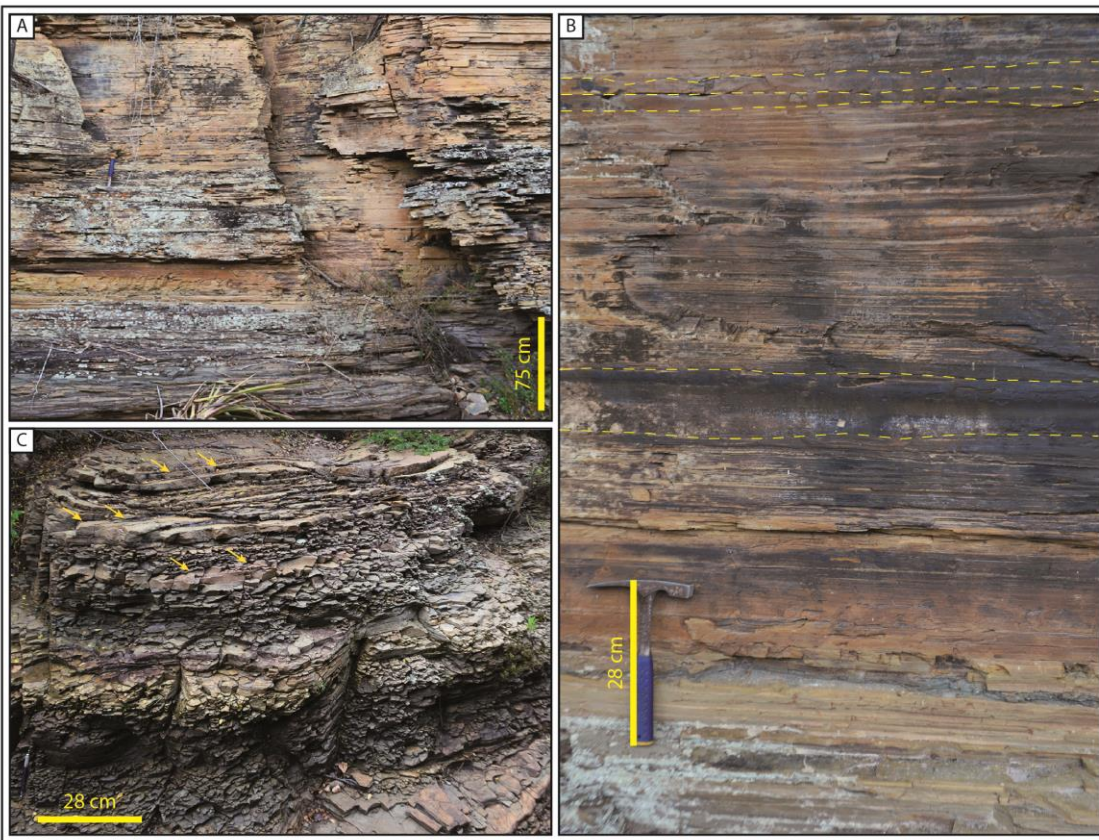


Fig. 3. Typical appearance of the offshore lithofacies association in outcrops. (A) Tabular packages composed predominantly of laminated mud. (B) Laminated mud and thin layered sandstones (dashed lines). (C) Note the thin layers of lenticular shaped sandstones (yellow arrows).

4.1.2. Offshore Transition

This lithofacies association comprises tabular packages up to 8 m thick characterized by the intercalation of sandstones and mudstones (Fig. 4). The mudstones are laminated or massive and 0.5 to 20 cm thick. The sandstones are very fine- to fine-grained, well-sorted and 1 to 30 cm thick. Internally the sandstones present isotropic undulated or scour and drape hummocks, wave ripples (Fig. 4A and D) and less frequently are massive. Erosive structures such gutter casts and pot casts are very common at the base of sandy layers (Fig. 4C).

The high-frequency intercalation of sandstones with oscillatory flow structures and mudstones deposited by decantation of suspended load, allied to the absence of features indicative of sub-aerial exposure, suggests a context of rapid and intense variations in energy in permanently subaqueous condition. These characteristics are compatible with the transition zone between shoreface and offshore, below the fair-weather wave-base and above the storm-weather wave-base (Dott and Bourgeois,

1982; Reading and Collinson, 1996). Fine sediments are settled by decantation during periods of fair-weather and the sandy sediments are transported and deposited by tractive, combined to oscillatory flows during storm-weather events. Massive sandstones were formed by hyperconcentrated gravitational flows associated to storm-generated turbidity currents (Aigner, 1982; Myrow and Southard, 1996; Bádenas and Aurell, 2001; Myrow et al., 2002; Brady and Bowie, 2017).

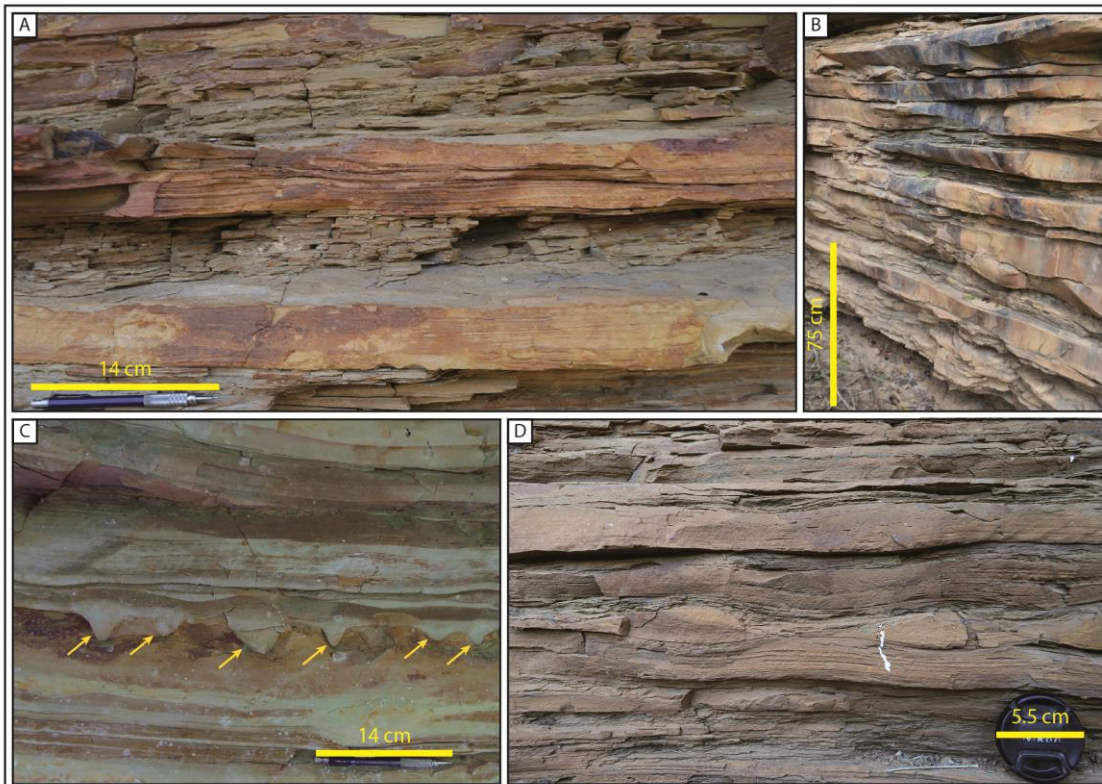


Fig. 4. Typical appearance of the offshore transition lithofacies association in outcrops. (A) Intercalation of hummocky cross-stratified sandstones and laminated mudstones. (B) Tabular and lenticular packages of sandstones separated by mudstones. (C) Succession of small gutter casts (yellow arrows) in the contact between a sandstone with wave ripple lamination and a mudstone. (D) High-frequency intercalation of mudstones and white sandstones with wave ripple lamination and hummocky cross-stratification.

4.1.3. Upper Shoreface

This lithofacies association forms packages up to 6 m thick. It is predominantly composed of amalgamated sandstones with swaley cross-stratification and wave ripple lamination (Fig. 5). Sometimes, interference wave ripples can be seen,

identified by the egg carton pattern (Fig. 5 B). Sandstones with low angle cross-stratification and horizontal lamination are subordinated. Convolute laminations are observed in some layers.

Amalgamated sandstones with structures indicative of oscillatory and combined flow suggest deposition in a high energy environment of shoreface, above the fair-weather wave-base (Dott and Bourgeois, 1982; Burchette and Wright, 1992; Reading and Collinson, 1996). Sandstones with swaley cross-stratification resulted from high-frequency storm events in nearshore areas. Low angle cross-stratification and horizontally laminated sandstones are interpreted as generated by unidirectional subcritical to supercritical currents in the surf zone, probably associated with rip or longshore currents (Dott and Bourgeois, 1982; Leckie and Walker, 1982). During periods of low energy, the reworking of the substrate by normal waves, with pure oscillatory flow, results in wave ripples. Interference wave ripples are consequence of two direction of wave currents (Allen, 1979; Clifton and Dingler, 1984). Convolute laminations are generated by liquefaction generated by stress of storm waves in water-saturated sand packages (Molina et al., 1998; Chen and Lee, 2013). This process causes overpressure in the pores, unpacking of grains and consequent deformation of depositional structures.

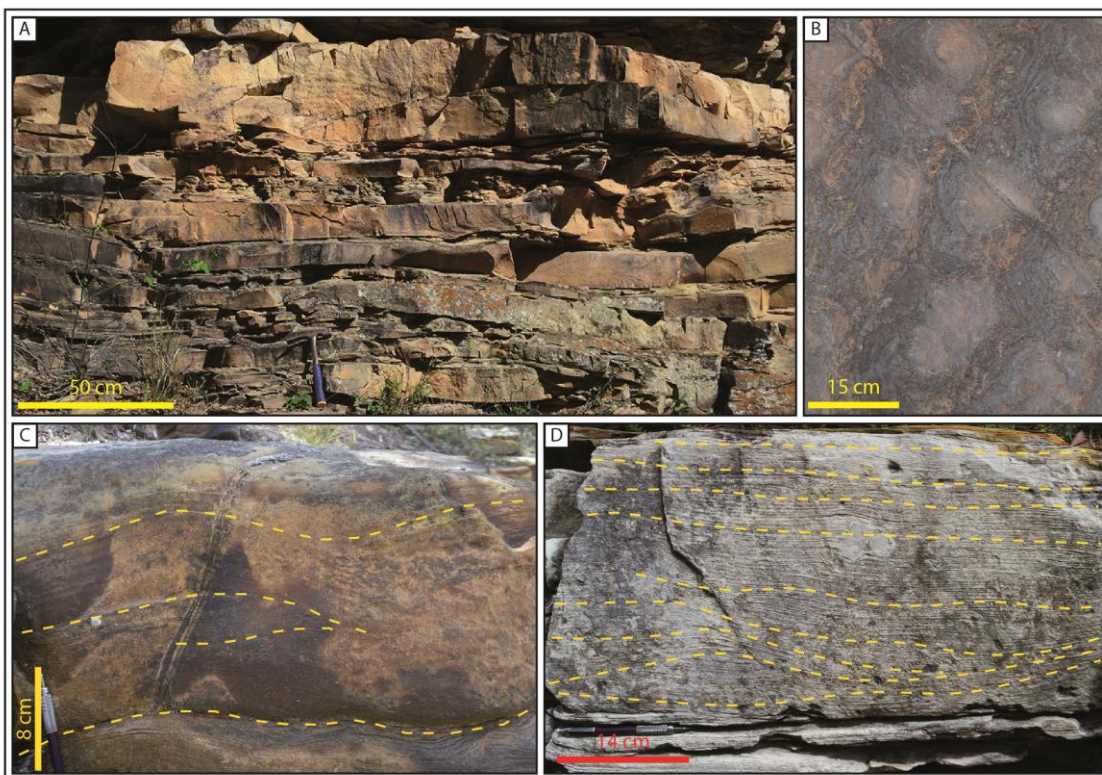


Fig. 5. (A) Typical appearance of the shoreface lithofacies association in outcrops; amalgamated sets of sandstones. (B) Interference wave ripples. (C) Swaley cross-stratified sandstone. Cut and fill structures, with undulated edges, filled by accretionary undulated lamination. (D) Swaley cross-stratified sandstone at the base transitioning upward to sandstone with low angle stratification. Dashed lines marking the laminations.

4.2. Stromatolites morphological types

Stromatolites in Caboclo Formation are present in two different lithofacies associations: (i) shoreface and (ii) offshore transition. The proximal shoreface stromatolites are characterized by silty to sandy fabric and poor lamination, and the distal ones by clay, silt grains, relatively less sand and distinct lamination. The volume of siliciclastic grains composing the stromatolites fabric is > 85% in the shoreface and > 30% in offshore transition.

4.2.1. Shoreface Siliciclastic Stromatolites

These stromatolites form structures from 0.1 to 1 meter thick, interspersed with the other shoreface sedimentary facies, occurring in an interval of 2 m thick in the Ventura River and of 3 m thick in the Preto River section (Fig. 2). According to the morphology and composition characteristics of the fabric, shoreface stromatolites are individualized into two types: (i) iron-rich siliciclastic domal stromatolites and (ii) siliciclastic sand mounds stromatolites. The vertical succession of facies indicates that the iron-rich domal stromatolites were established in portions slightly more distal of the shoreface zone than sand mounds.

4.2.1.1. Iron-Rich Siliciclastic Domal Stromatolites

Description:

The best examples of these stromatolites are found in an interval approximately 1 m thick in the Preto River. They form isolated to coalescent domes that are 0.1 to 0.2 m thick and 0.1 to 0.3 m wide, or elongated structures with the same thickness, but up to 1 m wide, with well-defined boundaries and steep flanks with dipping from > 45° to subvertical (Fig. 6). These stromatolites grow on top of and in abrupt lateral contact with shoreface sandstones. Their lamination is laterally continuous, without internal columns, weakly marked (almost thrombolitic), and in

outcrop, identified by the onion-skin pattern (Fig. 6A). They occur distributed over a stratigraphic interval, usually in groups that can cover an area of up to 2.5 m² (Fig. 6D). The inter-dome areas are filled with fine-grained sandstones with swaley cross-stratification, wave ripple lamination or low angle cross-stratification. Intraclasts can be found at the base of some constructions.

They are composed of well sorted silt and very fine to fine sand grains of quartz, feldspars and micas, as well detrital clay minerals composing thin brown laminae, amounting to 65 to 85% of total constituents (Fig. 7). As observed in macroscale, the lamination in microscopy is closely spaced and poorly developed, and is recognized by variations in iron mineral concentration and by the clay laminae (Fig. 7C). Framboidal pyrite or cryptocrystalline hematite replacing framboidal pyrite are common (15 to 35% of the total constituents). Sometimes, these iron minerals and brown clay minerals are vertically oriented, forming elongated structures (< 0.4 mm thick) perpendicular to the rock lamination and distributed throughout all samples (Fig. 7B). Subhedral microcrystalline dolomite has largely replaced clay minerals and siliciclastic silt and sand grains. The dominance of silt- to sand-sized siliciclastic grains allows to classify these deposits as sandstone stromatolites (Martín et al., 1993).

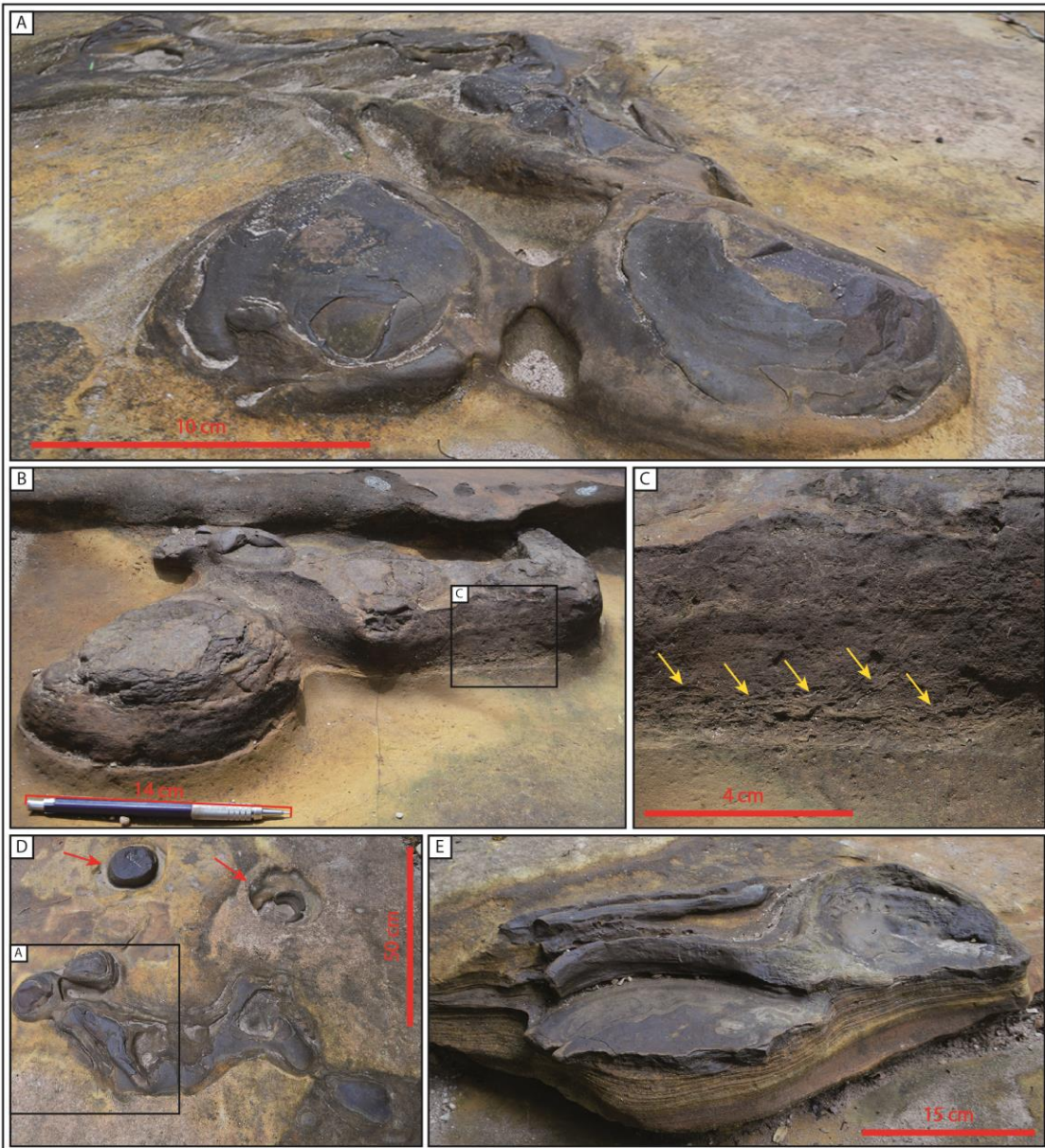


Fig. 6. Iron-rich domal stromatolites. (A and B) Coalescent domes in abrupt contact with shoreface sandstones. Note the well-defined boundaries and steep flanks. In 'A' the onion skin pattern represents a weakly marked lamination. (C) Detail of the contact between the sandstone and the stromatolite. Yellow arrows point to the disrupted lamination at the base of the stromatolite. (D) Plan view of a cluster of domes. Two isolated domes (red arrows) and a set of coalescent domes composing a ridge. (E) Two coalescent iron-rich domes that grew up over horizontally laminated sandstone.

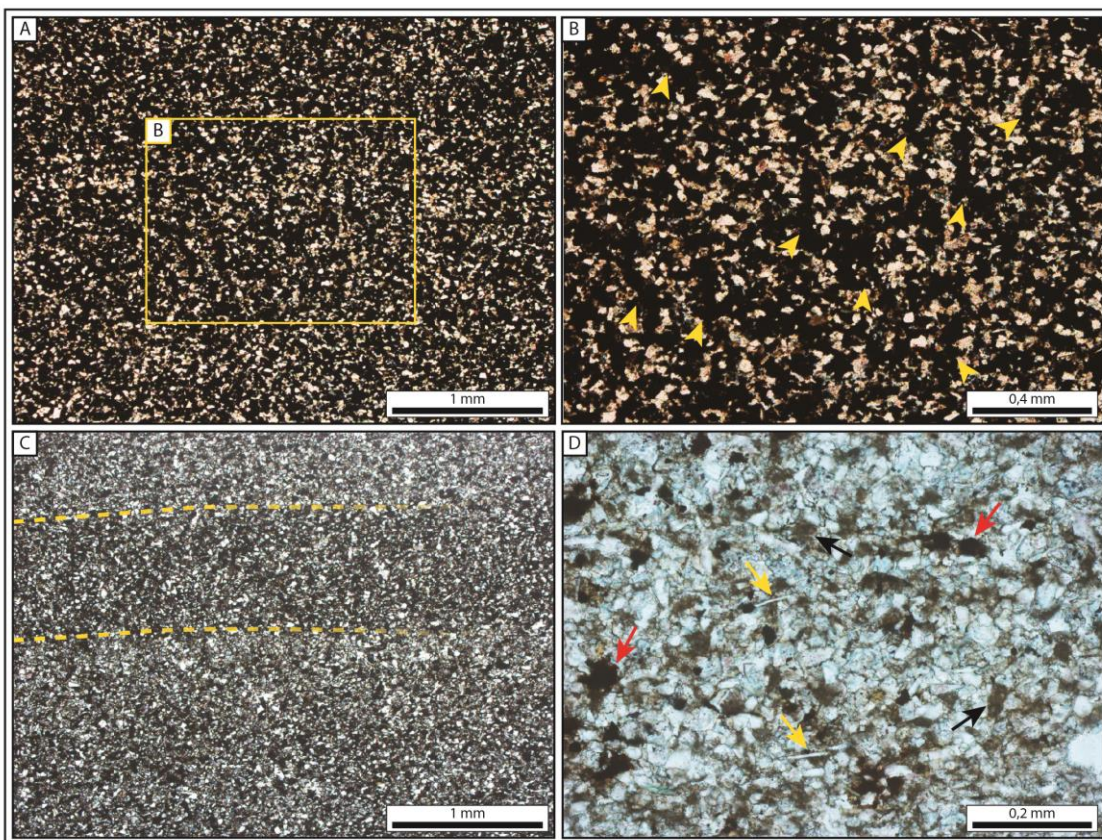


Fig. 7. Textural and fabric characteristics of the iron-rich domal stromatolites. (A) Well sorted silt and very fine to fine sand grains. Observe the high concentration of disseminated iron mineral (dark). (B) The yellow arrows indicate vertically oriented concentration of iron minerals (originally frambooidal pyrite, replaced by hematite), forming elongated structures perpendicular to the rock lamination. These microscopic structures are interpreted as replaced microbial filaments. (C) Microscopic stromatolite lamination (dashed yellow lines) recognized by variations in iron mineral concentration and by the clay laminae. (D) Red arrows: Concentrations of frambooidal pyrite or cryptocrystalline hematite replacing frambooidal pyrite; Black arrows: microcrystalline dolomite replacing clay minerals; Yellow arrows: muscovite grains.

Interpretation:

Benthic microbial colonies were established in high wave energy environment with low concentration of carbonate dissolved in water, in a system in which the available sediment was siliciclastic. Iron-rich siliciclastic domal stromatolites are formed almost exclusively by trapping and binding of silicate detrital grains by microbial filaments and EPS during the remobilization and transport of sediments by waves in shoreface environments (Reid et al., 2000; Riding, 2000; Draganits e

Noffke, 2004; Druschke et al., 2009; Suarez-Gonzalez et al., 2014, 2019; Frantz et al., 2015). Although the absence of primary particles, the presence of microcrystalline dolomite replacing clay minerals indicates that a small percentage of the fabric possibly is product of bio-induced precipitation in the form of micrite or microspar concentrated in thin laminae. No feature suggesting abiotic precipitation, as sparry crust, was identified. The progressive sedimentation and burial made the colony migrate towards the surface, binding more sediment and making the stromatolite grow. The thin clay laminae can be associated with periods of hiatus in sediment accretion, allowing the increase of microbial population, development of EPS-rich biofilm and its lithification/calcification (Gerdes et al., 2000; Druschke et al., 2009; Dupraz et al., 2011). Intraclasts were formed in periods of higher wave energy in the system when the laminations were disrupted, ripped out and transported by wave-induced currents.

The microscopic vertical structures filled by framboidal pyrites and carbonate clay suggest replaced microbial filaments. The high concentration of framboidal pyrite, in some cases subsequently oxidized to hematite, and microcrystalline dolomite can be related to the degradation of organic matter by bacteria (Gerdes et al., 2000; Mastrandrea et al., 2006; Druschke et al., 2009; Dupraz et al., 2011, Suarez-Gonzalez et al., 2014).

4.2.1.2. Siliciclastic Sand Mounds Stromatolites

Description:

This type of stromatolite was described in an interval approximately 1 m thick in Ventura River and Preto River. They occur as arch-shaped structures, forming large mounds up to 0.8 m thick and 2 m wide, with slightly dipping edges, which are flattened toward the base (Fig. 8A). Internally they are formed by well-sorted, very fine- to fine-grained sand with crude and crenulated laminations, usually marked by the concentration of muddy sediment (Fig. 8B). Disruption of muddy levels is very common (Fig. 8C). In some cases, at the top of the mounds, there are small domes and columns structures with laterally continuous laminations marked by iron minerals (Fig. 8D, E and F).

These stromatolites are composed mainly of silt to fine sand grains of quartz, feldspars and micas, and rare carbonate peloids. In thin sections were identified thin

and diffuse laminations of brown clay minerals, enriched in iron minerals and microcrystalline dolomite (Fig. 9). In some samples, it appears that microcrystalline dolomite has replaced vertical elongated structures (< 0.2 mm), that are oriented perpendicularly to the rock lamination (Fig. 9F). Compared to iron-rich siliciclastic domal stromatolites, the concentration of iron minerals is lower (< 15%), dispersed, concentrated in laminae or forming small clusters of microcrystalline framboidal pyrite, sometimes oxidized to hematite (Fig. 9B and D). The stromatolites are composed of a percentage of 90 to 100% of siliciclastic grains and up to 10% of carbonate peloids and can be classified as sandstone stromatolites (Martín et al., 1993).

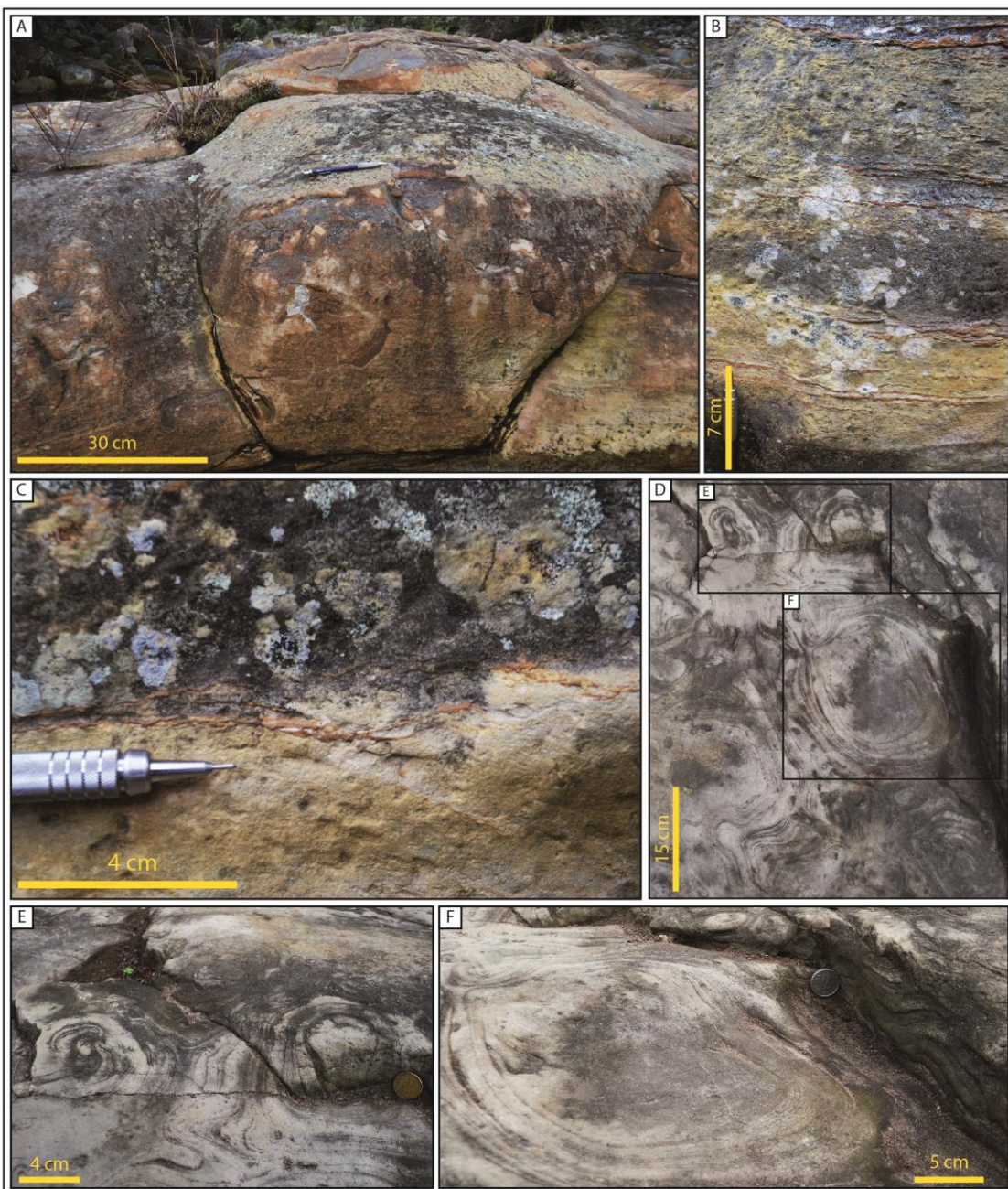


Fig. 8. Siliciclastic sand mounds stromatolites. (A) Stromatolite forming a large mound with arch-shaped structures. Note the slightly dipping edges flattened toward the base. (B) Crude and crenulated laminations, usually also marked by the concentration of muddy sediment (brown laminae). (C) Detail of a disrupted lamination. (D, E and F) Small, laterally linked columns that can be associated with mounds.

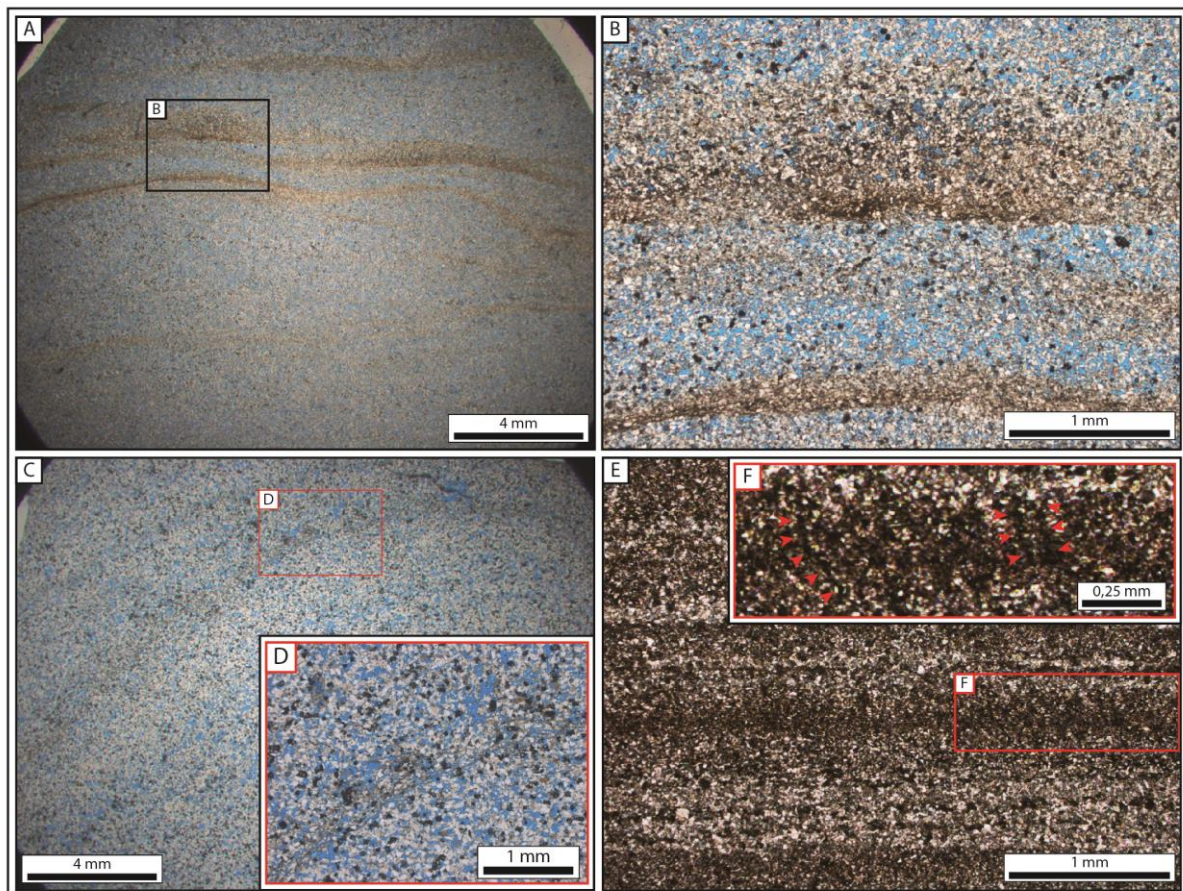


Fig. 9. Textural and fabric characteristics of the siliciclastic sand mounds stromatolites. (A, B and C) Well-sorted silt to fine sand grains. In 'B' it is possible to identify thin and diffuse laminations of brown clay minerals, enriched in iron minerals and microcrystalline dolomite. (D) Disseminated small clusters of microcrystalline frambooidal pyrite, sometimes oxidized to hematite. (E) Submillimetric lamination recognized by the differential concentrations of frambooidal pyrite or hematite and microcrystalline dolomite. (F) Detail of a lamination. The red arrows point to microcrystalline dolomite replacing vertical elongated structures oriented perpendicularly to the rock lamination.

Interpretation:

The environment conditions for formation of siliciclastic sand mounds stromatolites are very similar to the iron-rich domal stromatolites, representing a fair-weather to storm dominated shoreface with a low concentration of carbonate dissolved in the water. Sedimentological and petrographic features suggest that siliciclastic sand mounds stromatolites were formed mainly by agglutination of silt and sand grains by benthic microbial colonies in shoreface zone. Thin and irregular muddy layers present in these deposits suggest sedimentation by in situ carbonate precipitation processes as a response to microbial metabolism or degradation. These muddy laminae were deposited during intervals of relatively lower energy, causing a hiatus in detrital sediment accretion, increased of microbial population, development of EPS-rich biofilm and early lithification (Gerdes et al., 2000; Druschke et al., 2009; Dupraz et al., 2011). Subsequent periods of fair-weather to high energy storm oscillatory flow could erode part or all of the lithified microbial mat and return to move silt and sand grains that were partly agglutinated by the colony. The microcrystalline dolomite replacing vertical elongated structures, perpendicular to the rock lamination can be interpreted as microbial filaments.

4.2.2. Offshore Transition Bioherms and Biostromes

Description:

The offshore transition bioherms and biostromes occur in the top of Caboclo Formation succession (in contact with the Morro de Chapéu Formation), at an interval of approximately 5 m in Preto River and 9 m in the Ventura River (Fig. 2). These stromatolites were widespread in these intervals and coexisted with laminated or massive mudstones, very fine-grained sandstones with hummocky cross-stratification and wave ripple lamination (Fig. 10). Intraclastic conglomerate lenses are common. The stromatolites consist of bioherms with dome or columnar geometry up to 1 m thick and 2 m in diameter, or biostromes (Fig. 10A, B, D and F). Internally they are made up of small columns, usually < 3 cm wide and < 15 cm thick, which can be simple or branched with convex to parabolic/conic laminations (Fig. 10C and E).

The laminations are millimetric spaced, usually < 1 mm, crenulated, and characterized by the alternation between agglutinated silt to very fine-grained sands (30 to 60%) and clay minerals (40 to 70%), commonly disrupted (Fig. 11). In the mottled muddy laminae, the clay particles were commonly replaced by

microcrystalline dolomite, and frambooidal pyrite (partially oxidized to hematite) (Fig. 11D). The inter-columnar spaces were filled mainly with fine to very fine-grained sands, composed of quartz, feldspars, and peloids. Elongated and irregular intraclasts of microbial and mudstones were also common in inter-column spaces (Fig. 11A, B and C).

According to Martín et al., (1993), the offshore transition bioherms and biostromes described in Caboclo Formation are classified as siliciclastic stromatolites.

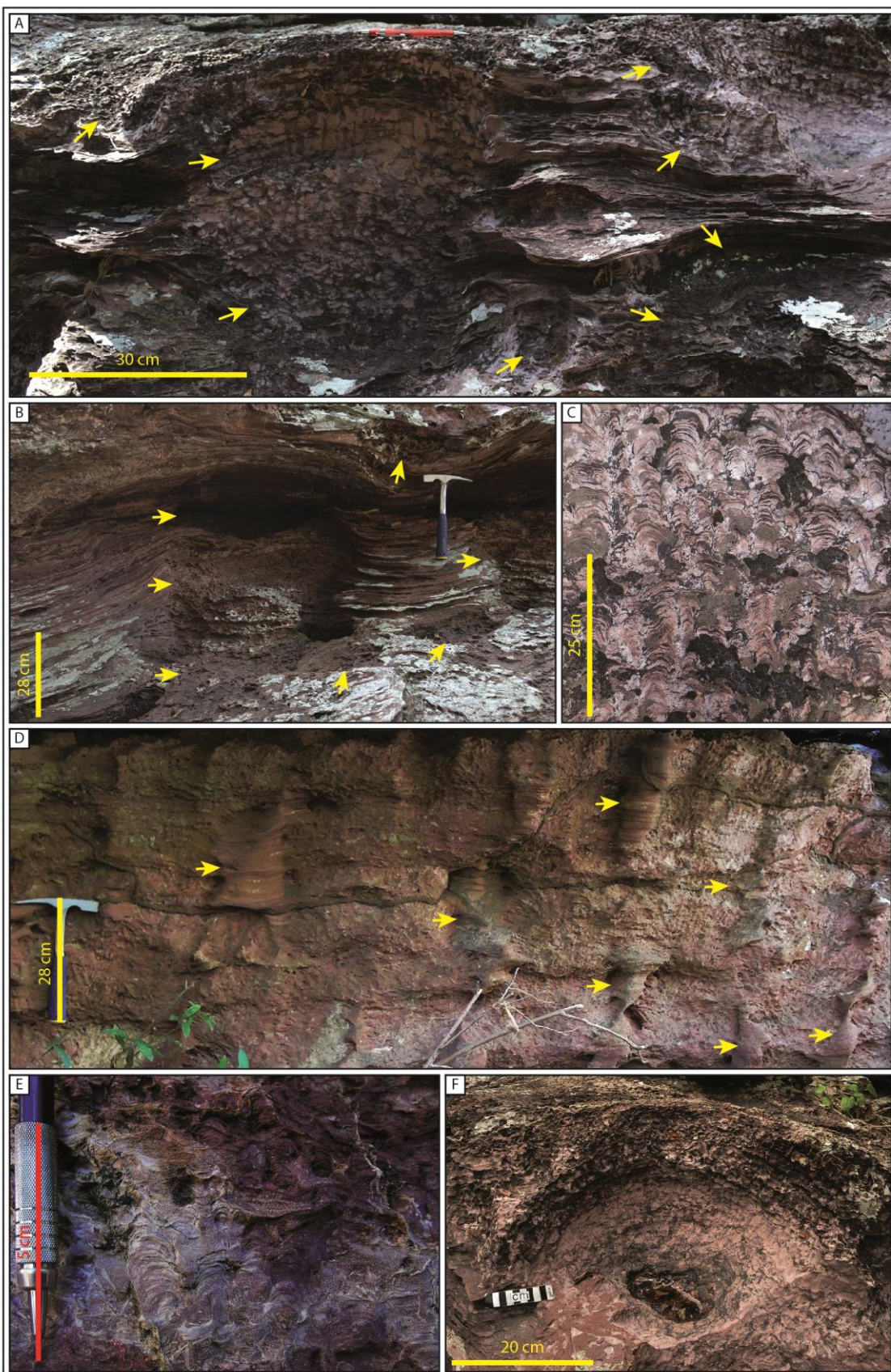


Fig. 10. Offshore transition bioherms and biostromes. (A and B) Columnar and domal bioherms (yellow arrows) and offshore transition clastic sediments filling the inter-bioherm area and covering them. (C) Small simple and branched columns. (D)

Tabular shaped biostrome compound of columnar stromatolites. The yellow arrows point to the inter-columns zones, which are filled with offshore transition clastic deposits. (E) Intraclasts concentration at the base of small columns. (F) Plan view of a domal bioherm.

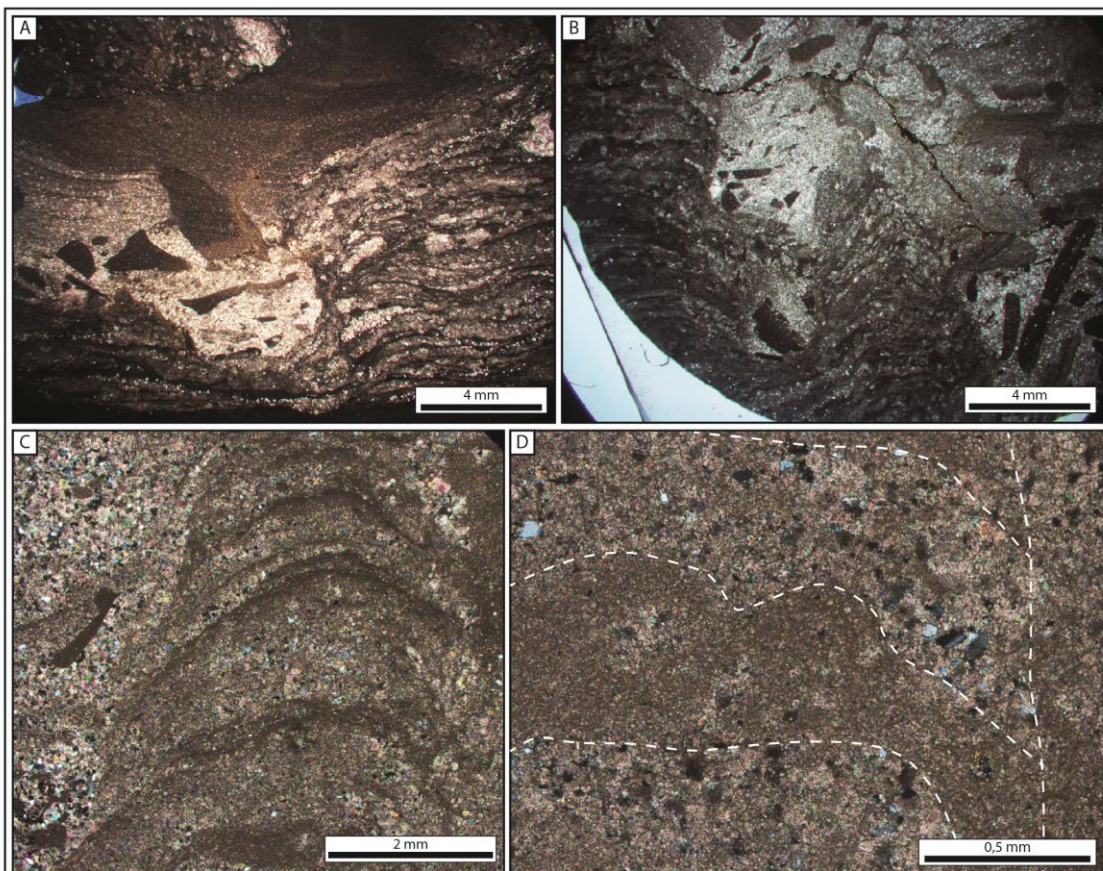


Fig. 11. Textural and fabric characteristics of the offshore transition bioherms and biostromes. (A and B) Small stromatolites columns partially eroded and covered by intraclastic conglomerates in 'B' and mudstone in 'A'. Note in 'A' stromatolites columns growing over a mud substrate. (C) Mud intraclasts and siliciclastic grains filling the inter-columns space. Observe the intercalation of dark brown clay laminae with light brown laminae with granular texture in the stromatolite column. (D) Detail of the lamination. Note the mottled texture and the fine-grained lamina forming submillimetric domes.

Interpretation:

These stromatolites were positioned in a zone with frequent energy variations, compatible with the transition between shoreface and offshore, between the fair-weather wave-base and the storm-weather wave-base. The alternation in the

composition of the laminae suggests different energy regimes during the growth of the stromatolites. In storm-weather events, silty and sandy sediments were transported from shoreface zones and part of these grains was agglutinated by microbial mats. In these high energy periods, microbial laminations were broken and sometimes transported in the form of intraclasts. In turn, in periods of fair-weather the offshore transition region was starved of siliciclastic sediments, establishing ideal conditions for colony stabilization and EPS development. During that period, fine-grained microbial induced clay laminae were deposited (Dupraz et al., 2009). Therefore, the alternation of processes forming the offshore transition stromatolite fabric refers to different energetic contexts, in which muddy laminae were deposited in periods of fair-weather and the agglutinated siliciclastic grains laminations in storm periods.

The shape of the small and large stromatolites structures was the result of the hydrodynamic conditions of the water column and the currents induced by oscillatory flows during storm-weather (Logan et al., 1964; Gebelein, 1969; Hofmann, 1973; Walter, 1977; Grotzinger and Knoll, 1999; Andres and Reid, 2006; Dupraz et al., 2006). The offshore transition bioherms and biostromes had a high vertical accretion rate. This is linked to the ‘light-driven’ growth of microbial mats (Dupraz et al., 2006). The lateral continuity and wide distribution of these stromatolites, when compared to shoreface stromatolites, is due to the fact that the wave action was more occasional, generating a more stable substrate and allowing wide nucleation and distribution of microbial colonies. The storm waves act disrupting the mats and initiating the columnar or domal morphologies. In addition, the storms transport grains from the shoreface to the offshore transition zone, sediments that were then trapped by the microbial mats.

5. DISCUSSION

5.1. Microbial evidences

Many authors list several features, both in the macro and the microscale, that may indicate biogenic signature in sedimentary deposits (Braga et al., 1995; Schieber, 1998; Grotzinger and Knoll, 1999; Gerdes et al., 2000; Chen et al., 2014; Awramik and Grey, 2005; Noffke et al., 2006; Druschke et al., 2009; Choudhuri et al.,

2020). The main characteristics that suggest microbial processes in the siliciclastic stromatolites of the Caboclo Formation are discussed below.

5.1.1. Macroscale evidence:

In shoreface stromatolites (Figs. 6 and 8) the diffuse irregular laminations, building isolated convex-upward laminated bodies with step angles of the boarders (generally $> 45^\circ$) suggest sediment binding by cohesive microbial mat surface (Schieber, 1998; Gerdes et al., 2000; Riding, 2011; Frantz et al., 2015). The stromatolites fabric is totally distinct from wave-generated deposits. The wave-generated bedforms forms smooth and symmetrical wavy laminations, composed by well defined, flat and continuous laminae. The absence of load structures, or successions of layers with deformed laminations indicate that these curved shaped structures do not represent soft-sediment deformation structures associated with fluidization or liquefaction processes. The diffuse lamination (Figs. 6C, 7B, C and F) is explained by the agglutination process, the main forming process of shoreface stromatolites laminations. Agglutinated stromatolites typically have crude lamination, and the definition of laminae is related to the size of the sediments trapped. Increased grain coarseness seems to correlate with crude layering, and coarse-grained laminae are at least partly thrombolitic (Awramik and Riding, 1988; Riding, 1991, 2000; Suarez-Gonzalez et al., 2014). These can explain why the lamination of the offshore transition bioherms and biostromes are better defined than the domes and mounds of the shoreface stromatolites.

Offshore transition bioherms and biostromes in outcrop have the classical anatomy of a stromatolite, composed of well-defined millimetric and crenulated convex-upward laminations forming small columns that coalesce into large domal or columnar bioherms and biostromes with sharp and high angle boundaries (Fig. 10). These features serve as good criteria to identify these microbial buildups and differentiate them from detrital deposits with structures generated by waves and settling of muddy material from inter-stromatolite portions.

5.1.2. Microscale evidence:

At microscale, the microbial signature is registered in the millimetric alternation of laminae with distinct composition and granulometry (Figs. 7, 9 and 11). The siliciclastic silt to fine-grained laminae is interpreted as sediment trapping and binding

by microbial filaments or by the EPS. The muddy laminae are interpreted as bio-induced precipitation of micrite or microspar. These characteristics are identified in shoreface and offshore transition stromatolites, but are better recognized in the offshore transition stromatolites.

Other evidence is the common presence of sulfides as early diagenetic frambooidal pyrite (Figs. 7, 9B and D), generated in response to the activity of sulfate-reducing microbial communities that benefit of in situ production of organic matter and the concentration of water dissolved sulfate (Canfield and Marais, 1993; Gerdes et al., 2000; Popa et al., 2004; Druschke et al., 2009; Noffke et al., 2006; Cai and Hua, 2007; Dupraz et al., 2009; Suarez-Gonzalez et al., 2014; Berg et al., 2020). With the progressive accretion, the colony migrate towards the top surface of the construction. The metabolic processes of microorganisms create an oxidizing zone at the top of the deposit, while in the regions towards the nucleus anoxic conditions are formed. Oxygen levels fall to zero near the base of photic zone, providing an ideal microenvironment for decomposition of organic matter via sulfate reduction and others microbial metabolic processes (Canfield and Des Marais, 1993; Grotzinger and Knoll, 1999; Gerdes et al., 2000; Druschke et al., 2009; Dupraz et al., 2009; Guan et al., 2017).

The high proportion of dolomite, disseminated or concentrated in the clay laminae, suggest mat mineralization by microbial activity (Figs. 7D, 9A, B and E). The microcrystalline dolomites possibly replaced the bioinduced early diagenetic micrite or microspar related to the calcification of EPS or microbe filaments, or has its genesis related to the precipitation of synsedimentary dolomite as a result of the degradation of organic matter by microbial sulfate-reducing metabolic activities (Visscher et al., 2000; Mastrandrea et al., 2006; Perri and Tucker, 2007, Druschke et al., 2009; Hips et al., 2015).

The vertical millimetric structures, that occur perpendicular to the rock lamination, replaced by microcrystalline dolomite or frambooidal pyrite can be interpreted as microbial fossil filaments in life position (Figs. 7B and 9F). These described features suggest a correlation between the bacteria, the degradation of organic matter and the genesis of frambooidal pyrite and microcrystalline dolomite (Bertrand-Sarfati, 1994; Popa et al., 2004; Mastrandrea et al., 2006; Perri and Tucker, 2007; Chen et al., 2014).

5.2. Stromatolite Preservation

The formation of agglutinated stromatolites depends on the sediment input and the preservation depends on the early lithification (Martin and Braga, 1993; Reid et al., 2000; Noffke, et al., 2002; Riding, 2011; Suarez-Gonzalez, 2019). According to Dupraz et al. (2009), with only trapping and binding it is not possible to construct a stromatolite. The key factor for the development and accumulation of a stromatolite is a hiatus in the sediment accretion and the development and lithification of a microbial biofilm.

For stromatolites that develop in high energy environments, the early lithification is essential to prevent erosion and transport of microbial trapped sediment. Potentially, two main processes influenced the preservation of Caboclo Formation stromatolites: (i) pyritization and (ii) lithification by bioinduced carbonate precipitation. Although these two processes are associated, pervasive pyritization was the main preservation process of the shoreface stromatolites, while synsedimentary carbonate precipitation of the offshore transition stromatolites.

5.3. Environmental Controls

According to Riding (2000), microbial deposits are biologically stimulated, but they also need favorable hydrodynamic conditions and saturation factors from the aqueous environment. Thus, the occurrence of these structures is dependent on a relationship between biotic and abiotic factors. Variations in these factors control the composition of the fabric, the growth and geometry of these organosedimentary deposits. According to Suarez-Gonzalez et al. (2019), the ideal conditions for agglutinated stromatolites to occur are: (i) availability of grains, (ii) common agitation by currents, (iii) abundance and diversity of electrolytes to enhance EPS adhesiveness and (iv) relatively low concentration of CaCO_3 , hindering very early and strong precipitation.

The Caboclo Formation stromatolites were deposited in a favorable environment for the trapping and binding of siliciclastic sediments. The upper part of the Caboclo Formation can be interpreted as wave-dominated siliciclastic ramp, with available siliciclastic sediments transported and deposited by oscillatory and combined flow generated by fair- and storm-weather waves. The marine environment is favorable to forming EPS with good adhesive properties. This is because there are

abundant and diverse ions in the marine environment that increase the capacity of EPS to adhere the grains transported by wave currents. Besides, the Caboclo Formation age (1.3 – 1.0 Ga) coincides with an abrupt fall in the amount of atmospheric CO₂, which is reflected in the degree of saturation of CaCO₃ dissolved in the oceans, reaching concentrations very similar to the current atmosphere (Grotzinger, 1990; Riding, 2011; Sheldon, 2013). This change in ocean chemistry may have led to a change in the stromatolite fabric, from sparry crust and fine-grained precipitated to agglutinated. Before this fall, the carbonate saturation was very high, making the calcification/lithification of the microbial mat, of both the EPS and the filaments and coccoids, very fast, not allowing the large agglutination of grains.

6. CONCLUSIONS

- The upper part of Caboclo Formation consists of a storm wave-dominated siliciclastic ramp, in which the deposition of sandstones and pelites dominates widely, with occasional development of siliciclastic agglutinated stromatolites. These stromatolites were described in two stratigraphic intervals of the Ventura River and Preto River, linked to shoreface and offshore transition lithofacies association.
- According to the morphological and composition differences of the fabric, shoreface stromatolites can be individualized into two types: (i) iron-rich siliciclastic domal stromatolites and (ii) siliciclastic sand mounds stromatolites. The offshore transition stromatolites occur as large bioherms and biostromes composed internally by small columns and domes. The proximal shoreface stromatolites are characterized by silty to sandy fabric and poor lamination, and the distal offshore transition by clay, silt grains, less sand and distinct lamination.
- Two main processes influenced the preservation of Caboclo Formation stromatolites: (i) pyritization and (ii) lithification by bioinduced carbonate precipitation. Although these two processes are associated, pervasive pyritization was the main preservation process of the shoreface stromatolites, while synsedimentary carbonate precipitation of the offshore transition stromatolites.

- At macroscale, the microbial signature of shoreface stromatolites is represented by the diffuse irregular laminations, building isolated convex-upward laminated bodies with step angles of the boarders suggest sediment binding by cohesive microbial mat surface. While offshore transition stromatolites presents well-defined millimetric and crenulated convex-upward laminations forming small columns that coalesce into large domal or columnar bioherms and biostromes. At microscale, the microbial signature is registered in the submillimetric to millimetric alternation of laminae with distinct composition and granulometry, presence of sulfides as early diagenetic frambooidal pyrite and the high proportion of dolomite, both disseminated or concentrated in the clay laminae.
- The Caboclo Formation stromatolites were deposited in a favorable environment for the trapping and binding of siliciclastic sediments: a marine environment with available siliciclastic sediments transported and deposited by constant fair-weather and storm-weather wave currents. And globally, the Caboclo Formation age coincides with an abrupt fall in the CaCO_3 saturation in the oceans, inhibiting the almost instantaneous calcification/lithification of the microbial mat.

REFERENCES

- Aigner, T., 1982. Calcareous tempestites: storm-dominated stratification in Upper Muschelkalk limestones (Middle Trias, SW-Germany). In: Einsele, G., Seilacher, A. (Eds.), Cyclic and event stratification. Springer-Verlag, Heidelberg, Heidelberg, pp. 180-198.
- Alkmim, F.F., Martins-Neto, M.A., 2012. Proterozoic first-order sedimentary sequences of the São Francisco craton, eastern Brazil. *Marine and Petroleum Geology* 33, 127-139.
- Allen, J.R.L., 1979. A model for the interpretation of wave ripple-marks using their wave-length, textural composition, and shape. *Journal of Geological Society* 136, 673-682.
- Allwood, A.C., Walter, M.R., Kamber, B.S., Marshall, C.P., Burch, I.W., 2006. Stromatolite reef from the Early Archean of Australia. *Nature* 441, 714-718.

- Andres, M.S., Reid, R.P., 2006. Growth morphologies of modern marine stromatolites: a case study from Highborne Cay, Bahamas. *Sedimentary Geology* 185, 319-328.
- Awramik, S.M., Riding, R., 1988. Role of algal eukaryotes in subtidal columnar stromatolite formation. *Proceeding of National Academy of Science, USA*, 85, 1327-1329.
- Awramik, S.M., 1991. Archaean and Proterozoic stromatolites. In: Riding, R. (Ed.), *Calcareous algae and stromatolites*. Springer-Verlag, Heidelberg, pp. 289-304.
- Awramik, S.M., Grey, K., 2005. Stromatolites: Biogenicity, Biosignature, and Bioconfusion. In: Hoover, R.B., Levin, G.V., Rozanov, A.Y., Gladstone, G.R. (Eds.), *Astrobiology and Planetary Missions*. Proceedings of SPIE 5906, pp. 5906P1.
- Babinski, M., Van Schmus, W.R., Chemale Jr, F., Brito Neves, B.B., Rocha, A.J. D., 1993. Idade isocrônica Pb/Pb em rochas carbonáticas da Formação Caboclo, em Morro do Chapéu, BA. *Simpósio sobre o Cráton do São Francisco 2*, 160-163.
- Bádenas, B., Aurell, M., 2001. Proximal-distal facies relationships and sedimentary processes in a storm dominated carbonate ramp (Kimmeridgian, northwest of the Iberian Ranges, Spain). *Sedimentary Geology* 139, 319-340.
- Basilici, G., de Luca, P.H.V., Poiré, D.G., 2012. Hummocky cross-stratification-like structures and combined-flow ripples in the Punta Negra Formation (Lower-Middle Devonian, Argentine Precordillera): a turbiditic deep-water or storm-dominated prodelta inner-shelf system? *Sedimentary Geology* 267, 73-92.
- Berg, J.S., Duverger, A., Cordier, L., Laberty-Robert, C., Guyot, F., Miot, J., 2020. Rapid pyritization in the presence of a sulfur/sulfate-reducing bacterial consortium. *Scientific Reports* 10, 8264.
- Bertrand-Sarfati, J., 1994. Siliciclastic-carbonate stromatolite domes, in the early Carboniferous of the Ajers Basin (Eastern Sahara, Algeria). In: Bertrand-Sarfati, J., Monty, C. (Eds.), *Phanerozoic Stromatolites II*. Kluwer, Dordrecht, pp. 395-419.
- Brady, M., Bowie, C., 2017. Discontinuity surfaces and microfacies in a storm-dominated shallow Epeiric Sea, Devonian Cedar Valley Group, Iowa. *The Depositional Record* 3, 136-160.

- Braga, J.C., Martin, J.M., Riding, R., 1995. Controls on Microbial Dome Fabric Development along a Carbonate-Siliciclastic Shelf-Basin Transect, Miocene, SE Spain. *Palaeos* 10, 347-361.
- Braga, J.C., Martín, J.M., 2000. Subaqueous Siliciclastic Stromatolites: A Case History from Late Miocene Beach Deposits in the Sorbas Basin of SE Spain. In: Riding, R.E., Awramik, S.M. (Eds.), *Microbial Sediments*. Springer-Verlag, Berlin, pp. 226–232.
- Branner, J.C., 1910. The Tombador Escarpment in the State of Bahia, Brazil. *American Journal of Science* 30, 335-343.
- Brito Neves, B.B., Kawashita, K., Delhal, J., 1979. A evolução geocronológica da Cordilheira do Espinhaço; dados novos e integração. *Revista Brasileira de Geociências* 9, 71–85.
- Brito Neves, B.B., Campos Neto, M.D.C., Fuck, R.A., 1999. From Rodinia to Western Gondwana: an approach to the Brasiliano-Pan African Cycle and orogenic collage. *Episodes-Newsmagazine of the International Union of Geological Sciences* 22, 155-166.
- Burchette, T.P., Wright, V.P., 1992. Carbonate ramp depositional systems. *Sedimentary geology* 79, 3-57.
- Cai, Y., Hua, H., 2007. Pyritization in the Gaojishan Biota. *Chinese Science Bulletin* 52, 645-650.
- Campos Neto, M.C., 2000. Orogenic systems from southwester Gondwana. In: Cordani, U.G., Milani, E.J Thomaz Filho, A., Campos, D.A. (Eds.), *Tectonic Evolution of South America, 31th International Geological Congress*. Rio de Janeiro, Brasil, pp. 335-365.
- Canfield, D.E., Des Marais, D.J., 1993. Biogeochemical cycles of carbon, sulphur, and free oxygen in a microbial mat. *Geochimica et Cosmochimica* 57, 3971-3984.
- Chemale Jr., F., Alkmim, F.F., Endo, I., 1993. Late Proterozoic tectonism in the interior of the São Francisco craton. In: Findlay, R.H., Unrug, R., Banks, M.R., Veevers, J.J. (Eds.), *Gondwana eight: assembly, evolution and dispersal*. Balkema, Rotterdam, pp. 29-41.
- Chemale Jr., F., Dussin, I.A., Alkmim, F.F., Martins, M.S., Queiroga, G., Armstrong, R., Santos, M.N., 2012. Unravelling a Proterozoic basin history through detrital

- zircon geochronology: The case of the Espinhaço Supergroup, Minas Gerais, Brazil. *Gondwana Research* 22, 200-206.
- Chen, J., Lee, H.S., 2013. Soft-sediment deformation structures in Cambrian siliciclastic and carbonate strom deposits (Shandong Province, China): Differential liquefaction and fluidization triggered by storm-wave loading. *Sedimentary Geology* 288, 81-94.
- Chen, Z., Wang, Y., Kershaw, S., Luo, M., Yang, H., Zhao, L., Feng, Y., Chen, J., Yang, L., Zhang, L., 2014. Early Triassic stromatolites in a siliciclastic nearshore setting in northern Perth Basin, Wesr Australia: Geobiolobic features and implications for post-extinction microbial proliferation. *Global and Planetary Change* 121, 89-100.
- Choudhuri, A., Banerjee, S., Sarkar, S., 2020. A review of biotic signatures within the Precambrian Vindhyan Supergroup: Implications on evolution of microbial and metazoan life on Earth. *Journal of Mineralogical and Petrological Sciences* 115, 162-174.
- Clifton, H.E., Dingler, J.R., 1984. Wave-formed structures and paleoenvironmental reconstruction. *Marine Geology* 60, 165-198.
- Collins, D.S., Johnson, H.D., Allison, P.A., Guipain, P., Damit, A.R., 2017. Coupled 'storm-flood' depositional model: Application to the Miocene–Modern Baram Delta Province, north-west Borneo. *Sedimentology* 64, 1203-1235.
- CPRM – SERVIÇO GEOLÓGICO DO BRASIL; 2003. Geologia e recursos minerais do Estado da Bahia: Sistema de Informações Geográficas – SIG. Versão 1.1. Salvador: CPRM, 1 CD-ROM. Convênio CPRM-CBPM.
- Dalrymple, M., 2010. Interpreting sedimentary successions: facies, facies analysis and facies models. In: James, N.P., Dalrymple, R.W. (Eds.), *Facies models 4*, Geological Association of Canada. St. John's, Newfoundland, GEO text 6, pp. 3-18.
- Davis, R.A., 1968. Algal stromatolites composed of quartz sandstone. *Journal of Sedimentary Petrology* 38, 953–955.
- Dickson, J.A.D., 1965. A modified staining technique for carbonates in thin section. *Nature* 205, 587.
- Dott Jr, R.H., Bourgeois, J., 1982. Hummocky stratification: significance of its variable bedding sequences. *Geological Society of America Bulletin* 93, 663-680.

- Draganits, E., Noffke, N., 2004. Siliciclastic stromatolites and other microbially induced sedimentary structures in an early Devonian barrier-island environment (Muth Formation, NW Himalayas). *Journal of Sedimentary Research* 74, 191-202.
- Druschke, P.A., Jiang, G., Anderson, T.B., Hanson, A.D., 2009. Stromatolites in the Late Ordovician Eureka Quartzite: implications for microbial growth and preservation in siliciclastic settings. *Sedimentology* 56, 1275-1291.
- Dupraz, C., Pattisina, R., Verrecchia, E.P., 2006. Translation of energy into morphology: Simulation of stromatolite morphospace using a stochastic model. *Sedimentary Geology* 185, 185-203.
- Dupraz, C., Reid, R.P., Braissant, O., Decho, A.W., Norman, R.S., Visscher, P.T., 2009. Processes of carbonate precipitation in modern microbial mats. *Earth-Science Reviews* 96, 141-162.
- Dupraz, C., Reid, R.P., Visscher, P.T., 2011. Modern microbialites. In: Reitner, J., Thiel, V. (Eds.), *Encyclopedia of Geobiology*. Springer, Berlin, pp. 617–635.
- Frantz, C.M., Petryshyn, V.A., Corsetti, F.A., 2015. Grain trapping by filamentous cyanobacterial and algal mats: implications for stromatolite microfabrics through time. *Geobiology* 13, 409-423.
- Gebelein, C.D., 1969. Distribution, morphology, and accretion rate of recent subtidal algal stromatolites, Bermuda. *Journal of Sedimentary Research* 39, 49-69.
- Gerdes, G., Klenke, T., Noffke, N., 2000. Microbial signature in peritidal siliciclastic sediments: a catalogue. *Sedimentology* 47, 279-308.
- Grotzinger, J.P., 1990. Geochemical model for Proterozoic stromatolite decline. *American Journal of Science* 290, 80-103.
- Grotzinger, J.P., Knoll, A.H., 1999. Stromatolites in Precambrian carbonates: evolutionary mileposts or environmental dipsticks? *Annual review of earth and planetary sciences* 27, 313-358.
- Guadagnin, F., Chemale Jr, F., Magalhães, A.J.C., Santana, A., Dussin, I., Takehara, L., 2015. Age constrains on crystal-tuff from the Espinhaço Supergroup – Insight into the Paleoproterozoic to Mesoproterozoic intracratonic basin cycles of the Congo-São Francisco Craton. *Gondwana Research* 27, 363-376.
- Guan, C., Wang, W., Zhou, C., Muscente, A.D., Wan, B., Chen, X., Yuan, X., Chen, Z., Ouyang, Q., 2017. Controls on fossil pyritization: Redox conditions,

- sedimentary organic matter content, and Chuaria preservation in the Ediacaran Lantian Biota. *Palaeogeography, Palaeoclimatology, Palaeoecology* 474, 26-35.
- Harwood, G., 1990. Sandstone Stromatolites' – An Example of Algal-Trapping of Sand Grains from the Permian Yates Formation, New Mexico, USA. *Sediments* 1990, 13th International Sedimentological Congress (Nottingham-England) Abstracts of Posters. pp. 97.
- Hips, K., Haas, J., Poros, Z., Kele, S., Budai, T., 2015. Dolomitization of Triassic microbial mat deposits (Hungary): Origin of microcrystalline dolomite. *Sedimentary Geology* 318, 113-129.
- Hofmann, H.J., 1973. Stromatolites: characteristics and utility. *Earth-Science Reviews* 9, 339-373.
- Knoll, A.H., Semikhatov, M.A., 1998. The genesis and time distribution of two distinctive Proterozoic stromatolite microstructures. *Palaios* 13, 408-422.
- Leckie, D.A., Walker, R.G., 1982. Storm-and tide-dominated shorelines in Cretaceous Moosebar-Lower Gates interval—outcrop equivalents of Deep Basin gas trap in western Canada. *AAPG bulletin* 66, 138-157.
- Logan, B.W., 1961. Cryptozoon and associate stromatolites from the Recent, Shark Bay, Western Australia. *The Journal of Geology* 69, 517-533.
- Logan, B.W., Rezak, R., Ginsburg, R.N., 1964. Classification and environmental significance of algal stromatolites. *The Journal of Geology* 72, 68-83.
- Loureiro, H.S.C., Lima, E.S., Macedo, E.R., Silveira, F.V., Bahiense, I.C., Arcanjo, J.B.A., Moraes Filho, J.C., Neves, J.P., Guimarães, J.T., Teixeira, L.R., Abram, M.B., Santos, R.A., Melo, R.C., 2008. Projeto Barra-Oliveira dos Brejinhos Geological map. Brazilian Geological Survey and Bahia Mineral Research Company, scale 1:200.000.
- Marcinowski, R., Szulczeński, M., 1972. Condensed Cretaceous sequence with stromatolites in Polish Jura Chain. *Acta Geologica Polonica* 22, 515-538.
- Martin, J.M., Braga, J.C., Riding, R., 1993. Siliciclastic stromatolites and thrombolites, late Miocene, S.E Spain. *Journal of Sedimentary Petrology* 63, 131-139.
- Martins-Neto, M.A., 2000. Tectonics and sedimentation in a paleo/mesoproterozoic rift-sag basin (Espinhaço basin, southeastern Brazil). *Precambrian Research* 103, 147-173.

- Mastandrea, A., Perri, E., Russo, F., Spadafora, A., Tucker, M., 2006. Microbial primary dolomite from a Norian carbonate platform: northern Calabria, southern Italy. *Sedimentology* 53, 465-480.
- Molina, J.M., Alfaro, P., Moretti, M., Soria, J.M., 1998. Soft-sediment deformation structures induced by cyclic stress of storm waves in tempestites (Miocene, Guadalquivir Basin, Spain). *Terra Nova* 10, 145-150.
- Monty, C.L.V., 1973. Precambrian background and Phanerozoic history of stromatolitic communities, an overview. *Annales de la Societe Geologique de Belgique* 96, 585-624.
- Myrow, P.M., Southard, J.B., 1996. Tempestite deposition. *Journal of Sedimentary Research* 66, 875-887.
- Myrow, P.M., Fischer, W., Goodge, J.W., 2002. Wave-modified turbidites: combined-flow shoreline and shelf deposits, Cambrian, Antarctica. *Journal of Sedimentary Research* 72, 641-656.
- Noffke, N., Knoll, A., Grotzinger, J.P., 2002. Sedimentary Controls on the Formation and Preservation of Microbial Mats in Siliciclastic Deposits: A Case Study from the Upper Neoproterozoic Nama Group, Namibia. *Palaios* 17, 533-544.
- Noffke, N., Eriksson, K.A., Hazen, R.M., Simpson, E.L., 2006. A new window into Early Archean life: Microbial mats in Earth's oldest siliciclastic tidal deposits (3.2 Ga Moodies Group, South Africa). *Geology* 34, 253-256.
- Pedreira, A.J., 1994. O Supergrupo Espinhaço na Chapada Diamantina centro oriental, Bahia: Sedimentologia, estratigrafia e tectônica. São Paulo, USP, Instituto de Geociências, 126 p.
- Pérez-López, A., Pérez-Valera, F., 2012. Tempestite facies models for the epicontinental Triassic carbonates of the Betic Cordillera (southern Spain). *Sedimentology* 59, 646-678.
- Perri, E., Tucker, M., 2007. Bacterial fossils and microbial dolomite in Triassic stromatolites. *Geology* 35, 207-210.
- Pesonen, L.J., Mertanen, S., Veikkolainen, T., 2012. Paleo-Mesoproterozoic supercontinents – a paleomagnetic view. *Geophysica* 48, 5-47.
- Pisarevsky, S.A., Elming, S.Å., Pesonen, L.J., Li, Z.X., 2014. Mesoproterozoic paleogeography: supercontinent and beyond. *Precambrian Research* 244, 207-225.

- Popa, R., Kinkle, B.K., Badescu, A., 2004. Pyrite Framboids as Biomarkers for Iron-Sulfur Systems. *Geomicrobiology Journal* 21, 193-206.
- Pratt, B.R., 1982. Stromatolite decline – A reconsideration. *Geology* 10, 512-515.
- Preiss, W.V., 1976. Basic field and laboratory methods for the study of stromatolites. In: Walter, M.R. (Ed.), *Stromatolites. Developments in Sedimentology*, Vol. 20. Elsevier, Amsterdam, pp. 5-13.
- Reading, H.G., Collinson, J.D., 1996. Clastic Coasts. In: Reading, H.G. (Ed.), *Sedimentary Environments: Processes, Facies and Stratigraphy*, 3rd. Edition, pp. 154-231.
- Reid, R.P., Visscher, P.T., Decho, A.W., Stoltz, J.F., Bebout, B.M., Dupraz, C., Macintyre, I.G., Paerl, H.W., Pinckney, J.L., Prufert-Bebout, L., Steppe, T.F., DesMarais, D.J., 2000. The role of microbes in accretion, lamination and early lithification of modern marine stromatolites. *Nature* 406, 989-992.
- Riding, R., 1991. Classification of microbial carbonates. In: Riding, R. (Ed.), *Calcareous Algae and Stromatolites*, Springer-Verlag, Berlin, pp. 21–51.
- Riding, R., 2000. Microbial carbonates: the geological record of calcified bacterial-algal mats and biofilms. *Sedimentology* 47, 179-214.
- Riding, R., 2011. Microbialites, stromatolites, and thrombolites. In: Reitner, J., Thiel, V. (Eds.), *Encyclopedia of geobiology, Encyclopedia of Earth Sciences Series*. Springer Netherlands, pp. 635-654.
- Rocha, A.J., Pereira, C.P., Srivastava, N.K., 1992. Carbonatos da Formação Caboclo (Proterozóico médio) na região de Morro do Chapéu - Estado da Bahia. *Revista Brasileira de Geociências* 22, 389-398.
- Schieber, J., 1998. Possible indicators of microbial mat deposits in shales and sandstones: examples from the Mid-Proterozoic Belt Supergroup, Montana, U.S.A. *Sedimentary Geology* 120, 105-124.
- Schwarz, H., Einsele, G., Herm, D., 1975. Quartz-sandy, grazing-contoured stromatolites from coastal embayments of Mauritania, West Africa. *Sedimentology* 22, 539-561.
- Sheldon, N.D., 2013. Causes and consequences of low atmospheric pCO₂ in the Late Mesoproterozoic. *Chemical Geology* 362, 224-231.
- Srivastava, N.K., 1988. Estromatólitos da Formação Caboclo na Região de Morro do Chapéu: relatório de consultoria I. Salvador: CPRM.

- Soudry, D., Weissbrod, T., 1995. Morphogenesis and facies relationships of thrombolites and siliciclastic stromatolites in a Cambrian tidal sequence (Elat area, southern Israel). *Palaeogeography, Palaeoclimatology, Palaeoecology* 114, 339-355.
- Suarez-Gonzalez, P., Quijada, I.E., Benito, M.I., Mas, R., Merinero, R., Riding, R., 2014. Origin and significance of lamination in lower cretaceous stromatolites and proposal for a quantitative approach. *Sedimentary Geology* 300, 11-27.
- Suarez-Gonzalez, P., Benito, M.I., Quijada, I.E., Mas, R., Campos-Soto., 2019. 'Trapping and binding': A review of the factors controlling the development of fossil agglutinated microbialites and their distribution in space and time. *Earth-Science Reviews* 194, 182-215.
- Tucker, M., 1982. Storm-surge sandstones and the deposition of interbedded limestone: Late Precambrian, southern Norway. In: Einsele, G., Seilacher, A. (Eds.), *Cyclic and event stratification*. Springer-Verlag, Heidelberg, pp. 363-370.
- Visscher, P.T., Reid, R.P., Bebout, B.M., 2000. Microscale observations of sulfate reduction: Correlation of microbial activity with lithified micritic laminae in modern marine stromatolites. *Geology* 28, 919-922.
- Walker, R.G., James, N.P., 1992. Facies models: response to sea level change. Newfoundland, Canada: Geological Association of Canada 409 p.
- Walter, M.R., 1977. Interpreting stromatolites. *American Scientist* 65, 563-571.

The screenshot shows a software interface for managing journal submissions. At the top, there's a red header bar with the text 'PRECAMBRIAN RESEARCH' and 'Editorial Manager'. Below this, a black navigation bar includes links for 'HOME', 'LOGOUT', 'HELP', 'REGISTER', 'UPDATE MY INFORMATION', 'JOURNAL OVERVIEW', 'MAIN MENU', 'CONTACT US', 'SUBMIT A MANUSCRIPT', 'INSTRUCTIONS FOR AUTHORS', and 'PRIVACY'. The user is logged in as 'Author' with the username 'joaopedroformolo@hotmail.com'. The main content area is titled 'Submissions Being Processed for Author João Pedro Formolo Ferronatto'. It displays a table with one row of data. The columns are 'Action', 'Manuscript Number', 'Title', 'Initial Date Submitted', 'Status Date', and 'Current Status'. The 'Action' column contains a link labeled 'Action Links'. The 'Title' column shows the manuscript title: 'Mesoproterozoic siliciclastic stromatolites of Chapada Diamantina (Brazil): morphological types, genesis and environmental context.'. The 'Initial Date Submitted' and 'Status Date' both show 'Mar 24, 2021'. The 'Current Status' is 'Submitted to Journal'. Below the table, there are two pagination controls: 'Page: 1 of 1 (1 total submissions)' and 'Display 10 results per page.'.

Confirming submission to Precambrian Research

Precambrian Research <em@editorialmanager.com>

Qua, 24/03/2021 22:33

Para: João Pedro Formolo Ferronatto <joaopedroformolo@hotmail.com>

This is an automated message.

Mesoproterozoic siliciclastic stromatolites of Chapada Diamantina (Brazil): morphological types, genesis and environmental context.

Dear Mr Formolo Ferronatto,

We have received the above referenced manuscript you submitted to Precambrian Research.

To track the status of your manuscript, please log in as an author at <https://www.editorialmanager.com/precam/>, and navigate to the "Submissions Being Processed" folder.

Thank you for submitting your work to this journal.

Kind regards,
Precambrian Research

ANEXO I

Título da Dissertação/Tese:

**ESTROMATÓLITOS EM SISTEMA PLATAFORMAL DOMINADO POR ONDAS
DO MESOPROTEROZOÍCO DA CHAPADA DIAMANTINA**

Área de Concentração: Estratigrafia

Autor: **João Pedro Formolo Ferronatto**

Orientador: Prof. Dr. Claiton Marlon dos Santos Scherer

Examinador: Prof. Dr. Roberto Iannuzzi

Data: 14/05/2021

Conceito: A

PARECER:

O documento apresentado referente à tese de João P. F. Ferronatto está muito bem organizado e escrito. O conteúdo é apropriado e atualizado sobre o tema, bem como a metodologia. O objeto de estudo foi investigado com profundidade adequação, de forma que as interpretações e conclusões são coerentes e estão concatenadas com as existentes na literatura internacional sobre o tema, tanto que o primeiro artigo já foi aceito em periódico internacional nível A1 do Qualis-CAPES. Sem dúvida o trabalho realizado atingiu o nível de doutorado. Infelizmente, todas as figuras do texto integrador não foram traduzidas para o português, o que deveria ter ocorrido, pois se trata de documento a ser escrito em língua portuguesa, além do que algumas delas não estão reproduzidas em boa resolução para leitura. Isso não tira o brilho da pesquisa que alcançou alto nível, mas fica como um alerta ao candidato quando da elaboração de futuros documentos formais. Quanto à defesa, o candidato apresentou no tempo estabelecido de forma clara e objetiva, e demonstrou conhecimento e segurança durante a arguição. Assim sendo, considero o candidato APROVADO.

Assinatura:

Data: 14/05/2021

Ciente do Orientador:

Ciente do Aluno:

ANEXO I

Título da Dissertação/Tese:

**ESTROMATÓLITOS EM SISTEMA PLATAFORMAL DOMINADO POR ONDAS
DO MESOPROTEROZOÍCO DA CHAPADA DIAMANTINA**

Área de Concentração: Estratigrafia

Autor: **João Pedro Formolo Ferronatto**

Orientador: Prof. Dr. Clayton Marlon dos Santos Scherer

Examinador: Prof. Dr. Juliano Kuchle

Data: 14/05/21

Conceito: A - Excelente

PARECER:

Tese apresentada com volume textual e apresentação oral bem estruturados, organizados, com informação clara e bem escrita e bem apresentada. Tema relevante, com definição de hipóteses e objetivos bem elaborados. Artigos bem escritos e relevantes, em revistas de alto impacto (A1), um já publicado e um submetido. O doutorando apresenta grande domínio do tema, o que demonstra sua capacitação plena. A arguição desenvolveu discussão em alto nível e idéias relevantes tanto no tema específico da tese, quanto temas em paralelo.

Parabenizo o doutorando João e seu Orientador Clayton pelo trabalho realizado.

Assinatura: Juliano Kuchle Data: 14/05/21

Ciente do Orientador:

Ciente do Aluno: